LIGAND-RECEPTOR INTERACTION MODELLING USING PET IMAGING

by

Stefano Zamuner

Thesis submitted in partial fulfilment of the requirement for the degree of

Doctor of Philosophy

Centre of Measurement and Information in Medicine

City University

2003

ABSTRACT

A basic problem in the discovery and development of novel drugs to be used in the treatment of neurological and psychiatric disorders is the absence of relevant *in vitro* or *in vivo* animal models that can yield results which can be extrapolated to man. Drug research now benefits from the fast development of functional imaging techniques such as positron emission tomography (PET) which trace radiolabelled molecules directly in the human brain. PET uses molecules that are labelled with short-lived radionuclides and injected intravenously into experimental animals, human volunteers or patients.

The current work provided novel knowledge in the ligand-receptor interaction between GR205171 and neurokinin 1 (NK1) receptor. GR205171 is a high affinity and selective NK1-receptor antagonist. Clinical studies were performed both in monkeys and humans to obtain information about the suitability of the ligand with regard to its affinity and penetration.

The specific objectives of this thesis were to define an appropriate model for GR205171 tracer and to calculate receptor occupancy in the monkey and human brain, introducing also novel methodological approaches. The definition of a relationship between plasma drug concentration and receptor occupancy was another important aim of this work. In fact, the demonstration of quantitative relationships between drug binding *in vivo* from plasma concentration data and drug effects in patients can be used to validate targets for drug action, to correlate pharmacological and physiological effects, and to optimise clinical treatment.

In conclusion, the modelling of GR205171 PET data, including different methodological approaches, demonstrated its utility in assessing NK1 receptor occupancy after drug challenge and its relationship with plasma concentration.

TABLE OF CONTENTS

Page

TABLE OF FIGURES

TABLE OF TABLES

ACKNOWLEDGMENT

I would like to thank Dr. Roman Hovorka for his support, encouragement and for his invaluable advice. I am indeed grateful to Dr. Roberto Gomeni for his important support and for his time. I am also thankful to Dr. Alessandra Bertoldo and Professor Claudio Cobelli to have introduced me in the "magic world" of modelling of imaging data. A special thanks to Dr. Alan Bye for supporting this PhD study. Finally, I am thankful to my friends and colleges, in particular to Dr. Laura Iavarone, who supported and helped me to achieve this point.

I would like to express my grateful appreciation to my family for their ongoing support.

GLOSSARY

AIC	Akaike information criterion
BBB	Blood brain barrier
B_{max}	Total receptor concentration (µmol)
BP	Binding potential (unitless)
C'_i	Unlabelled ligand concentration in compartment i (µmol · ml^{-1})
C_i	Labelled ligand concentration in compartment i (µCi · ml^{-1})
CNS	Central nervous system
EC_{50}	Concentration resulting in 50% maximum effect
E_{max}	Maximum effect
GR205171	A high affinity and selective NK1-receptor antagonist
K_D	Equilibrium dissociation constant (µmol · ml^{-1})
k_{ij}	Transfer rate constant of tracer kinetics (min^{-1})
k_{off}	Dissociation rate (min^{-1})
k_{on}	Association rate (units mol^{-1} · ml · min^{-1})
NK1	Neurokinin 1 receptor
PET	Positron emission tomography
RO	Receptor occupancy (%)
ROI	Region of interest
SUV	Standard uptake value (unitless)
WSS	Sum of squared weighted residuals

1 INTRODUCTION

In the discovery and the development of new drugs imaging techniques have become an important feature to accelerate and improve these processes (Farde, 1996; Paans and Vaalburg, 2000). In terms of efficacy, the use of these techniques allows crucial information to be obtained in a non invasive way near to the target of the drug. It allows biological processes of mechanistic relevance to be monitored in real time, with high resolution and with the preservation of the structural integrity of the experimental model, both animals and humans, during and after the study. Especially in the central nervous system (CNS) area, where non invasive methods are necessary for in vivo studies, the utility of imaging consists of identifying whether the drug has reached the target (i.e. a region rich of specific receptors) and obtaining meaningful information (i.e. the distribution of the drug, binding to the target site, the duration of binding).

Neuroimaging can be used to identify biological or functional changes that are related to the disease state and are surrogate markers to be used for the assessment of novel compounds (Grasby, 1999). One of the meaningful imaging techniques is positron emission tomography (PET). PET has become an important non-invasive methodology to investigate ligand-receptor binding in the living brain (Farde, 1995; Halldin *et al.*, 2001).

Receptor/transporter imaging studies conducted using PET determine the interaction of the drug of interest with a putative binding site and measure neurotransmitter concentration changes indirectly in animals and man after administration of the drug whose putative mode of action is through neurotransmitter release. As positron labels can be used, PET also provides a continuum of data allowing simulations from animals to human experimental design.

Mainly, the aim of this technique is to quantify physiological parameters from the experimental data. The processes involved in the ligand receptor interaction are

basically the tracer penetration of the blood brain barrier and the binding with specific and non specific receptors.

In summary, neuroimaging techniques can provide relevant information to facilitate decision-making for target and compound development, in particular for dose selection, proof-of-concept (PoC) design, and surrogate marker identification for reducing attrition by early use of human disease models.

Different PET studies have been conducted to estimate the brain penetration and receptor occupancy of some compounds developed by GlaxoSmithKline. Several methods, based on a compartmental analysis of the ligand-receptor interactions, for quantitatively measuring the binding parameters have been devised. The subject of this project is the study, the application, and the development of ligand-receptor models in the CNS area using PET imaging.

We focus on the ligand-receptor interaction between a NK_1 antagonist developed by GlaxoSmithKline and the NK_1 receptor. This receptor belongs to the family of NK_1 receptors (NK_1, NK_2, and NK_3) and its binding with tachykinin neurotransmitters mediates the release of intracellular calcium. This binding could be related to many neurological diseases.

The first part of the thesis introduces the principles of ligand-receptor interaction and the methodologies to study this interaction with PET (Chapter 2-4). We introduce the models currently used to analyse PET data in the field of brain receptor studies. The main objective of this review is to describe the different models to analyse PET data with a particular attention to the limitations and the advantages of the different approaches proposed in the literature. Basic concepts of the PET system are given.

To investigate the characteristics of a new NK_1 antagonist drug, both monkey and human studies were performed.

In Chapter 5 the monkey study is presented. The aim of this study is to obtain information about tracer penetration across the blood brain barrier and to define the

most appropriate models to estimate the parameters that describe the ligand receptor interaction with a particular emphasis upon receptor occupancy. Since arterial tracer concentration corrected for metabolites was not available, a modelling approach that uses a region void of specific receptors as the reference was applied.

In Chapter 6, an intravenous human study is presented. In this analysis our aim was to define the appropriate model in humans and to estimate receptor occupancy after different doses of the drug. The time course of receptor occupancy was also evaluated. In the human study it was possible to use two different methodologies: one based on the reference region and the other based on plasma radioactivity corrected for metabolites as an input function. A secondary objective of this study was to compare the results of the receptor occupancy estimates using these two approaches.

A new data analysis approach based on a mixed effect model is proposed to take into account inter- and intra-subject variability in Chapter 7. The conventional data analysis approach is based on the independent modelling of data for each subject and for each PET scan. As a result, the parameter estimation and the precision of receptor time varying occupancy do not account for the variability induced by the complex methodology of data acquisition and by the intra- and inter-subject variability in individual responses. Alternative parameter estimation strategies were considered based on the use of non-linear mixed effect models accounting for intra- and inter-subject variability using covariate measurements.

A mathematical model linking plasma concentration to the receptor occupancy is developed in Chapter 8. The model is then validated using data collected in a complementary experiment. This approach is helpful to forecast receptor occupancy after a drug administration from the PK profile.

In Chapter 9, a simulation study to forecast the expected receptor occupancy after single oral dose was performed. The prediction of the PK/PD modelling was assessed using the estimated receptor occupancy (RO) from an oral dosing study in humans.

2 AIMS AND OBJECTIVES

The aim of this thesis is to study the ligand-receptor interaction between GR205171 and neurokinin 1 (NK1) receptor. GR205171 is a high affinity and selective NK1-receptor antagonist. The compound was labelled with ^{11}C in the Uppsala University PET Centre (Bergstom *et al.*,1998). Clinical studies were performed both in monkeys and humans to obtain information about the suitability of the ligand with regard to its affinity and penetration.

The specific objectives of this thesis are:

1. to define an appropriate model for GR205171 tracer;
2. to calculate receptor occupancy in monkey and human brain;
3. to define a relationship between plasma drug concentration and receptor occupancy; and
4. to forecast receptor occupancy for different dose regimens.

3 BACKGROUND

3.1 Receptor-ligand interaction

3.1.1 Definitions

Receptors are specialised cellular or tissue elements with which a drug interacts to produce its characteristic pharmacological effects. Structurally, receptors appear to be macromolecules such as proteins, enzymes, lipoproteins, and nucleic acids.

When a ligand (hormone, neurotransmitter, intracellular messenger molecule, or exogenous drug) combines with a receptor, cell function changes. Each ligand may interact with multiple receptor subtypes. Activated receptors directly or indirectly regulate cellular biochemical processes (e.g. ion conductance, protein phosphorylation, DNA transcription).

The formation of a complex between a drug (ligand) and receptor is thought to trigger a series of events that alter a biological system and lead to a pharmacological effect. These effects may be as diverse as inhibition of an enzyme or release of a neurotransmitter. However, the effect may be separated both in time and nature from the drug receptor interaction, which initiates a series of events that only eventually results in the observed response.

A ligand can be agonist or antagonist. An agonist is a signalling molecule (hormone, neurotransmitter or synthetic drug) which binds to a receptor, inducing a conformational change which produces a response such as contraction, relaxation, secretion, change in enzyme activity, etc.

An antagonist is a drug which attenuates the effect of an agonist. Antagonists may be divided either on the basis of being surmountable or, on the basis of being competitive, non-competitive, or uncompetitive. Surmountable and insurmountable are functional descriptions, depending on whether or not the effect of the antagonist may be overcome by increasing the concentration of agonist. The other terms describe

the mechanism by which the antagonist exerts its effect. Thus, competitive antagonists bind to a region of the receptor which overlaps with the binding site for the agonist, but occupy the site without activating the effector mechanism. The agonist and antagonist therefore compete for the same binding site and cannot simultaneously occupy the receptor.

Antagonists interact selectively with receptors but do not lead to an observed effect; they reduce the action of another substance (agonist) at the receptor site involved. Receptor antagonists thus possess affinity but lack intrinsic efficacy.

Receptor antagonists can be classified as reversible or irreversible. Reversible antagonists readily dissociate from their receptor; irreversible antagonists form a stable chemical bond with their receptor. Pseudoirreversible antagonists slowly dissociate from their receptor.

3.1.2 Ligand-receptor interaction

Several theories of drug-receptor interaction have been proposed, but most experimental observations are best explained by a combination of current hypotheses. The law of mass action and the reversibility of drug-receptor interaction served as the basis for the receptor occupation theories (Young, 1986), which postulate that the magnitude of the drug-induced effect is proportional to the concentration of the drug-receptor complex. Inherent in this theory are the concepts of affinity (the propensity of a drug to bind with a given receptor) and intrinsic activity or efficacy (the biological effectiveness per unit of drug-receptor complex).

3.1.2.1 Analysis of ligand action: Principles

A great deal of pharmacology theory deals with the interaction between a receptor molecule and an agonist either alone or in the presence of a competing antagonist. The simplest case is that one molecule of ligand (L) binds reversibly to a receptor molecule (R) to form an active ligand-receptor complex (LR), which generates a pharmacological response while the ligand remains bound

$$L + R \Leftrightarrow LR \rightarrow response$$

Such interactions frequently obey the law of mass action, which states that the rate of reaction is proportional to the concentration of reactants (so it is not really a law in the strict physical sense, it is more an assumption that seems to apply to many pharmacological interactions). If it does apply, then the rate of the forward reaction is proportional to the ligand and receptor concentration. The rate of the reverse reaction is simply proportional to ligand-receptor complex concentration, since there is no other molecular species involved in the dissociation. At equilibrium, the rate of the forward reaction is equal to the rate of the reverse reactions, and so (using k_{on} and k_{off} as the respective proportionality constants)

$$k_{on} L \cdot R = k_{off} LR \qquad (1)$$

Rearranging,

$$\frac{L \cdot R}{LR} = \frac{k_{off}}{k_{on}} = K_D \qquad (2)$$

The K_D value (units mol $\cdot$ ml^{-1}) is called the equilibrium dissociation constant for the ligand (agonist or antagonist) and is equal to the ratio of the reverse and forward rate constants. K_D is an inverse measure of the ligand's affinity for the receptor.

Arranging the previous equation, we obtain

$$R = \frac{K_D \cdot LR}{L} \qquad (3)$$

To find an expression relating the proportion of receptors occupied by ligand, LR, to the total receptor population, R_T, we first note that R_T must equal the total of occupied receptors, LR, plus unoccupied receptor, R,

$$R_T = LR + R \qquad (4)$$

Substituting for R, we obtain

$$R_T = \frac{K_D \cdot LR}{L} + LR \tag{5}$$

Then, dividing both sides by LR gives

$$\frac{R_T}{LR} = \frac{K_D}{L} + 1 = \frac{K_D + L}{L} \tag{6}$$

and taking reciprocals results in

$$\frac{LR}{R_T} = \frac{L}{K_D + L} \tag{7}$$

The left-hand side of this equation represents the fraction of receptor occupied by ligand, and the right-hand side shows that it varies with the concentration of ligand with a rectangular hyperbolic relationship. This equation is called Hill-Langmuir adsorption isotherm.

When $L = K_D$, then

$$LR = \frac{L \cdot R_T}{L + L} = \frac{1}{2} R_T \tag{8}$$

and half maximal binding occurs. Note that L refers to free ligand concentration, which is sometimes hard to quantify. Practically, if binding conditions in which LR is less than 10% of the total amount of the ligand, L could be considered equal to L_T.

Usually in binding experiments, the symbol used in Equation 8 are B = bound ligand (LR), F = free ligand (L), and B_{max} = total receptor binding site (R_T).

3.1.3 Occupancy

Occupancy represents the proportion of receptors to which a drug is bound. It may be calculated from the Hill-Langmuir adsorption isotherm, which gives the fraction of receptors occupied by a drug (substituting D for L in Equation 7)

$$RO = \frac{D}{K_D + D} \qquad (9)$$

Early drug occupation theory assumed that a pharmacological response was directly proportional to receptor occupancy (Stephenson, 1956); a maximal effect occurred when all receptors were occupied or activated. Current theory includes kinetic processes (onset/offset rates) of ligand-receptor occupancy, multiple activation states (active/inactive) of receptors, and the lack of apparent proportionality between ligand-receptor occupancy and ultimate tissue or organ response (Mackay, 1988).

3.1.4 Receptor binding techniques

Receptor binding studies are possible because of the high affinity that some agonists and antagonists have for their receptor. Consequently, at low concentrations of drug, a high proportion is bound to the receptor compared to the proportion which binds to non-receptor sites.

Although only minute amounts of receptor are present in most cells and tissues (typically less than a few pmol/mg protein), the amount of drug bound can be measured by radiolabelling it and measuring the amount of radioactivity bound to the tissue. It is essential to distinguish the receptor-bound drug from that which is free in solution.

Radioligand binding techniques are commonly used to determine the equilibrium dissociation constant, K_D, and maximal specific binding, B_{max}, of a radioligand by saturation analysis and to measure the affinity of competing ligands by competition analysis (Qume, 1999).

Moreover, these techniques are used to investigate whether a particular receptor type is present in the particular cell or tissue. The validity of these data would depend on the selectivity of the radioligand used for the purpose.

3.1.4.1 Saturation analysis

In the saturation analysis the aim is to determine the equilibrium dissociation constant, K_D, and maximal specific binding, B_{max}, of a radioligand. The observed total binding consists of specific binding to the receptor itself, plus non-specific binding to non-receptor sites. The specific binding should saturate at sufficiently high concentrations of radioligand, and the K_D value is equal to the concentration of radioligand occupying 50% of the B_{max} value.

Scatchard analysis was, until recently, the standard method for analysing the equilibrium binding parameters of a radiolabelled drug with its receptor determined by saturation analysis. This method of analysis suffers from various statistical drawbacks and has now been superseded by computer-modelling to fit a mathematical model of one or more binding sites to the data (see Figure 1).

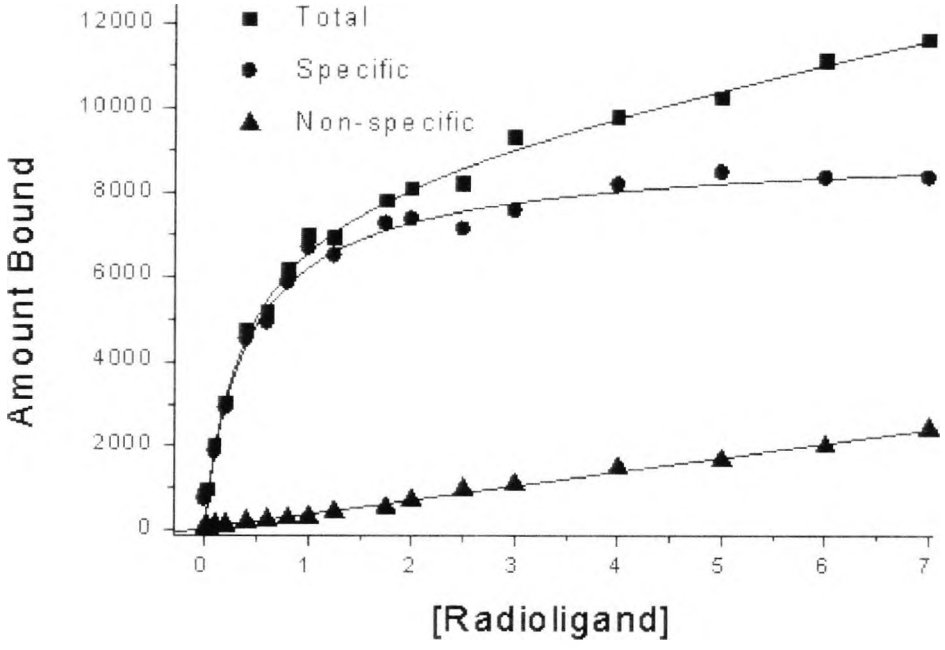

Fig. 1. Saturation plot for a radiolabelled ligand. The x axis represents the concentration of radioligand. The y axis shows the amount bound (in counts per minute) for total binding, non-specific binding, and specific binding (the difference between the other two).

However, it is still frequently used in the form of a Scatchard plot as a visual summary of the data. The method is only valid where the drug binds to a single receptor population. If it binds to more than one type of site, the result will be a curved Scatchard plot.

Equation 7 is not a linear relationship and therefore R_T and K_D can not be directly estimated. The equation can be rearranged to yield a linear relationship which gives more accurate estimates of R_T and K_D. Using Equation 2 and $R_T = R + LR$,

$$\frac{K_D}{L} = \frac{R}{LR} = \frac{R_T - LR}{LR} \tag{10}$$

$$\frac{LR}{L} = \frac{R_T - LR}{K_D} \tag{11}$$

Since LR is determined experimentally and $L = L_T$, if $R_T << L_T$, then a plot of $\frac{LR}{R_T}$ versus LR will give a straight line with a slope of $-\frac{1}{K_D}$, a y-intercept of $\frac{R_T}{K_D}$ and an x-intercept of R_T. This type of plot is termed a Scatchard plot (see Figure 2). The main consequence of the linearisation procedures is that the model parameters are not estimated using the observed measurements but using derived data. The final parameter values resulting from this analysis are potentially biases for non-linear transformation applied (the ratio between LR and R_T) and the error propagation on the measurements. For this reason the most appropriate procedure to estimate the parameters remains the non-linear regression analysis applied to Equation 7.

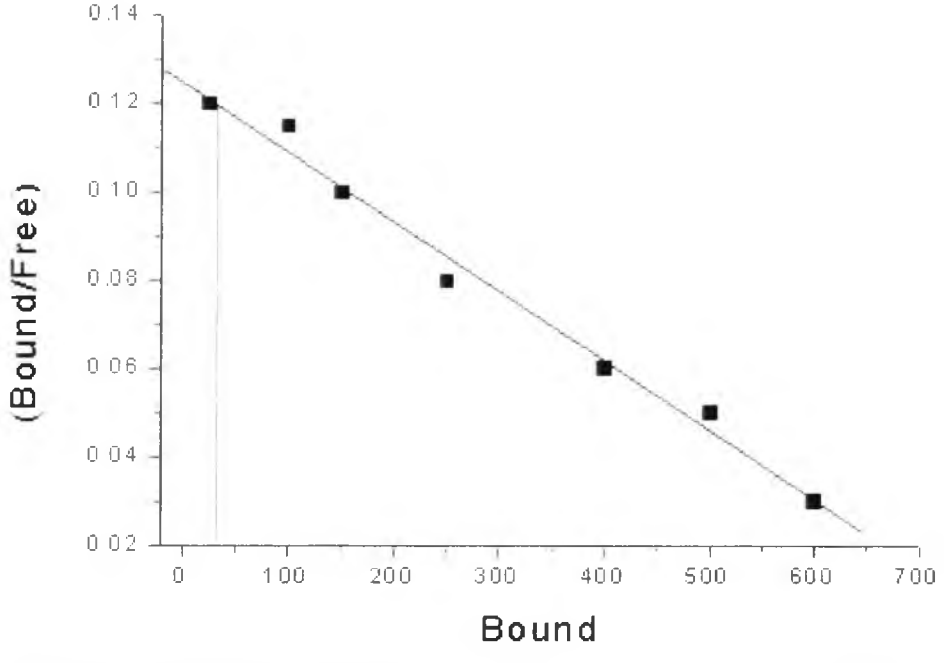

Fig. 2. Scatchard plot from a radioligand saturation experiment. The Scatchard plot is a graph of (on the y axis) the amount of radioligand bound divided by the amount of radioligand free in the solution, versus (on the x axis) the amount of radioligand bound. The B_{max} value is equal to the intercept on the x axis when y = 0, and the absolute value of the slope is equal to the K_D value.

3.1.4.2 Competition analysis

Equilibrium experiments can be performed in the presence of various concentrations of competitors to determine both binding and inhibitory constants.

In the competition analysis a single concentration of radioligand is used for every assay point (unlike in saturation analysis, in which the radioligand concentration is varied). The ligand is used at a low concentration, usually at or below its K_D value. The level of specific binding of the radioligand is then determined in the presence of a range of concentrations of other competing non-radioactive compounds in order to measure the potency with which they compete for the binding of the radioligand. The data for each competing ligand are usually fitted to a hyperbolic equation from which the IC_{50} value can be determined.

In the presence of inhibitor I, the equations that need to be considered are those originating from competitive kinetics

$$R + L = LR \tag{12}$$

$$R + I = IR \tag{13}$$

Then it follows that

$$K_D = \frac{R \cdot L}{LR} \text{ and } K_I = \frac{R \cdot I}{IR} \tag{14}$$

and

$$R = \frac{K_D \cdot LR}{L} \tag{15}$$

$$IR = \frac{R \cdot I}{K_I} = \frac{K_D \cdot LR \cdot I}{K_I \cdot L} \tag{16}$$

Since in the presence of inhibitor, $R = R_T - LR - IR$, substituting this in Equation 16 and rearranging we obtain

$$LR = \frac{R_T \cdot L}{L + K_D \cdot (1 + I/K_I)} \quad (17)$$

In practice, competition experiments determine an IC_{50} concentration of an inhibitor, that is, the concentration of an inhibitor that reduces binding by 50% under conditions in which L and R are constant. In this case

$$K_I = \frac{IC_{50}}{1 + (L/K_D)} \quad (18)$$

In fact,

$$LR = \frac{R_T \cdot L}{L + K_D \cdot (2 + L/K_D)} \quad (19)$$

$$\frac{LR}{R_T} = \frac{1}{1 + K_D/L \cdot (2 + L/K_D)} = \frac{1}{2} \cdot \frac{1}{1 + K_D/L} \quad (20)$$

and the second term in Equation 7 is reduced by 50%.

When competition experiments are carried out at ligand concentrations well below K_D, then $IC_{50} = K_I$. When the ligand concentration is high, IC_{50} can be considerably higher than the K_I.

The K_I can be estimated from the slope of the Scatchard plot as in the presence of inhibitor, the slope is

$$-1/K_D \cdot (1 + I/K_I) \quad (21)$$

3.2 PET technique

3.2.1 Principle of PET

Positron emission tomography (PET) is a technique for measuring the concentrations of positron-emitting radioisotopes within a three dimensional object by the use of external measurement of the radiation from these isotopes (Hoffman and Phelps, 1986).

Proton-rich radioisotopes can reduce the excess positive charge on the nucleus in two different ways: a) the nucleus captures an orbital electron and neutralizes positive charge with the negative charge of the electron, b) a positive electron (positron) can be emitted from the nucleus.

The positron is an anti-electron that, after travelling a short distance, will combine with an electron from the surrounding and annihilate itself. On annihilation the masses of both the electron and the positron are converted to electromagnetic radiation formed by two gamma rays of equal energy (511 keV), which are emitted 180° to each other. It is this annihilation radiation that can be detected externally and is used to measure both the quantity and the location of the positron emitter.

The external detection takes advantage not only of the fact that the two annihilation photons are admitted at 180° to each other, but also of the fact that they are created simultaneously. Simultaneous or coincidence detection of two of these photons by detectors on opposite sides of an object places the site of the annihilation on or about a line connecting the centres of the two detectors (see Figure 3). If the annihilation originates outside the volume between the two detectors, only one of the photons can be detected, and since the detection of a single photon does not satisfy the coincident condition, the event is rejected.

This concept of PET could only be realized when the inorganic scintillation detectors for the detection of gamma radiation, the electronics for coincidence measurements,

and the computer capacity for data acquisition and image reconstruction became available essential for synthesis of the desired complex molecules.

PET employs mainly short-lived positron-emitting radioisotopes. The most widely used radio-nuclides are: ^{11}C ($t_{1/2}$ 20 min), ^{13}N ($t_{1/2}$ 10 min),^{15}O ($t_{1/2}$ 2 min), and ^{18}F ($t_{1/2}$ 110 min). Because of this short half-life, the radio-nuclides have to be produced in house, preferably with a small, dedicated cyclotron (Paans *et al.*, 2002).

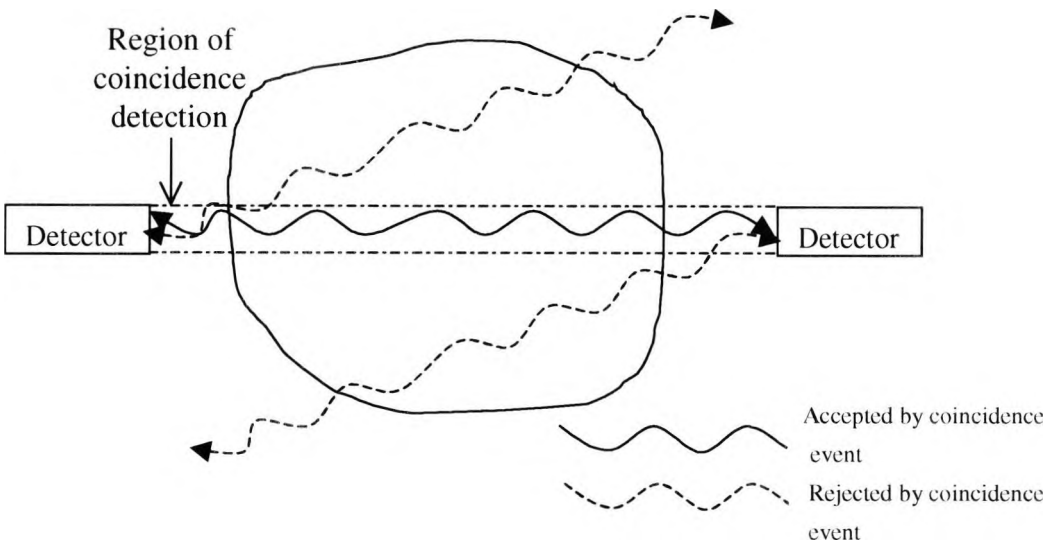

Fig. 3. Diagram of the principle of annihilation coincidence detection. When two gamma rays produced by the annihilation of two particles are detected by opposite detectors a coincidence event occurred. In this case the annihilation is localised to the region between the two detectors (between the dashed line). Any radiation occurring outside the volume between the two detectors is not considered.

The accuracy of the localisation in PET depends primarily on the physical size and geometry of the detectors. Moreover, the detector materials themselves affect the detection efficiency for the annihilation radiation and also affect the shape of response near the edge of the detector. Every couple of radiation produced by a positron emitter will be detected in a coincidence event by the two adjacent detectors and consequently a count rate profile as a function of the position will be determined (line spread function LSF). The LSF of the individual coincidence detectors pairs define the limit

of spatial resolution for the final PET image (LSF is gaussian for cylindrical detector and trapezoidal for rectangular detectors).

The physical limit of the accuracy of localisation in PET depends both on the energy of emission of the positron and the fact that not all the annihilations are emitted at exactly 180°. Since the measurement of interest is the location of the positron-emitting nuclide, the fact that the positron annihilates at same distance from the nucleus reduces the accuracy of this localisation.

Since the annihilation coincidence detection can only localise in one dimension, it is necessary to obtain measurements from a number of directions to determine the three-dimensional isotope distribution.

An adequate data sampling in each profile and an adequate data number of angular views are equivalent to having sufficient independent linear equations to solve for all the unknown variables and then to reconstruct an image of the isotope concentrations in a slice through the object.

3.2.2 Quantitation in PET

The PET measurement represents the in vivo regional or local tissue concentration of positron emitter. This measurement can be related to a physiological or metabolic process through the application of an appropriate mathematical model of the process.

Since a PET system will detect only a fraction of the emitted radiation, it is necessary to calibrate the efficiency of the machine. Usually, the calibration requires the measurement of a source of positron emitter (a uniform solution of activity in a cylindrical container much larger than the spatial resolution of the tomograph) by the PET system followed by the measurement of the amount of the same activity in a well counter. This type of calibration will give the efficiency of the response of the system in terms of activity per unit volume or concentration. Thus, it is possible to correct by this calibration factor the activity detected in a region of interest (ROI).

The amount of activity is to be considered irrelevant to the physiological system (an amount that does not change the system). Anyway, the relationship between its concentration in the blood (the input of the system) and the response of the PET system (the output) allows the investigation of the physiological system.

The usual method of obtaining the input function is to catheterise an artery of the subject and to take a series of blood samples following the injection of the labelled compound. The blood samples must be obtained with a frequency and a length of time adequate to define the level and the shape of the input function.

In same cases only one component of the blood is involved in the input function (for example in metabolic studies with fluorodeoxyglucose (FDG), the plasma concentration of FDG is used).

Two methods have been developed to avoid arterial samples to define the input function. The first consists on arterialising the blood in the veins (using a mechanism that heats the hand). This produces a very high blood flow in the hand without an increase in the metabolic function, and the extraction of the substrate in the hand is typically small. The second method consists of measuring the input function directly by measuring the amount of activity in the left ventricle, aorta, or other large artery as a function of time. This method requires that the PET system be capable of accumulating images rapidly enough to satisfy the temporal sampling requirements of the particular input function. In brain receptor studies it is possible to use a region void of specific receptors as input function (see the model section).

3.2.3 Limitation of quantitation in PET

In the PET technique, as with all measurement techniques, there are different sources of errors that should be taken into account in order to provide a proper interpretation of the results of PET measurements.

Resolution

The primary limitation of PET is its spatial resolution. The limiting resolution due to the physics of the annihilation process and the required physical size of the PET system is of the order of 2 to 3 mm.

In the PET field there are a number of types of resolution that can be defined. First of all the intrinsic resolution, that is the resolution of the individual detector pairs in the system. It is usually given in terms of the LSF of a pair detector at the centre of the field of view. The intrinsic resolution essentially defines the limit of resolution of the particular PET system.

The image resolution stays beyond the effect of the intrinsic resolution and depends on a number of different factors: the sampling of the PET system, the grid of the final image, and the amount of spatial smoothing during the reconstruction process.

Usually, in *in vivo* imaging the activity at any one point in the image provides a signal for that point and is a background noise for all other points. The signal to noise ratio is much worse with the distributed source, and a noise reduction in a system can only be achieved by increasing the total number of events accumulated during the measurement process or by spatial averaging or smoothing of the data. Because of dose limitations related to the patient, spatial averaging is usually required.

The purpose of spatial averaging is to provide an imaging in which the structures can be confidently identified and located for the purpose of defining the ROIs for quantitative measurements and qualitative interpretation of the image.

The resolution is also affected by patient motion during a scan. Often, to solve this problem, a restraint system, such as a head holder, is applied.

Partial volume effect

The partial volume effect occurs when the object of interest has at least one dimension smaller than the width of the LSF of the PET system. In this situation the object occupies only partially the sensitive volume of detectors. Consequently, in the reconstructed image the apparent activity concentration is underestimated.

Accidental and scatter coincidences

Accidental and scatter coincidences are to be considered the principle sources of the background noise in PET.

The accidental coincidences are related to the fact that two different events are detected at the same time. In fact, to establish that annihilation photons are in coincidence in a PET system, it is necessary to perform timing measurements for hundreds to thousands of combinations of detector pairs. The simplest method of accomplishing this task is with an overlap coincidence method. When a detector absorbs a photon, an electronic pulse is generated with a width, amplitude, and time relation to the absorption of the photon by the detector. Summing this pulse with all the pulses from the other detectors in the system that could be in coincidence with the first detector makes it possible to determine when a coincidence condition is satisfied. The accuracy of the timing depends on the property of the detector. In most PET systems, the detector is a scintillation crystal that absorbs the gamma ray. The energy of the gamma ray produces a number of excited states in the crystal, which produce a visible light and that light is detected by a photomultiplier. The excited states decay with half lives in the range of 0.5 to 300 nsec. Because of the decay time there is an inherent jitter between the actual annihilation event and the production of the timing signal. As a consequence, there is the probability that unrelated photons will accidentally produce timing signals that will overlap and produce accidental or random coincidences.

The scatter coincidences are related to the fact that the original photon can interact with other electrons presented in the adjacent space. These interactions will produce photons scattered in other directions different from the original ones.

In human tissue the annihilation photon has an interaction distance with a half value of about 7 cm. Most of the interactions are Compton scatters and most of those are scatters in the forward direction. Since most cross-sections of the human body are several multiply of 7 cm and very little energy is lost by a forward-scattered 511 keV, this means that a large fraction of the radiation striking the detectors in a PET system consists of scattered photons with energy similar to the original annihilation photon. Electronically, these events are indistinguishable from true events and they will be misplaced in the image.

3.3 Review of existing modelling methods

3.3.1 Introduction

Different methods have been proposed in the literature for modelling receptor-ligand interaction (Mintum *et al.*, 1984; Wong *et al.*, 1986; Perlmutter *et al.*, 1986; Lammertsma *et al.*, 1996; Lammertsma and Hume, 1996; Delforge *et. al.*, 1993). The general description of receptor-ligand interaction must account for the free-ligand penetration through the blood brain barrier (BBB) and the ligand receptor binding in the tissue. Many factors are involved in these processes: the BBB penetration, the presence of metabolites, the non specific binding, the affinity and selectivity of specific binding.

The most important parameters that describe the ligand-receptor interaction are the equilibrium dissociation constant (K_D) and the receptor concentration (B_{max}). A tracer experiment on the system in a steady state does not allow estimation of these parameters. Only an aggregated parameter can be estimated, the potential binding (BP) that equals the ratio between the receptor concentration and the equilibrium dissociation constant (B_{max}/K_D). Using this parameter an estimation of the percent receptor occupancy (%RO) can be obtained using the binding potential computed before (BP) and after treatment (BP') experiment as %RO=100*(BP-BP')/BP.

3.3.2 Description of models

The general description of ligand kinetics assumes three possible environments for the ligand. The first two are compartments representing the blood and brain tissue, the third compartment represents a chemical compartment environment, i.e. being bound to a specific binding site (see Figure 4). The ligand may enter via arterial blood flow into the blood compartment, then crosses the blood brain barrier into the tissue compartment by passive linear diffusion. Only in the tissue compartment is it free to react with drug binding sites according to classical kinetics: bimolecular association and unimolecular dissociation. Additionally, there are non specific, nonsaturable binding sites in both blood and tissue compartments.

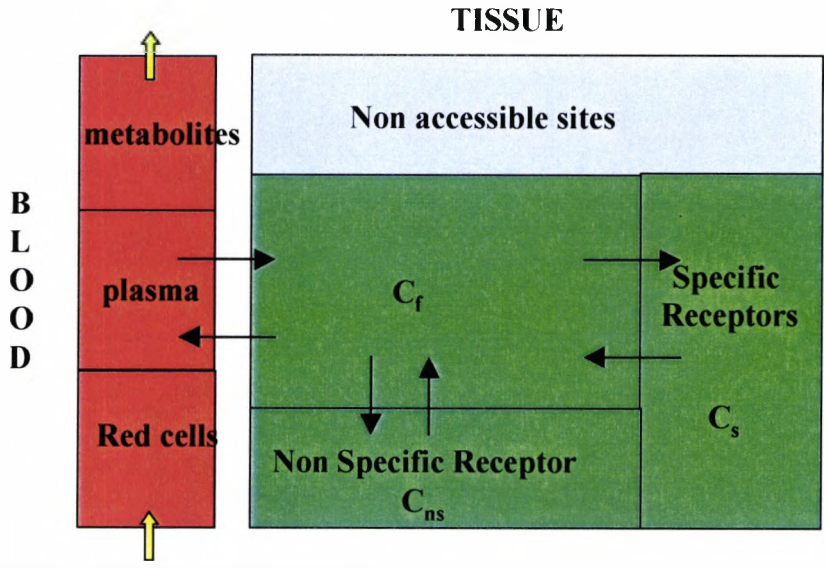

Fig. 4. Scheme of the ligand kinetic. The ligand may cross the blood brain barrier into the tissue compartment by passive linear diffusion. In the tissue compartment the ligand binds with specific sites and non specific sites. C_f is the concentration of the free ligand, C_s is the concentration of specifically bound ligand, and C_{ns} is the concentration of not specifically bound ligand.

As the rate of transport to tissue is not highly dependent on blood flow (Phelps *et al.*, 1986), it is possible to assume that the arterial plasma concentration of the ligand well approximates the vascular compartment near to the brain tissue.

According to these assumptions a four compartment model as illustrated in Figure 5 can be used to describe the ligand kinetics in *in vivo* experiments.

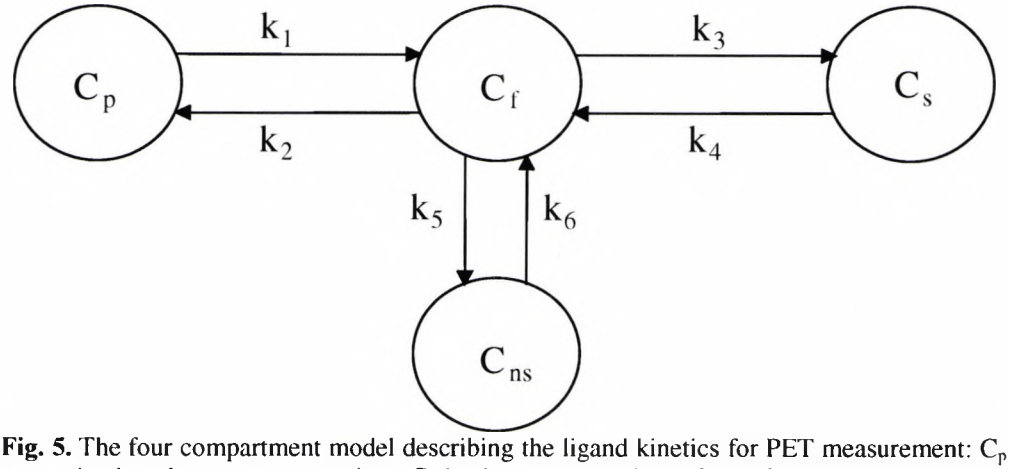

Fig. 5. The four compartment model describing the ligand kinetics for PET measurement: C_p is the plasma concentration, C_f is the concentration of the free ligand, C_s is the concentration of specifically bound ligand, and C_{ns} is the concentration of not specifically bound ligand.

The model equations are

$$\frac{dC_f(t)}{dt} = k_1 C_p(t) - k_2 C_f(t) - k_3 C_f(t) - k_5 C_f(t) + k_4 C_s(t) + k_6 C_{ns}(t) \qquad (22)$$

$$\frac{dC_s(t)}{dt} = k_3 C_f(t) - k_4 C_s(t) \qquad (23)$$

$$\frac{dC_{ns}(t)}{dt} = k_5 C_f(t) - k_6 C_{ns}(t) \qquad (24)$$

where C_p ($\mu Ci \cdot ml^{-1}$) is the plasma concentration, C_f ($\mu Ci \cdot ml^{-1}$) is the concentration of the free ligand, C_s ($\mu Ci \cdot ml^{-1}$) is the concentration of specifically bound ligand, and C_{ns} ($\mu Ci \cdot ml^{-1}$) is the concentration of not specifically bound ligand. The symbol k_1 represents the transfer rate from plasma to the free ligand compartment ($ml_{blood}/ml_{tissue} \cdot min^{-1}$), k_2 is the rate constant from the free ligand to the plasma compartment (min^{-1}). The interaction between the ligand and specific receptor compartments is described by k_3 and k_4, k_3 is the rate from the free ligand to the specifically bound compartment (min^{-1}), k_4 is the rate from the specifically bound ligand to the free ligand compartment (min^{-1}). Finally k_5 (min^{-1}) and k_6 (min^{-1}) are, respectively, the rates from free to non specifically bound compartment and vice versa.

Bimolecular association and unimolecular dissociation describe the interaction between ligand and specific receptor sites as shown in Equation 1. The dynamic relationship between free ligand and specifically bound ligand is described by

$$\frac{dC_s}{dt}(t) = k_{on} C_r(t) \cdot C_f(t) - k_{off} C_s(t) \qquad (25)$$

where $C_r(t)$ represents the available receptors for the specific binding. According to equations 23-24 it is possible to derive that

$$k_3(t) = k_{on} C_r(t) \qquad (26)$$

and

$$k_4=k_{off} \tag{27}$$

with $k_3(t)$ being a time dependent variable. All other rates can be assumed time invariant.

Since the quantity of radiolabelled ligand used in PET experiments occupies only a very low number of the specific receptor sites, the concentration of the receptor occupied by the ligand can be considered negligible compared with the available receptors ($C_s << C_r$). Then, the available receptors can be approximated by the total receptor density,

$$B_{max} = C_s+C_r \cong C_r \tag{28}$$

Then, it follows that

$$k_3= k_{on}\, B_{max} \tag{29}$$

and in such a case a constant rate k_3 is obtained. According to these assumptions the system is not perturbed during the PET experiment.

The PET measurement in ROI takes into account both vascular and tissue components (see Figure 6). The following measurement equation applies

$$C_t(t) = (1-V_b)(C_f(t)+C_{ns}(t)+C_s(t))+V_bC_b(t) \tag{30}$$

where $C_t(t)$ represents the radiolabelled concentration in ROI, V_b the fractional vascular component (unitless) and $C_b(t)$ the radiolabelled concentration in the blood.

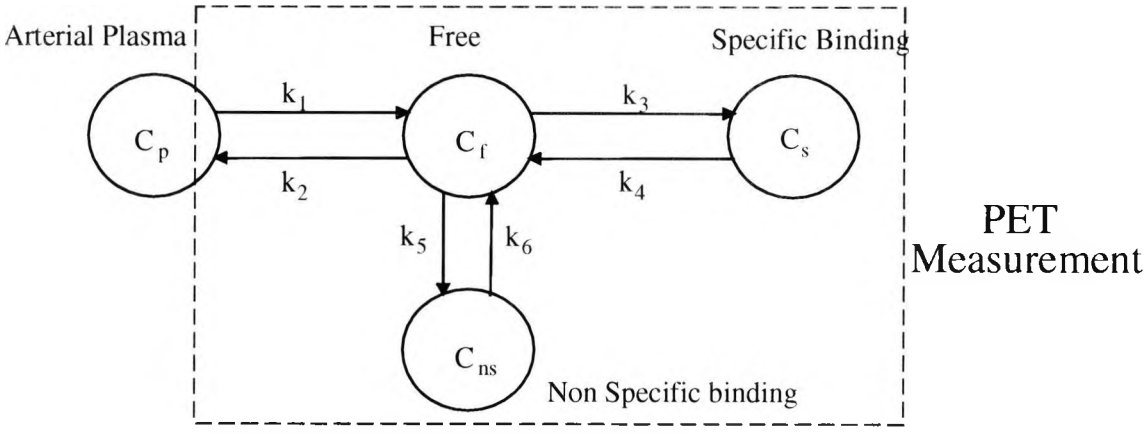

Fig. 6. PET measurement includes a tissue and a vascular component.

The parameters of the model are V_b, k_1, k_2, k_3, k_4, k_5 and k_6. Usually, to obtain a better precision of parameter estimates, the value of V_b is a priori fixed (its standard value is about 5%).

Non-specific binding is assumed to be reversible and to have a fast binding and release rates. According to this assumption the equilibrium between the two compartments is quickly achieved, and non-specific binding sites and the free ligand in the tissue can be considered to be positioned in a common compartment. The simplified model is illustrated in Figure 7.

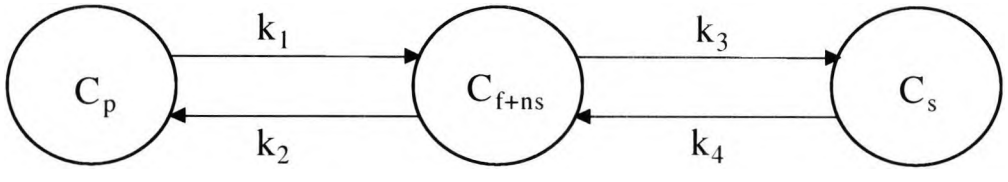

Fig. 7. The three compartment model, C_{f+ns} represents the free plus non specifically bound ligand compartment.

The following equations describe the simplified model

$$\frac{dC_{f+ns}(t)}{dt} = k_1 C_P(t) - k_2 C_{f+ns}(t) - k_3 C_{f+ns}(t) + k_4 C_s(t) \qquad (31)$$

$$\frac{dC_s(t)}{dt} = k_3 C_{f+ns}(t) - k_4 C_s(t) \qquad (32)$$

where C_{f+ns} represents the non specifically bound plus free ligand compartment. In this model the estimated parameters are k_1, k_2, k_3, k_4 and V_b.

In this case the PET measurement is

$$C_t(t) = (1 - V_b)(C_{f+ns}(t) + C_s(t)) + V_b C_b(t) \tag{33}$$

a PET experiment which using only a tracer concentration does not enable the estimation of the *in vivo* equilibrium dissociation constant ($K_D=k_{off}/k_{on}$) and the receptor density (B_{max}). However, the binding potential (BP) defined as the ratio between the receptor density and affinity can be estimated.

$$BP = \frac{B_{max}}{K_D} = \frac{B_{max} \cdot k_{on}}{k_{off}} = \frac{k_3}{k_4} \tag{34}$$

BP is proportional to the available receptors and the ligand-receptor affinity. This variable reflects the capacity of the tissue for ligand-binding site interaction. In a tracer experiment the available receptors for the binding coincide with the receptor density.

In the models presented above, the parameter identification requires the presence of both the PET measurement and the arterial plasma concentration (the input of the system). Since the arterial blood sampling is to be considered invasive, different approaches that avoid arterial blood samples were evaluated. An interesting alternative approach for the receptor-ligand model (Lammertsma *et al.* 1996) consists of using a region void of specific receptor as a reference site (see Figure 8).

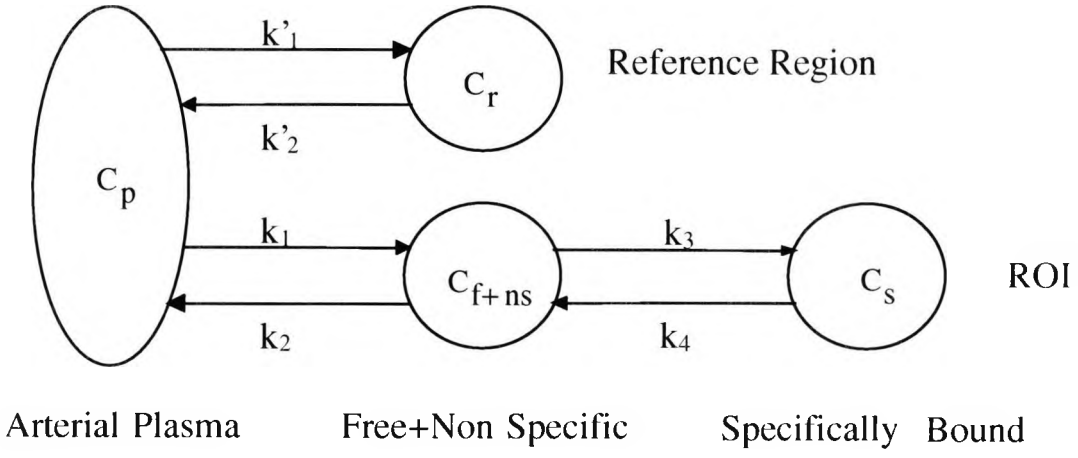

Fig. 8. The Reference Tissue Model. The upper part is related to the region void of specific receptor (reference region), while the lower part is related to the region of interest (ROI).

The differential equations governing this model are

$$\frac{dC_r(t)}{dt} = k_1' C_p(t) - k_2' C_r(t) \tag{35}$$

$$\frac{dC_{f+ns}(t)}{dt} = k_1 C_p(t) - k_2 C_{f+ns}(t) - k_3 C_{f+ns}(t) + k_4 C_s(t) \tag{36}$$

$$\frac{dC_s(t)}{dt} = k_3 C_{f+ns}(t) - k_4 C_s(t) \tag{37}$$

where C_p is the plasma concentration, C_r is the concentration in the reference region, C_{f+ns} is the concentration of the free plus not specifically bound ligand, and C_s is the concentration of specifically bound ligand; k_1 is the transfer rate from plasma to the free plus non specific bound ligand compartment ($ml_{blood}/ml_{tissue} \cdot min^{-1}$), k_2 is the rate constant from the free plus non specific bound ligand to the plasma compartment (min^{-1}), k_3 is the rate constant from the free plus non specific bound ligand to the specific bound compartment (min^{-1}), k_4 is the rate constant from the specific bound to the free plus non specific bound ligand compartment (min^{-1}), k'_1 is the transfer rate from the plasma to the reference compartment ($ml_{blood}/ml_{tissue} \cdot min^{-1}$), and k'_2 is the rate constant from the reference to the plasma compartment (min^{-1}).

We assume that the free and non-specifically bound ligand distribution volume (DV) are the same in the reference region and in the region of interest. DV represents the tissue to plasma partition coefficient of the labelled ligand concentration and its dimension is ml_{blood}/ml_{tissue} (unitless). At steady state the DV is equal to

$$DV = \frac{C_r}{C_p} = \frac{k_1}{k_2}$$

for the reference region and

$$DV = \frac{C_{f+ns}}{C_p} = \frac{k_1}{k_2}$$

for the ROI. From the assumption of the same distribution volume of the non-specifically bound ligand for the reference region and the region of interest the following equalities apply

$$DV = \frac{k_1}{k_2} = \frac{k_1'}{k_2'}. \qquad (38)$$

We define R as ratio between k_1 and k'_1

$$R = \frac{k_1}{k_1'} \qquad (39)$$

From Equations 35 to 37 it is possible to derive a relationship between $C_t(t)$ (where $C_t = C_{f+ns} + C_s$) and $C_r(t)$

$$C_t(t) = R \cdot \left[C_r(t) + a \cdot C_r(t) \otimes \exp(-c \cdot t) + b \cdot C_r(t) \otimes \exp(-d \cdot t)\right] \qquad (40)$$

where a, b, c, d are model parameters containing k_2, k_3, k_4, and R, and $\otimes$ is the convolution operator.

In this approach, the vascular component in the reference region and in the region of interest is not considered. The measurement equation C_t contains only the tissue component.

The parameters estimated by this model are: R, k_2, k_3, k_4. BP is derived as the ratio k_3 over k_4.

A simplified version of the Reference Tissue Model has been proposed (Lammertsma and Hume, 1996) to obtain an improved precision of parameter estimates.

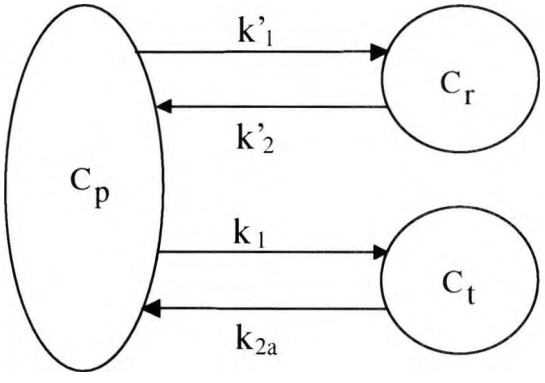

Fig. 9. The Simplified Reference Tissue Model

In this model (Figure 9) a single compartment description is used for the free and bound ligand in the tissue ($C_t(t)= C_s(t)+ C_{f+ns}(t)$). The model equations are

$$\frac{dC_t(t)}{dt} = k_1 C_p(t) - k_{2a} C_t(t) \tag{41}$$

where k_{2a} is obtain as

$$k_{2a} = \frac{k_2}{(1+BP)} \tag{42}$$

From the equilibrium conditions it follows that

$$C_t = C_{f+ns} + C_s \tag{43}$$

and at equilibrium

$$C_s = \frac{k_3}{k_4} C_{f+ns} \text{ and } C_{f+ns} = \frac{k_1}{k_2} C_p \tag{44}$$

The total distribution volume is

$$DV_T = \frac{C_t}{C_p} = \frac{k_1}{k_{2a}} = \frac{k_1}{k_2}(1+\frac{k_3}{k_4}) \tag{45}$$

where in the second part of the equation the distribution volume of the original model is introduced. From Equation 45 and 34 the expression for k_{2a} given in Equation 42 is derived.

From Equations 35 and 41 the following expression can be derived

$$C_t(t) = R\,C_r(t) + \left[k_2 - \frac{R\,k_2}{1+BP}\right] C_r(t) \otimes \exp\left[\frac{-k_2 t}{1+BP}\right] \qquad (46)$$

where $C_t(t)$ and $C_r(t)$ are the tracer concentrations in the region of interest and in the reference tissue, respectively. R, k_2, and BP are parameters to be estimated.

3.3.3 Receptor occupancy

To investigate the percentage of receptors occupied by an endogenous compound, an experiment with a non-negligible quantity of unlabelled ligand has to be performed. When an unlabelled compound is injected, the condition of the system will change and the available receptors will be less than the total receptor density B_{max}.

According to the Equation 26, $k_3(t)$ depends on the number of available receptors $C_a(t)$. After an administration of unlabelled ligand the total receptor concentration can be derived as

$$B_{max} = C_s(t) + C_a(t) + B(t) \cong C_a(t) + B(t) \qquad (47)$$

where B(t) represents the receptors occupied by the unlabelled ligand. The receptor occupied by the labelled compound is always considered negligible ($C_s << C_a$), but the unlabelled compound occupies a non-negligible number of receptor sites. Consequently the association rate is described by a time dependent relationship

$$k_3(t) = k_{on} C_a(t) = k_{on}(B_{max} - B(t)) \qquad (48)$$

However, if a constant value of occupied receptor sites (B) is assumed during the PET experiment, the available receptors can also be considered constant

$$C_a = B_{max} - B \tag{49}$$

and then

$$k_3 = k_{on}\,(B_{max} - B). \tag{50}$$

If we perform a tracer experiment at baseline followed by a tracer experiment after an unlabelled compound injection, it is possible to calculate the receptor occupancy (RO). From the tracer experiment at baseline (all receptors are available), it follows that

$$BP = \frac{B_{\max}}{K_D} \tag{51}$$

and from the PET experiment after the administration of the unlabelled compound it follows that

$$BP' = \frac{B_{\max} - B}{K_D} \tag{52}$$

Then, from Equations 51 and 52, the percentage of receptor occupied can be calculated as

$$\%RO = \frac{BP - BP'}{BP} = \frac{B}{B_{\max}} \tag{53}$$

3.3.4 Time varying model

In all models described above the information about affinity and receptor concentration cannot be obtained. Performing a sufficient number of PET experiments

after the administration of increasing doses of unlabelled ligand should allow the estimation of B_{max} and K_D with the Scatchard analysis.

It is possible to estimate both B_{max} and K_D using a complex protocol during a PET experiment (Delforge *et. al*, 1990; Delforge *et. al*, 1993). This involves achieving different values of receptor occupancy during the same PET experiment. A displacement (an injection of unlabeled ligand) and a co-injection (a simultaneous injection of labelled and unlabelled ligand) experiments have to be performed during the same PET scan.

Two identical models for the labelled and unlabelled ligand describe the experiment (see Figure 10).

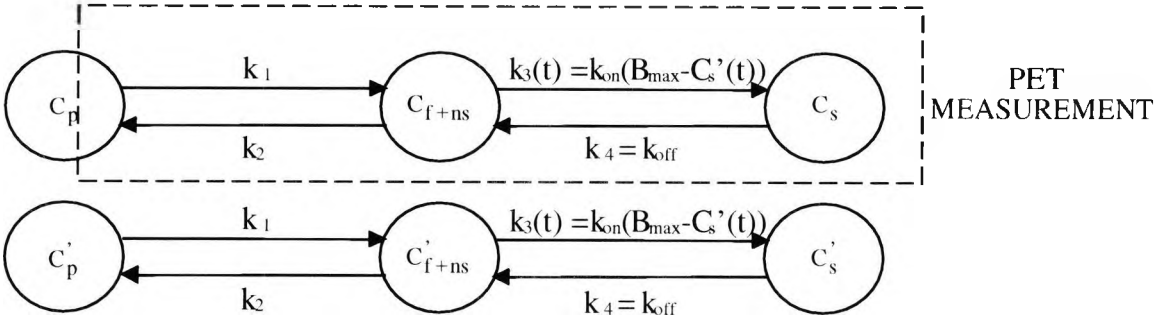

Fig. 10. The time varying model describing both labelled and unlabelled ligand kinetics. The upper part describes the labelled ligand kinetics detected by the PET system. The lower part describes the unlabelled ligand kinetics.

We assume that the kinetics of the unlabelled and labelled ligand are indistinguishable. Then model equations describing both labelled and unlabelled kinetics are

$$\frac{dC_{f+ns}(t)}{dt} = k_1 C_P(t) - k_2 C_{f+ns}(t) - k_3(t) \cdot C_{f+ns}(t) + k_4 C_s(t) \qquad (54)$$

$$\frac{dC_s(t)}{dt} = k_3(t) \cdot C_{f+ns}(t) - k_4 C_s(t) \qquad (55)$$

$$\frac{dC'_{f+ns}(t)}{dt} = k_1 C'_p(t) - k_2 C'_{f+ns}(t) - k_3(t) \cdot C'_{f+ns}(t) + k_4 C'_s(t) \quad (56)$$

$$\frac{dC'_s(t)}{dt} = k_3(t) \cdot C'_{f+ns}(t) - k_4 C'_s(t) \quad (57)$$

where $C_s(t)$ is the concentration of the specifically bound labelled ligand, and $C'_s(t)$ is the concentration of the specifically bound unlabelled ligand, C_{f+ns} is the concentration of free and non specifically bound labelled ligand, C'_{f+ns} is the concentration of free and non specifically bound unlabelled ligand, $C_p(t)$ is the plasma labelled ligand concentration and $C'_p(t)$ is the plasma unlabelled ligand concentration.

The key feature is in the time-varying parameter $k_3(t)$

$$k_3(t) = k_{on}(B_{max} - C_s(t) - C'_s(t)) \quad (58)$$

The available number of receptors $C_a(t)$ is equal to

$$C_a(t) = B_{max} - C_s(t) - C'_s(t) \quad (59)$$

and since $C_s(t)$ can be considered negligible, the following relationship for $k_3(t)$ is obtained

$$k_3(t) = k_{on}(B_{max} - C'_s(t)) \quad (60)$$

This non-linear model is a priori identifiable from the labelled ligand PET data and the measured plasma concentration of non-metabolised labelled ligand $C'_p(t)$. The parameters to be estimated are k_1, k_2, k_{on}, B_{max}, and k_4.

The plasma concentration of non-metabolised labelled ligand $C'_p(t)$ can be obtained directly from $C_p(t)$

$$C_p^*(t) = \frac{D}{d} C_p(t) \qquad (61)$$

where D is the dose of the unlabelled compound, and d is the dose of the labelled compound.

3.4 PK/PD modelling

From a drug development perspective the principle aim of PET studies is to estimate the percentage of occupied receptor in order to link this information with a therapeutic effect (Aboagye et al., 2001). The receptor occupancy could be considered in this case a surrogate marker of therapeutic effectiveness. Since it is feasible to perform a PET study only with a limited number of subjects it is desirable to link the pharmacokinetic information (the drug plasma concentration) to RO as a function of the plasma drug concentration. In this way, it is possible to understand the link between the plasma concentration of the compound and the blocking effect of the drug at the site of action. This represents a PK/PD modelling approach since using the estimated PK and PD parameters (in this case RO) a link between the plasma concentration and the receptor occupancy can be established.

A range of models can be formulated with the aim to describe accurately the relationship between the plasma concentration and the receptor occupancy.

3.4.1 The linear model

The simplest model assumes a proportional relationship between the concentration of the drug and the pharmacological response

$$E = S \cdot C + E_0 \qquad (62)$$

where E is the effect, C is the drug concentration, S is the rate of change in response with a given change in the concentration, and E_0 is the effect without the presence of the drug.

This model does not consider a maximal response. Another limitation of this model is that for most drugs the concentration-effect relation is not linear.

3.4.2 The E_{max} model

The equation for this model describes a hyperbolic concentration-effect relationship

$$E = \frac{E_{\max} \cdot C}{EC_{50} + C} \tag{63}$$

where E and C are as defined above, E_{max} is the maximum drug effect, and EC_{50} is the concentration giving 50% of the maximal effect. Unlike the linear model, this model predicts a maximal response.

An alternative model with the same structure is the inhibitory E_{max} model. In this case E_0 is the effect when no drug is present, and E_{max} is the maximum reduction in response.

$$E = E_0\left(1 - \frac{C}{EC_{50} + C}\right) \tag{64}$$

3.4.3 The sigmoid E_{max} model

Often the concentration-effect curves take on a more pronounced S-shape not adequately described by an inhibitor E_{max} model. A model adapting the Hill equation is usually introduced to improve data fitting (Keller *et al.*, 2002). The model involves the use of an exponent, a, which determinates the slope of the curve. The model collapses to an E_{max} model when the exponent has a value of 1

$$E = \frac{E_{\max} \cdot C^a}{EC_{50}{}^a + C^a} \tag{65}$$

Similar to the E_{max} model, an inhibitory response can be incorporated into this model.

3.5 Parameter estimation approaches

Three different parameter estimation approaches were used in this thesis. The first approach uses the standard weighted non-linear least squares methodology as utilised by almost all published studies in the PET field. With this approach, data from PET scans are considered separately and are analysed independently. The inter- and intra-subject variability is not considered. When problems of convergence occurred a Bayesian approach was used by introducing an a priori information. Finally the non-linear mixed effect model was used in order to consider both fixed effects and random effects due to inter- and intra-subject variability.

The non-linear mixed effect approach has been described in numerous publications (Sheiner and Beal, 1980; Sheiner and Beal, 1983; Sheiner and Ludden, 1992). In this thesis, the first order approximation method (implemented in NONMEM) has been used.

3.5.1 Fixed effect approach

The model parameters can be estimated by weighted non-linear least squares. The cost function is

$$\mathrm{WRSS}(\mathbf{p}) = \sum_{i}^{N} w_i (y_i - \hat{y}_i(\mathbf{p}))^2 \qquad (66)$$

where y_i is the i-th data, w_i is the weight associated with y_i, N the number of the data points, and the vector **p** represents the model parameters.

Measurement error was assumed to be multiplicative, uncorellated, Gaussian, with zero mean, and a variance described as follows

$$\sigma^2(t_i) = v\frac{y_i}{t_i - t_{i-1}} \qquad (67)$$

where $(t_i - t_{i-1})$ is the scan duration and v is a scale factor estimated a posteriori from the fitting of the data. In fact, the variance of the PET measurement is assumed to be a non-homogenous Poisson process according to (Mazoyer *et al.*, 1986). Then, weights were chosen optimally as:

$$w_i = \frac{t_i - t_{i-1}}{y_i} \qquad (68)$$

In this way the weight is proportional to the scan duration and inversely proportional to the value of tissue concentration.

The precision of the estimates was calculated from the covariance matrix which is given by

$$\mathrm{cov}(\hat{\mathbf{p}}) = v \cdot \mathbf{M}^{-1} \qquad (69)$$

where M is the Fisher Information matrix, and $\hat{\mathbf{p}}$ is the vector of the estimated parameters. The standard deviation of the j-th parameter estimate is given by the square root of the j-th diagonal element of the covariance matrix. The smaller value of the standard deviation the more precise is the parameter estimate.

3.5.2 Bayesian approach

The least square estimator returns a parameter vector, or a point estimate. An alternative approach is the Bayesian estimator in which a parameter probability distribution is considered.

Formally, the set of individual parameter values is regarded as a set of random variables characterised by a priori probability distribution. This approach involves the

use of the Bayes' formula to adjust the prior probability distribution of the parameters in light of measurements, and thus arrive at a revised posterior distribution. The posterior distribution could have a different mode than the prior distribution. The updated probability, the a posteriori probability $\pi(\mathbf{p})$, is obtained according to the Bayes' theorem

$$\pi(\boldsymbol{p}) = p(\boldsymbol{p} \mid \boldsymbol{y}) = \frac{p(\boldsymbol{y} \mid \boldsymbol{p}) \cdot p(\boldsymbol{p})}{p(\boldsymbol{y})} \tag{70}$$

where $\boldsymbol{y}$ is the vector of measurements, $p(\boldsymbol{p})$ is the prior probability of parameters, $p(\boldsymbol{y})$ is the prior probability of measurements, and $p(\boldsymbol{y}|\boldsymbol{p})$ is the conditional probability of measurements given parameters.

To apply the Bayes' theorem, a form for the a priori probability distribution must be assumed. Usually a normal distribution is assumed. In this case an expression for the posterior distribution of the parameters can be written and the mode of this distribution can be found by a numerical minimisation.

In the Bayesian context, one of the most utilised estimator is the Maximum a Posteriori estimator (implemented also in SAAMII package). This estimator assumes that the prior distribution of parameters and the conditional distribution of the observed measurements are both normal, and that the different parameters and the different data measurements are independent, then the mode of the posterior distribution of parameters minimises the expression

$$\sum_{i}^{N} \frac{(y_i - \hat{y}_i(\mathbf{p}))^2}{\sigma_i^2} + \sum_{i}^{M} \frac{(p_i - \hat{p}_i)^2}{\sigma_{p_i}^2} \tag{71}$$

where y_i is the i-th measurement, p_i is the i-th parameter in the parameter set, $\hat{y}_i$ is the i-th predicted observation, $\hat{p}_i$ is the mean value of prior distribution of the i-th parameter, $\sigma_{p_i}^2$ is the prior variance, and σ_i^2 is the error variance of the i-th

measurement. In this case, the second term in (71) is added to the objective function (66).

When N is very large, abundant measurement information is available and the first term of (71) dominates the expression. Prior information is ignored and the observations alone determine the mode. The expression (71) is therefore minimised by those parameter values that minimise the weighted sum of squares (66). When N is moderate, the expression (71) weights squared deviations of parameters and measurements from their expectations, with weights equal to the inverted variances. This weighting reduces all deviations from expectations to a common probability scale taking into account both measurements and information about prior parameter values.

3.5.3 Non-linear mixed effect approach

In this approach the population characteristics are defined by two moments of the distribution of the vector parameter p, the mean values (μ) or fixed effects, and the elements of the variance covariance matrix (Ω) that characterise random effects (η).

Consider the model for a given observation in a given individual

$$y_{ij} = f_{ij}(\mu + \eta_i) + \varepsilon_{ij} \qquad \text{for i} = 1,\ldots,n_j,\ j = 1,\ldots\ldots,N \qquad (72)$$

where $\mu + \eta_j = p$. The population mean (μ) is the fixed effect, and η_j is the (random) individual shift from the mean for individual j. By definition, the random effects η_j have a zero mean and a variance Ω; ε_{ij} is the additive error.

The extended least squares criterion used in NONMEM with respect to parameters μ and Ω is

$$O(\mu,\Omega) = \sum_{i=1}^{N}\left[(y_i - E(y_i))\cdot v_i^{-1}\cdot(y_i - E(y_i)) + \ln\det v_i\right] \qquad (73)$$

where $v_i = \mathrm{Var}(y_i)$.

Because of the non-linear dependence of observations on parameters through the vector-valued function f_i, a closed form solution for μ and Ω can be obtained only for specific kinetic models. A general (approximate) solution is provided by the first order method.

To derive the moments of y_{ij}, in (Beal and Sheiner, 1992) it is suggested linearising the model using the first-order Taylor series expansion around the random effect η_j evaluated at the expected value (i.e., zero). Then,

$$y_{ij} = f_{ij}(\mu) + \frac{\partial f_{ij}^{t}(\mu)}{\partial \eta_J} \cdot \eta_j + \xi_{ij} + \varepsilon_{ij} \tag{74}$$

where the partial derivatives are denoted G_{ij}, and ξ_{ij} is the approximation error between the true value and the forecast of the linearised version of the model.

In the vector notation, for subject j, equation (74) translates into

$$y_j = f_j(\mu) + G_j(\mu) \cdot \eta_j + \xi_j + \varepsilon_j \tag{75}$$

where $G_j(\mu)$ is the n_j x p Jacobian matrix whose ith line contains the p-vector G_{ij} and ξ_j is the n_j-vector of the approximation errors. In this case, the expected value $\mathrm{E}(y_i)$ for the jth subject is

$$E(y_j) = f_j(\mu) + G_j(\mu) \cdot E(\eta_j) + E(\xi_j) + E(\varepsilon_j) \tag{76}$$

Because $\mathrm{E}(\eta_j) = 0$ by definition and assuming $\mathrm{E}(\varepsilon_j)$ equal to zero, we obtain

$$E(y_j) = f_j(\mu) + E(\xi_j) \tag{77}$$

According to the previous equation and provided that the approximation error has a zero mean (i.e. $E(\xi_j) = 0$), the expected value for the profile of subject j is the profile calculated according to the same equation f_j for the population mean p.

The variance-covariance matrix of y_j, $Var(y_j)$, can be derived in a similar way. Because a variance of a linear combination of random variables is a linear combination of the variances and covariances of its constituent variables, assuming that η_j and ε_j are independent and not considering all terms including ξ_j in the variance calculations, $Var(y_j)$ is given by

$$Var(y_j) = G_j(\mu) \cdot \Omega \cdot G_j(\mu)' + Var(\varepsilon_j) \qquad (78)$$

Any assumptions about the variance of the residual error ε_j can be easily incorporated.

3.5.4 Model selection

The evaluation of models was based on the weighted residual plots, the precision of parameter estimates, the comparison of the model predicted vs observed values.

The statistical criteria used in model selection (Ludden *et al.*, 1994) were

- Akaike Information Criterion

$$AIC = N \ln WSS + 2p \qquad (79)$$

where N is the number of data points, p is the number of model parameters, and WSS is the sum of squared weighted residuals;

- F-test (used only for the comparison between hierarchical models, the Reference Tissue Model and the Irreversible model)

$$F = \frac{WSS_j - WSS_k}{WSS_k} \frac{df_k}{df_j - df_k} \cdot with \cdot df_j > df_k \qquad (80)$$

where df = N-p is the degree of freedom, j denotes the reduced model, and k the full model.

4 NK1 PLAN

4.1 Background

The tachykinins are a conserved family of peptide neurotransmitters subdivided into three groups, substance P, neurokinin A, and neurokinin B. Tachykinin neurotransmitters mediate the release of intracellular calcium via binding to a group of conserved transmembrane neurokinin receptors named NK_1, NK_2 and NK_3 (Saria, 1999). The tissue distribution of these receptors varies between species and tissue types. As neurotransmitter dysfunction in the central nervous system (CNS) is believed to be the basis of many neurological diseases (Parkinson's disease, Altzheimers disease, depression and anxiety) compounds that can modulate the effects of these intercellular signals could be of importance for the development of new therapeutic interventions (Rupniak and Kramer, 1999).

Substance P (SP) is a member of the neurokinin family and is one of the well-established neuromodulators and neurotransmitters in the mammalian CNS. It is present at high concentrations in the striatum, brainstem, spinal cord and cortex.

Neurokinin receptors have been pharmacologically classified in NK1, NK2 and NK3 receptors and SP exerts its pleiotropic role by binding preferentially to the NK1 receptor. The latter is a G-protein coupled receptor and, when activated by the agonist, induces intracellular phospholipase C (PLC) activation and intracellular increase of calcium concentration through the release from internal stores.

The evidence for a role of SP in the regulation of mood is not conclusive and still lacks clear understanding of the mechanism of action of NK1 antagonists as antidepressants (Nutt, 1998). It is suggested that SP is released centrally following traumatic or noxious stimulation. Patients with mental disorders complain of 'emotional pain', a state in which the type of effect caused by trauma is expressed but devoid of the sensation of pain. Many patients suffering from depression, anxiety or related disorders reports histories of adult or childhood trauma. Thus, the hyperactivity

in SP neurotransmission might contribute to or be the source of anxiety, fear, and emotional pain that accompany affective disorders. As described above, SP and NK1 receptors are widely expressed throughout the fear-processing pathways of the brain (amygdala, septum, hyppocampus, hypothalamus and periaqueductal gray). Neurochemical studies showed changes in SP levels in discrete brain regions and internalisation of NK1 receptor in guinea pig amigdala in response to stressful stimuli such as immobilization stress. Interestingly, pretreatment with brain penetrating NK1 antagonists could inhibit neuronal response to stress and reduce receptor endocytosis.

Activation of the pathways innervated by SP, by direct central injection of agonist, produces a range of defensive behavioral and cardiovascular changes in animals. These include conditioned place aversion, anxiogenic effects, potentiation of the acoustic startle response, distress vocalisation, escape behaviors and cardiovascular changes resembling the defense response to threatening stimuli. Consistently, NK1 antagonists have been shown to be anxiolytic in the social interaction test in rat, in the acoustic startle response test, and the mouse light-dark box model.

However, these studies do not demonstrate that SP is released in response to psychological stress, or more importantly, if the blockade of NK1 receptors alter behavioral stress response. Recent studies showed the ability of NK1 antagonists to block vocalisation elicited by transient maternal separation of guinea pig pups. This is a pharmacological effect observed also with clinically effective antidepressants and anxiolytic agents.

The aforementioned series of pre-clinical experiments on psychological stress responses probably led to test the selective NK1 antagonist, MK-869 (300mg/day) in a six-week clinical trial in depressed patients with anxiety (Kramer *et al.*, 1998). The effect of MK-869 was comparable to that of paroxetine (20mg/day) as a 4.3 point difference (mean change from base line to six weeks) between MK-869 and placebo in the total Hamilton depression score. MK-869 was well tolerated since fewer side effects (insomnia, sexual dysfunction, and gastrointestinal effects) were observed in the MK-869 treated group with respect to paroxetine group. Also the percentage of

discontinuation was lower in the MK-869 group with respect to the paroxetine group. Therefore, it was concluded that MK-869 demonstrated a significant antidepressant activity without the classical side effect of SSRIs. Interestingly, MK-869 also showed anxiolytic activity in the population of depressed patients utilised for the study, an effect that was still improving after six weeks of treatment.

In a recent report (Kramer *et al*, 1998) the MK-869 dose (300 mg) was found active in healthy subjects. As a result, 24h after administration of the last dose, the binding at the striatum level of a labelled NK1 antagonist was markedly inhibited (> 90%). Accordingly, a sufficient (and likely) therapeutic effect is expected to be achieved when receptor occupancy in relevant brain areas is maintained over 90% during 24 hours in a chronic treatment.

4.2 Rationale of PET studies

GR205171 is a potent and selective neurokinin 1 (NK_1) receptor antagonist developed by GlaxoSmithKline as a potentially effective compound in neurological diseases. A set of positron emission tomography studies has been planned to investigate the GR205171 penetration properties of the blood brain barrier in monkey and humans and the uptake in brain with particular interest to striatum, an area predicted to contain NK_1 receptors, and furthermore to understand the relationship between the monkey and human brain results. The compound was labelled with ^{11}C in the Uppsala University PET Centre and all the PET studies were conducted in this centre. The protocol design for monkey and human was different. In the monkey study two different experiments were performed administering GR205171 by IV route: a single tracer experiment (baseline) and one with tracer injected after a treatment with an unlabelled ligand injection experiment. Two different studies were conducted in human: the first using increasing IV doses and the second using oral administration with different dosage regimens. The protocol design for human study was more complex than the one used for monkey. It was composed from a baseline experiment, a co-injection experiment, and a series of tracer experiments following the unlabelled ligand injection.

The aim of this study was to estimate directly the B_{max} and K_D using a non-linear model approach. Furthermore, the time varying receptor occupancy after different IV doses was investigated.

The oral PET study was performed to estimate the receptor occupancy after an oral administration of the unlabeled compound and consequently to investigate the effect of bioavailability on receptor occupancy.

In both human studies, the relationship between the plasma concentration of the unlabeled compound and the receptor occupancy was investigated.

5 A PET MODELLING STUDY IN MONKEY

5.1 Introduction

The purpose of this study is to study the ligand-receptor interaction between GR205171 and neurokinin 1 (NK1) receptor in the monkey brain. GR205171 is a high affinity and selective NK1-receptor antagonist. The compound was labelled with ^{11}C in the Uppsala University PET Centre (Bergstom *et al.*,2000). Two different experimental protocols were performed, a single tracer experiment (baseline) and one with tracer injected after a pre-treatment with an unlabelled ligand injection experiment.

Since arterial tracer concentrations corrected for metabolites were not available, we applied a modelling approach that uses a region void of specific receptors as the reference region (Lammertsma *et al.*, 1996; Lammertsma and Hume, 1996). Since cerebellum is usually considered a region without NK-1 receptors we used this region as the reference region.

We considered two different scenarios. In the first we assumed that it is possible to estimate both the association (k_3) and dissociation (k_4) rate constants of ligand-receptor interaction. The Reference (Lammertsma *et al.*,1996) and the Simplified Reference (Lammertsma and Hume, 1996) Tissue Models were used.

In the second case it was assumed that the dissociation rate during the PET experiments was negligible and a new modified version of the Reference Tissue Model that does not take into account the dissociation rate constant (k_4) was introduced. In this last case we consider an irreversible binding.

Only the first two but not the third model allow the estimation of BP. In theory all these models allow the estimation of receptor occupancy.

Our first objective was to assess which of the three models was the most plausible to interpret the experimental data. Then, we estimated the receptor occupancy.

5.2 Theory and methods

5.2.1 Data

The PET studies were performed in the Uppsala PET Centre (Bergstom *et al.*, 2000). GR205171 was labelled with ^{11}C. The experiments were done in 5 rhesus monkeys weighting between 7 and 12 kg. The monkeys were anaesthetised during the experimental period. Two different experiments were done in each monkey: a tracer injection experiment and an unlabelled ligand injection followed by a tracer injection (pre-treatment tracer experiment). 15 sequential PET scans (1-10 min long) were acquired and then reconstructed.

The tracer dose was given as a rapid bolus injection. The various doses of the cold injection were given as a 5 min intravenous infusion. In subject #528, the cold injection dose was 0.1 mg/kg, in subjects #297, #259 and #636 two different doses were used (0.05 mg/kg and 0.5 mg/kg), and finally in subject #779 the injected dose was 1mg/kg. The modelling analysis was not performed for subject #528, because of data problems.

The time activity curves are expressed in SUV (standardised uptake value), which equals the radioactivity concentration divided by the dose of injected radioactivity normalised to body weight (normalised dose radioactivity).

The monkey data supplied by the Uppsala University PET Centre belong to two different regions of interest (ROI): cerebellum which is considered a region without specific NK1 receptors and striatum which is considered a large uptake region from previous studies.

In Figure 11A, the mean tracer data of 4 subjects (#297, #259, #636 and #779) of the tracer experiment are shown. In Figure 11B, the mean tracer data of the pre-treatment

experiment are shown, respectively, for the 0.5 mg/kg and 0.05 mg/kg cold dose (#297, #259 and #636). In Figure 11C, the tracer data of subject #779 of the pre-treatment experiment for 1 mg/kg cold dose are shown.

A. Mean data for 4 subjects (#297, #259, #636, #779). Tracer only experiment.

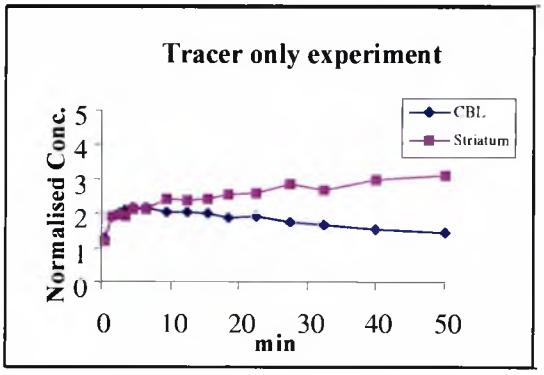

B. Mean data of the pre-treatment experiment for three subjects (#297, #259, #636).

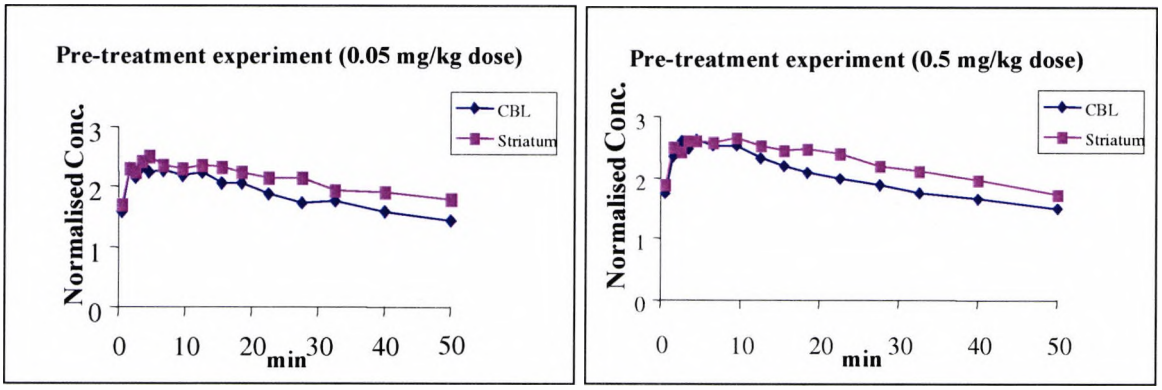

C. Data of the pre-treatment experiment for subjects #779.

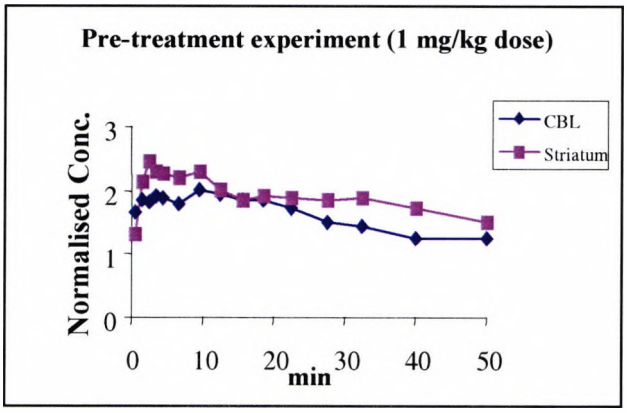

Fig. 11. PET monkey data for tracer only and pre-treatment experiments in striatum and cerebellum (CBL) regions.

5.2.2 Modelling analysis

We performed the modelling analysis using the striatum and cerebellum ROIs. Modelling analysis was performed in 4 subjects (see above) and used three different models to interpret PET data. We considered the cerebellum as the reference region.

The first two models are presented in Section 3.3.2: the Reference Tissue Model and the Simplified Reference Tissue Model.

The third model (the Irreversible Binding Model) is another simplified version of the model in Figure 8 (Section 3.3.2) and is based on the assumption that the dissociation rate constant (k_4) is negligible during the PET experiment. This hypothesis leads to the model shown in Figure 12. In this model we estimate R, k_2 and k_3. The model does not allow the estimation of BP, i.e. the ratio between k_3 and k_4.

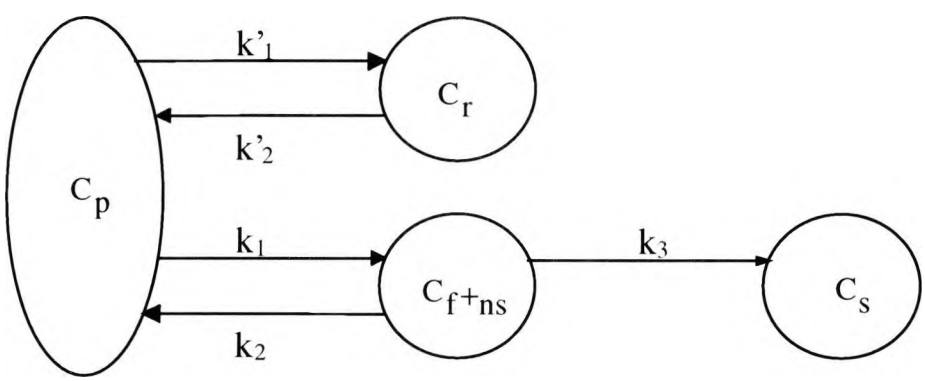

Fig. 12. The Irreversible Binding Model

For the Reference Tissue Model and the Simplified Reference Model it is possible to calculate RO according to Equation 53. Since the Irreversible Binding Model does not allow the estimation of BP, it is possible to calculate the receptor occupancy from Equation 53 at the baseline and after treatment as follows

$$\%RO = \frac{k_3' - k_3}{k_3} = \frac{B}{B_{max}'} \qquad (81)$$

We note that Equation 81 also allows the estimation of receptor occupancy for the Reference Tissue Model, but, due to an improved parameter precision of BP with respect to k_3, the calculation of receptor occupancy using Equation 53 is more robust. Finally, the Simplified Reference Tissue Model only provides BP for calculating receptor occupancy.

Parameter Identification

We performed the identification of the three models by using the SAAMII software package (Barrett *et al.*, 1998).

The evaluation of the three models was based on the weighted residual plots, i.e. the difference between the observed and the predicted values weighted by the accuracy of the measured value, the precision of the parameter estimates (expressed as percent CV), and the parsimony criterion of Akaike (AIC).

5.3 Results

5.3.1 Tracer experiment (baseline)

The results of the three models are shown in Table 1. In Figures 13-18 the fits and the mean weighted residuals for all subjects respectively for the Reference Tissue Model, the Simplified Reference Tissue Model, and the Irreversible Binding Model are reported.

Table 1 **Tracer only experiment. Estimates of the parameters for the Reference Tissue Model, the Simplified Reference Tissue Model and the Irreversible Binding Model. BP in the Reference Tissue Model is derived from the estimated parameters.**

	Reference Tissue Model					Simplified Reference Tissue Model			Irreversible Binding Model		
	R	**k2**	**k3**	**k4**	**BP**	**R**	**k2**	**BP**	**R**	**k2**	**k3**
#297	0.891	0.056	0.130	0.081	1.617	0.844	0.039	2.052	0.852	0.256	0.022
CV%	5	75	204	166	50	5	22	37	10	45	9
#259	0.886	0.066	0.053	0.040	1.321	0.845	0.030	2.109	0.861	0.163	0.019
CV%	10	448	649	633	32	5	31	71	8	44	14
#636	0.839	0.055	0.067	0.033	2.064	0.747	0.036	2.536	0.805	0.097	0.029
CV%	8	Fixed*	62	153	94	6	Fixed*	16	10	48	27
#779	1.036	0.043	0.656	0.237	2.769	1.010	0.040	2.894	1.169	0.172	0.032
CV%	18	85	766	712	104	9	43	89	11	Fixed*	7
	R	**k2**	**k3**	**k4**	**BP**	**R**	**k2**	**BP**	**R**	**k2**	**k3**
Mean	0.913	0.055	0.227	0.098	1.943	0.862	0.036	2.398	0.922	0.172	0.026
SD	0.085	0.009	0.288	0.095	0.630	0.109	0.004	0.395	0.167	0.065	0.006

*Fixed parameter due to the non-convergence of the minimisation algorithm (we fixed k_2 to the mean value obtained in all the other tracer only experiments in the same model).

We note from Figures 13, 15 and 17 that all three models describe the data well. As far as parameter estimates are concerned, the Simplified Reference Tissue Model and the Irreversible Binding Model provide estimates with a good precision. In contrast, the Reference Tissue Model provides non acceptable CVs especially for parameters k_3 and k_4. However, as expected from the theory, parameter BP is estimated with acceptable precision. The BP estimates obtained from the Reference Tissue Model in all subjects are in a good agreement with those obtained from the Simplified Reference Tissue Model.

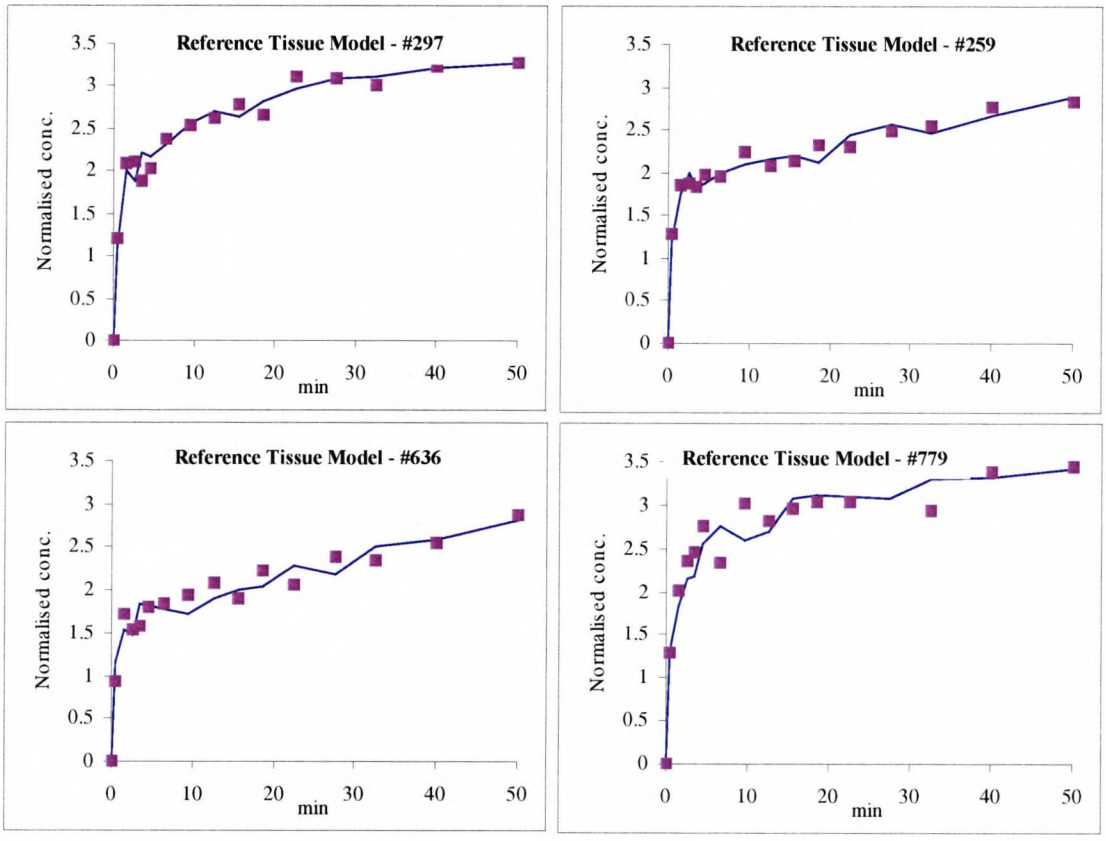

Fig. 13. Model fits for 4 subjects (#297, #259, #636, #779). Tracer only experiment.

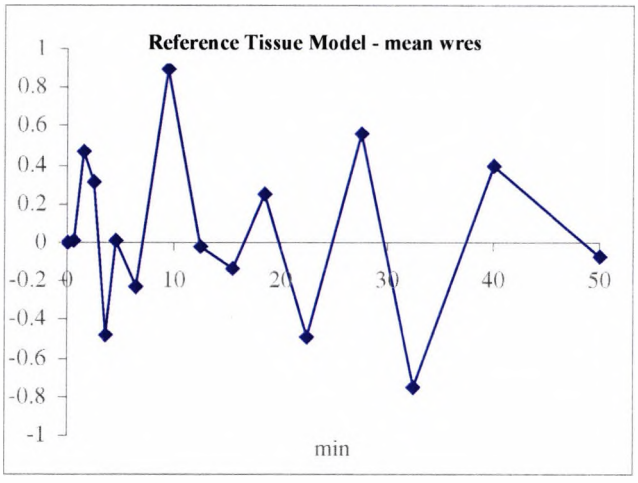

Fig. 14. Mean weighted residuals for 4 subjects (#297, #259, #636, #779). Tracer only experiment.

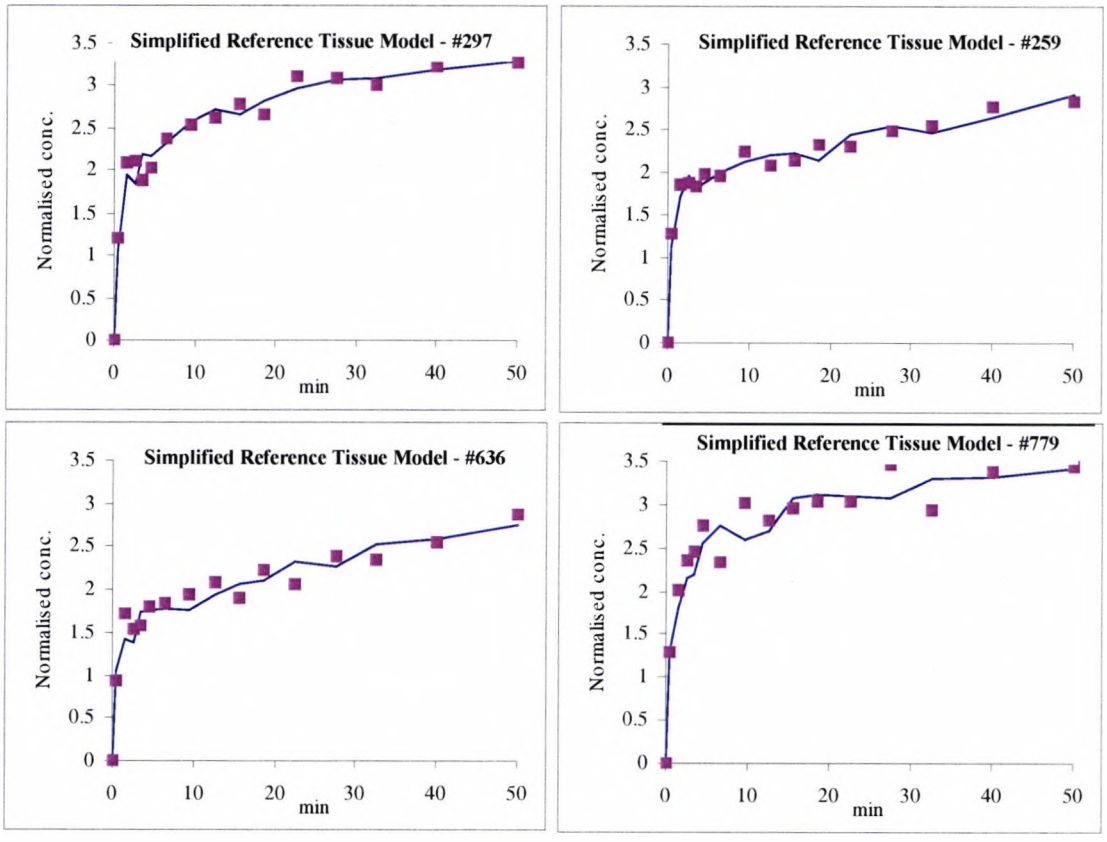

Fig. 15. Model fits for 4 subjects (#297, #259, #636, #779). Tracer only experiment.

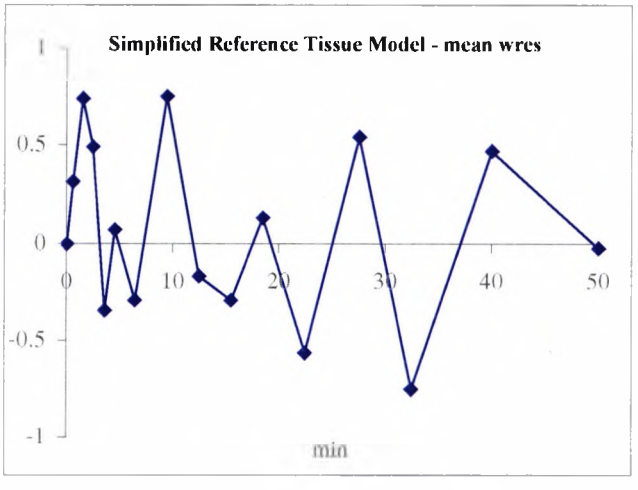

Fig. 16. Mean weighted residuals for 4 subjects (#297, #259, #636, #779). Tracer only experiment.

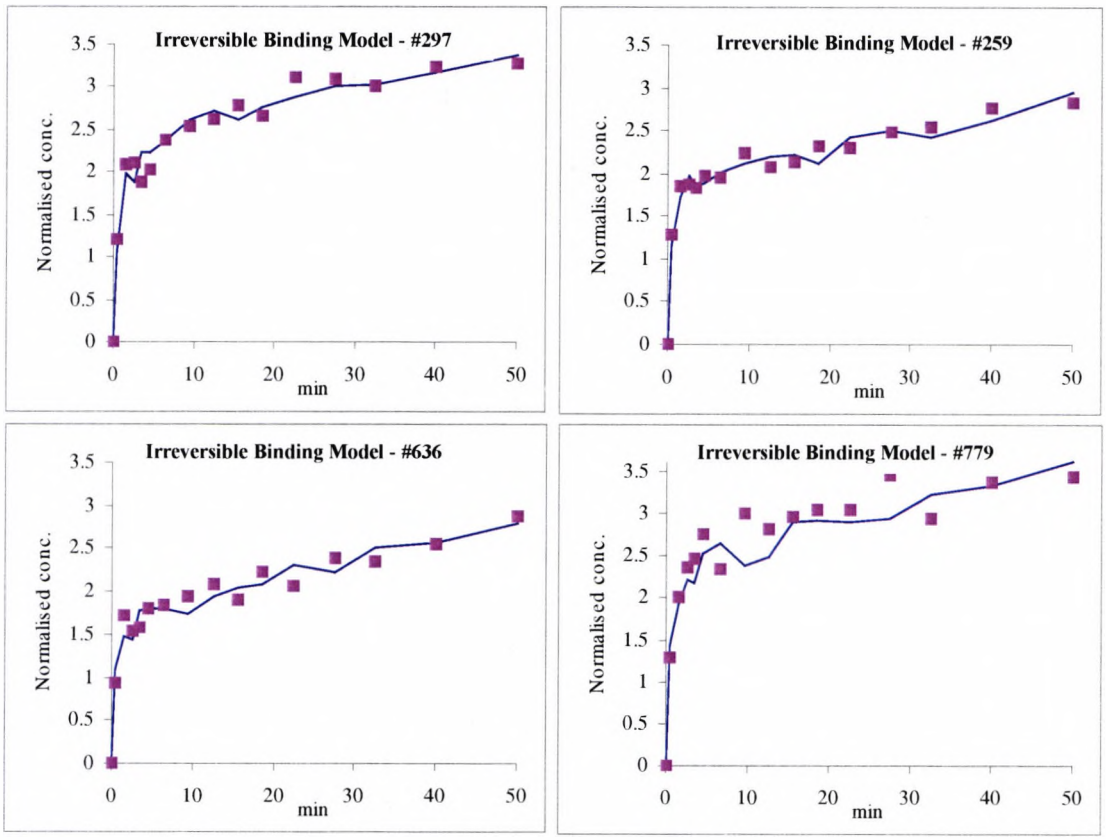

Fig. 17. Model fits for 4 subjects (#297, #259, #636, #779). Tracer only experiment.

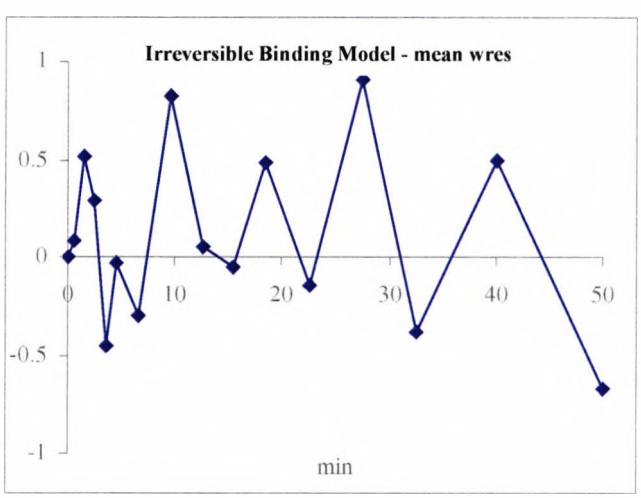

Fig. 18. Mean weighted residuals for 4 subjects (#297, #259, #636, #779). Tracer only experiment.

The Akaike criterion (AIC) provided similar values for the three models, see Table 2. The Simplified Reference Tissue Model has a lower AIC in all subjects.

In conclusion, the weighted residual plots, the precision of the parameter estimates, and the parsimony criterion indicate the Simplified Reference Tissue Model to be the best model to describe the tracer only experiment data.

Table 2 Tracer only experiment. Value of the Akaike information criterion (AIC) for the Reference Tissue Model, the Simplified Reference Tissue Model and the Irreversible Binding Model.

	Reference Tissue Model	Simplified Reference Tissue Model	Irreversible Binding Model
# 297	-0.405	-0.430	-0.295
# 259	-0.427	-0.437	-0.379
# 636	-0.106	-0.155	-0.139
# 779	0.380	0.313	0.421

5.3.2 Tracer experiment after unlabelled administration

We performed the same modelling analysis on the pre-treatment tracer data. Results are shown in Table 3. Figures 19-24 show the fits and weighted residuals for subjects with 0.5 and 1 mg/kg pre-treatment cold dose.

In this situation the best model to interpret the data seems again the Simplified Reference Tissue Model. The Reference Tissue Model is numerically non-identifiable and has a similar weighted residual plot to the Simplified Reference Tissue Model which is numerically identifiable. For the lower cold dose (0.05 mg/kg) The Simplified Reference Tissue Model and the Irreversible Binding Model give good precision of parameters estimates except for subject #259. In this case it was necessary to fix one parameter for The Irreversible Binding Model identification. However, for the other cold doses, the Irreversible Binding Model (Figure 23) does not fit the experimental data well, i.e. weighted residuals plot (Figure 24) shows a non-random behaviour. Moreover, for the Irreversible Binding Model, it was necessary to fix one parameter (k_2) for all subjects but one (#636, pre-treatment with the higher dose, see Table 3) since convergence of the minimisation algorithm was not reached.

Table 3 **Pre-treatment experiment. Estimates of the parameters for the Reference Tissue Model, the Simplified Reference Tissue Model, and the Irreversible Binding Model. BP in the Reference Tissue Model is derived from the estimated parameters.**

		Reference Tissue Model					Simplified Reference Tissue Model			Irreversible Binding Model		
Dose	**Subj**	**R**	**k2**	**k3**	**k4**	**BP**	**R**	**k2**	**BP**	**R**	**k2**	**k3**
0.05mg/kg	**#297**	1.368	0.480	0.673	3.227	0.209	1.345	0.471	0.209	1.272	0.021	0.006
	CV%	15	212	1370	1369	8	9	137	8	4	71	22
0.5mg/kg	**#297**	1.066	0.078	0.059	0.257	0.231	1.048	0.051	0.249	1.113	0.256	0.005
	CV%	7	175	360	343	26	5	69	29	9	Fixed*	14
0.05mg/kg	**#259**	0.886	0.168	0.006	0.019	0.313	0.901	0.047	0.208	0.876	0.216	0.004
	CV%	10	114	109	304	198	6	68	45	10	86	20
0.5mg/kg	**#259**	1.019	0.217	0.022	0.115	0.192	0.986	0.080	0.201	1.058	0.163	0.005
	CV%	4	569	368	378	12	4	38	11	6	Fixed*	12
0.05mg/kg	**#636**	0.767	0.049	0.095	0.252	0.379	0.752	0.045	0.395	1.045	0.166	0.008
	CV%	10	125	855	803	64	8	41	40	9	Fixed*	13
0.5mg/kg	**#636**	0.836	0.166	0.020	0.263	0.075	0.820	0.147	0.074	0.823	0.235	0.001
	CV%	21	539	2611	2617	40	12	68	39	18	120	63
1mg/kg	**#779**	1.097	0.088	0.017	0.058	0.295	1.047	0.023	0.400	1.123	0.172	0.006
	CV%	13	475	247	227	65	8	280	193	10	Fixed*	17

*Fixed parameter due to the non-convergence of the minimisation algorithm (for the Irreversible Binding Model we fixed k_2 to the value obtained in the tracer only experiment).

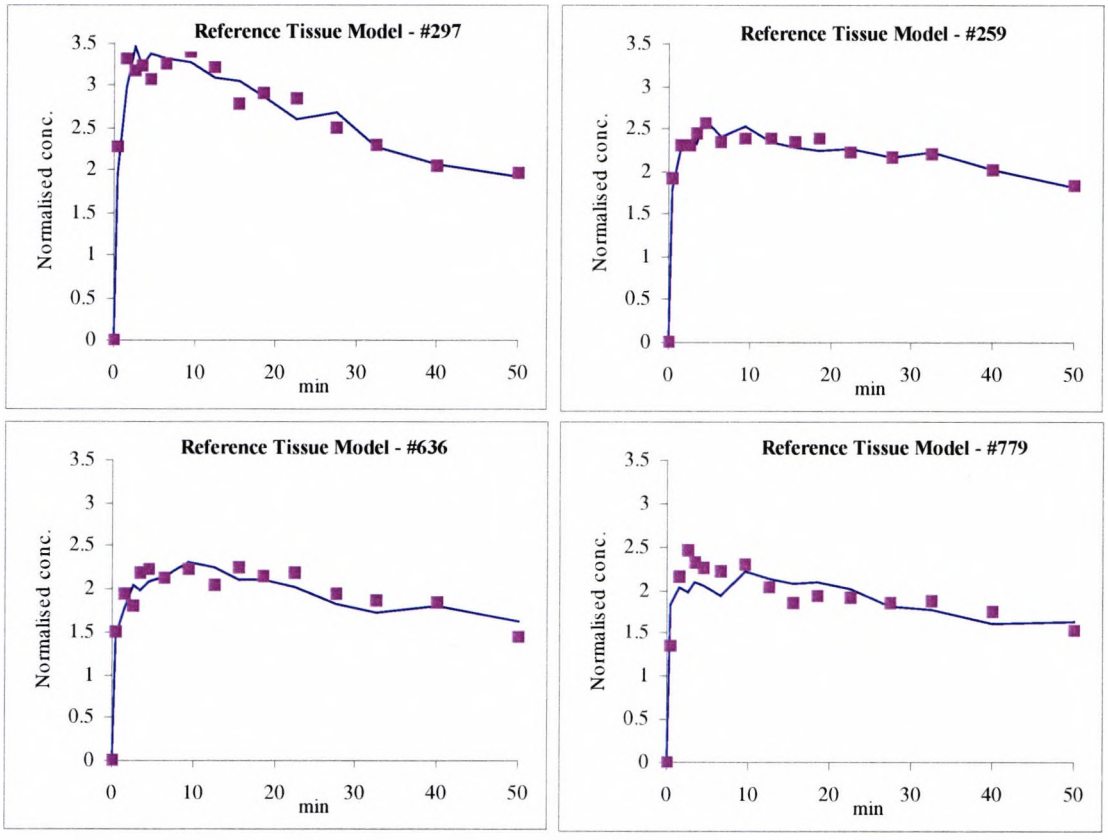

Fig. 19. Model fits for 4 subjects (#297, #259, #636, #779) in the pre-treatment experiment. The cold doses are 0.5mg/kg in subjects #297, #259 and #636; 1 mg/kg in subject #779.

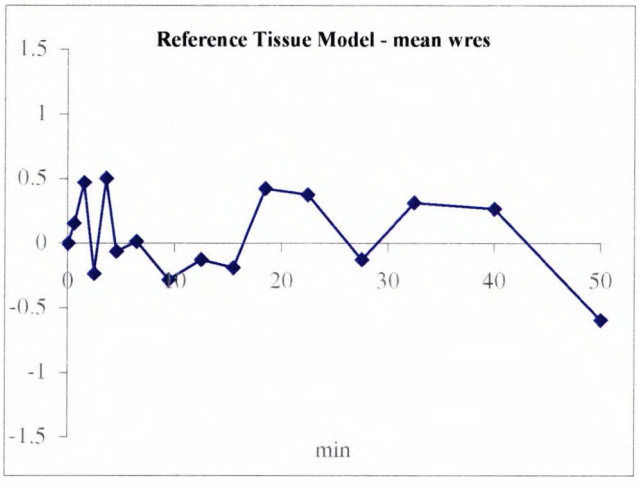

Fig. 20. Mean weighted residuals for the 3 subjects with 0.5 mg/kg cold dose (#297, #259, #636).

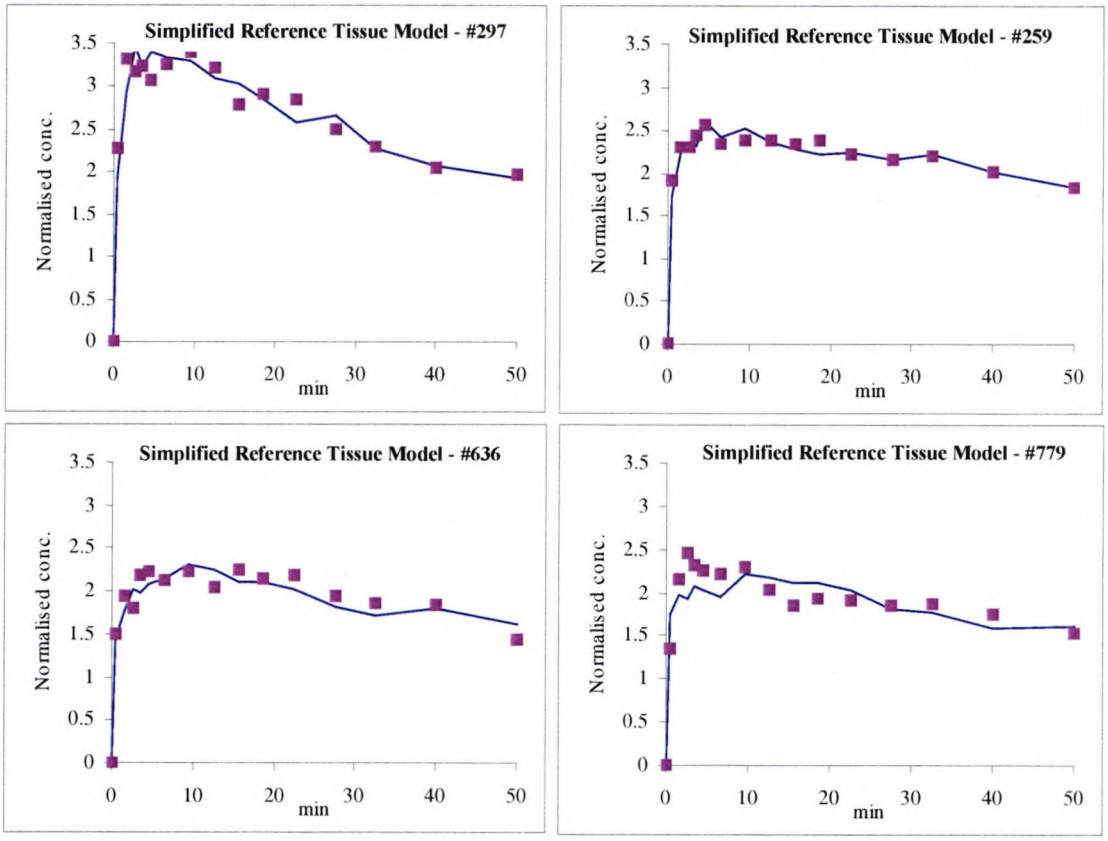

Fig. 21. Model fits for 4 subjects (#297, #259, #636, #779) in the pre-treatment experiment. The cold doses are 0.5mg/kg in subjects #297, #259 and #636; 1 mg/kg in subject #779.

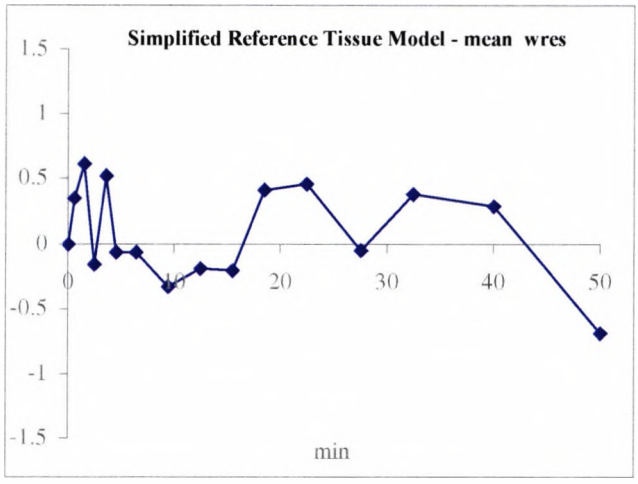

Fig. 22. Mean weighted residuals for the 3 subjects with 0.5 mg/kg cold dose (#297, #259, #636).

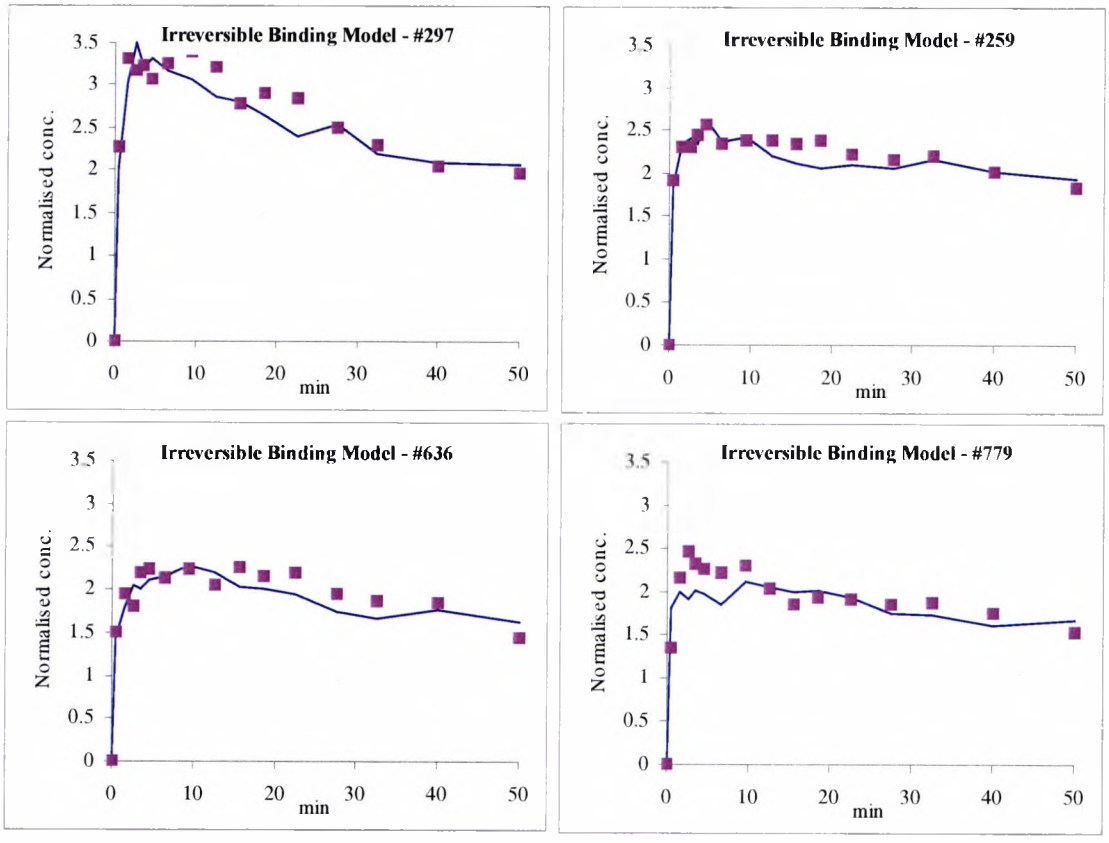

Fig. 23. Model fits for 4 subjects (#297, #259, #636, #779) in the pre-treatment experiment. The cold doses are 0.5mg/kg in subjects #297, #259 and #636; 1 mg/kg in subject #779.

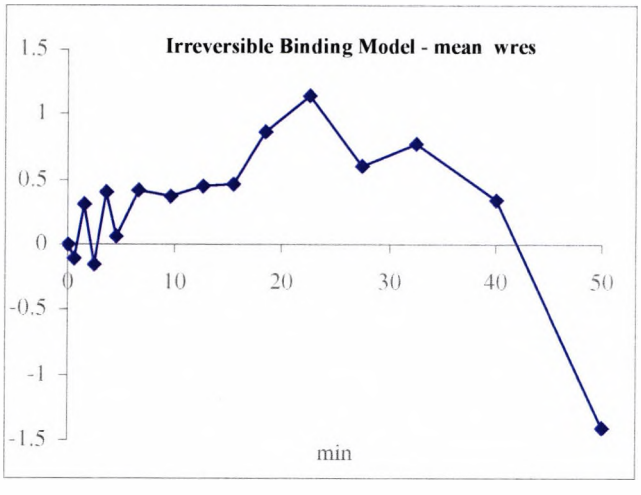

Fig. 24. Mean weighted residuals for the 3 subjects with 0.5 mg/kg cold dose (#297, #259, #636).

Table 4 gives the receptor occupancy for different subjects and models. The receptor occupancy reflects the differences between the models discussed above. Results from

the Reference Tissue Model and the Simplified Reference Tissue Model are very similar.

It is crucial to point out that for the pre-treatment experiments with cold doses of 0.05 and 0.5 mg/kg the receptor occupancy (about 90%) is similar. This suggests that during the pre-treatment experiments the specific receptors have been completely saturated.

Table 4 **Receptors occupancy calculated using Equation 53 (the Reference Tissue Model and the Simplified Reference Tissue Model) and Equation 66 (the Irreversible Binding Model)**

		Reference Tissue Model			Simplified Reference Tissue Model			Irreversible Binding Model		
Subj	Dose	BP	BP'	RO	BP	BP'	RO	k3	k3'	RO
#297	0.05	1.617	0.209	87%	2.052	0.208	90%	0.0217	0.0060	73%
#297	0.5	1.617	0.249	85%	2.052	0.231	89%	0.0217	0.0053	76%
#259	0.05	1.321	0.313	76%	2.109	0.209	90%	0.0186	0.0040	78%
#258	0.5	1.321	0.201	85%	2.109	0.192	91%	0.0186	0.0053	72%
#636	0.05	2.064	0.379	82%	2.526	0.395	84%	0.0289	0.0080	73%
#636	0.5	2.064	0.074	96%	2.526	0.075	97%	0.0289	0.0014	95%
#779	1	2.769	0.401	86%	2.894	0.295	90%	0.0324	0.0061	81%

5.4 Discussion

5.4.1 Tracer experiment.

Since it is very difficult to resolve the Reference Tissue Model, the Simplified Reference Tissue Model and the Irreversible Binding Model are the two candidate models to interpret the data.

In the tracer only experiment, weighted residuals plots and parameter precision do not allow the choice of the best model. However, the Akaike information criterion supports the Simplified Reference Tissue Model as the best model. In Figure 25, simulated responses of the two models during 90 minutes are shown. The increase of the observation time interval would allow to assess further which of the two models is

the most appropriate. This simulation highlights the importance of a longer experiment duration.

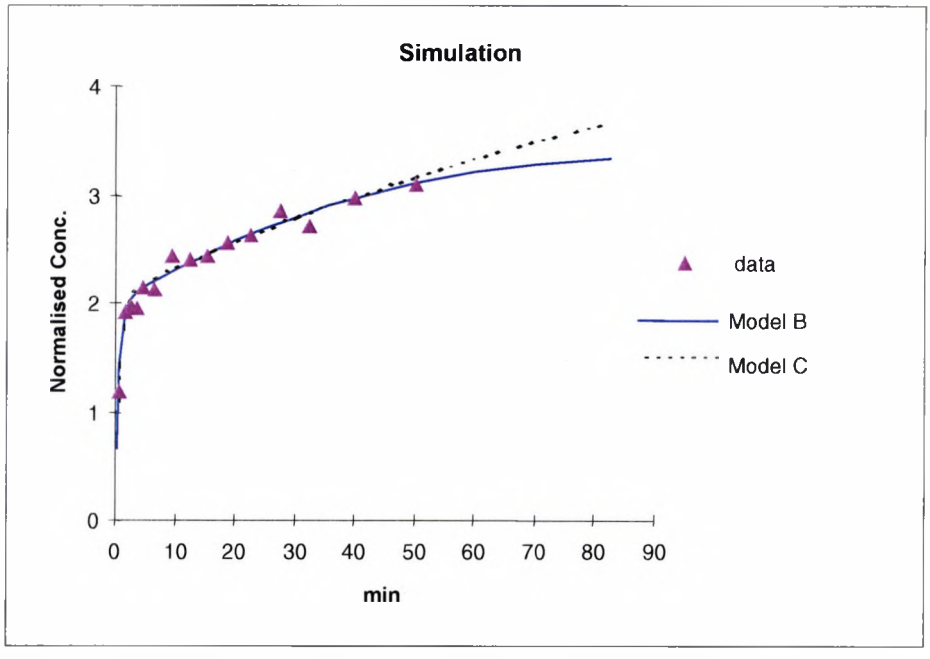

Fig. 25. Simulated profile for the Simplified Reference Tissue Model and the Irreversible Binding Model.

5.4.2 Tracer experiment after unlabelled administration

Regarding the pre-treatment experiment, the results again support The Simplified Reference Tissue Model. The assumption was made that for all models the concentration of the unlabelled specifically bound ligand compound was constant. This is unlikely to be true. However, in order to consider the possibility of a time-varying specifically bound ligand concentration, a new model approach has to be used. The k_3 parameters has to be considered time-varying. Here k_3 is assumed to be constant. In the literature, non-linear models that take into account the presence of the unlabelled compound have been proposed (Delforge et. al, 1990; Delforge et. al, 1993).

Two ingredients are essential in order to estimate the time varying parameter $k_3(t)$. The first is to design an appropriate protocol allowing different levels of receptor occupancy during the PET experiment (the so-called displacement or co-injection experiment). The second is the use of a metabolite corrected plasma concentration as an input function. This model approach would allow the estimation of both B_{max} and k_{on} which is not possible with the present protocol.

Given this scenario, it is worth re-emphasising that the estimated value of receptor occupancy is only an indicative index of an average receptor occupancy during the PET experiment.

On the basis of this modelling analysis a new design protocol was designed for a [^{11}C]GR205171 human study that includes a co-injection experiment. The experiment should last at least 90 minutes and required the measurement of metabolite corrected plasma concentrations of the labelled ligand.

6 A PET MODELLING STUDY IN HUMANS WITH IV DOSING

6.1 Introduction

The purpose of this analysis is to study the ligand-receptor interaction between GR205171 and neurokinin 1 (NK1) receptor in the human brain. A complex experimental protocol was performed using a single tracer experiment followed by two infusions of the unlabelled drug (one co-injected with a tracer) and a series of PET tracer experiments.

The main objective of this study is to estimate the degree and duration of receptor occupancy achieved following different doses of GR205171.

A secondary objective of this study is to estimate the equilibrium dissociation constant (K_D) and the receptor concentration (B_{max}). A tracer experiment on the system in a non-perturbed condition does not allow these parameters to be estimated but only an aggregated parameter, i.e. the potential binding (BP) which is the ratio B_{max}/K_D. An experiment in which the system is perturbed, i.e. one that also includes an administration of unlabelled ligand (co-injection or displacement experiment), is necessary to estimate K_D and B_{max} and to obtain quantitative information on receptor occupancy.

Three different methods have been used to analyse the data: a model approach that uses a region void of specific receptors as the reference region (Lammertsma *et al.*, 1996; Lammertsma and Hume, 1996), a model using a plasma concentration corrected for metabolites as the input function (Mintum *et al.*, 1984; Perlmutter *et al.*, 1986) and a non-linear model to evaluate the possibility of estimating K_D and B_{max} from the co-injection experiment data (Delforge *et al.*, 1990; Delforge *et al.*, 1993). Since cerebellum is usually considered a region without NK-1 receptors we used this region as the reference region. A comparison analysis was also performed to select the most appropriate model among the reference tissue ones.

6.2 Data

6.2.1 Experimental protocol

Six subjects were studied using a protocol comprising a tracer experiment (baseline), a co-injection of the tracer and the drug, and a series of tracer experiments following the infusion of the drug (pre-treated experiment). Details are given in Table 5.

Table 5 **Study Design Protocol** (the experiments at 2 hours are co-injection of the drug plus tracer, x represents the PET scan experiment).

Subj.	0 hours	2 hours	4 hours	24 hours	26 hours	28 hours	48 hours
3825	X	5 mg + x	X	X	5 mg	X	x
3827	X	5 mg + x	X	X	5 mg	X	x
3830	X	0.1 mg + x	X	X	-		x
3831	X	0.1 mg + x	X	X	-		x
3832	X	Placebo + x	X	X	1 mg	X	x
3834	X	0.01 mg + x	X	X	1 mg	X	x

The first two subjects (# 3825 and # 3827) on day 1 following the baseline PET scan with ^{11}C- GR205171 (time 0) received 5mg GR205171 (0.07mg/kg based on a 70kg male) given as an infusion over 2 minutes at 2 h. This infusion was accompanied by a tracer dose of ^{11}C- GR205171 (co-injection) and a series of PET frames was taken. Two PET scans with ^{11}C- GR205171 were performed at 4 and 24 hours and a repeated dose of 5mg unlabelled GR205171 was given as an infusion over 2 minutes on day 2 at 26 h. Then two PET scans were performed at 28 and 48 h.

The second pair of subjects (# 3830 and # 3831) following the baseline PET scan with ^{11}C- GR205171 (time 0) received 0.1mg GR205171 (0.0014mg/kg based on a 70kg male) given as an infusion over 2 minutes at 2 hours. This infusion was accompanied by a tracer dose of ^{11}C- GR205171 (co-injection) and a serious of PET frames was taken. Three PET scans with ^{11}C- GR205171 were performed at 4, 24, and 48 h (pre-treatment experiments).

Finally, the last pair of subjects received, after a baseline experiment, respectively, a placebo (# 3832) and 0.01 mg dose (# 3834) of GR205171 (0.00014mg/kg based on a

70kg male) given as infusion over 2 minute at 2 hours (co-injected with a tracer dose of ^{11}C-GR205171) and a serious of PET frames was taken. Two PET scans with ^{11}C-GR205171 were performed at 4 and 24 h and both subjects received a new infusion of 1 mg GR205171 (0.014mg/kg based on a 70kg male) at 26 h. Then two PET scans with ^{11}C- GR205171 were performed at 28 and 48 h.

The dose of labelled GR205171, administrated as a rapid bolus, were variable but in the μg range.

6.2.2 PET

The PET studies were performed using two equal whole body PET cameras, Siemens ECAT EXACT HR+. These systems generate 63 contiguous slices with a distance of 2.5 mm between planes and an in-plane resolution of 4 mm. For evaluation of the PET images, four regions of interest were out-lined in the images: the striatum, the lateral, medial and occipital cortex.

Each scan lasted approximately 90 minutes and involved the capture of 27 sequential frames (1 x 1 min, 4.x 0.5 min, 4 x 1 min, 4 x 2 min, 13 x 5 min, 1 x 10 min).

6.2.3 Blood sampling for assay of ^{11}C- GR205171

Serial 2ml arterialised blood (venous blood from a warmed arm) samples for the analysis of whole blood and plasma ^{11}C- GR205171 were taken during each PET scan (prior to ^{11}C-GR205171 injection and then at 1,1.5, 2, 2.33, 2.66, 3, 3.5, 4, 5, 7, 10, 15, 30, 45, 60 and 90 min). In addition 2ml blood samples were taken for the metabolite analysis of radiolabelled GR205171 (prior to ^{11}C-GR205171 injection and at 5, 10, 30, 60 and 90 min post tracer injection).

6.3 Methods

Three different approaches were used to analyse the PET data. A model using a reference tissue (cerebellum) was first selected among the three models presented in

the monkeys' analysis, then a model using the plasma data as an input function was also used. These two models assume that the system is not perturbed during the PET experiment. Finally, the data from co-injection experiments were analysed with a time varying model, which assumes that the system is perturbed during the PET.

In these modelling studies the PET scans for the same subject were analysed independently. This analysis follows the standard approach in which the intra-subject variability is not considered.

6.3.1 Time invariant model

6.3.1.1 Plasma input model

The model using plasma radioactivity corrected from metabolites as an input function (Mintum *et al.*, 1984; Perlmutter *et al.*, 1986) is the most general approach to estimate parameters describing the binding interaction. The basic assumption in this approach is that metabolites do not cross the blood brain barrier. The model is described by three compartments (plasma, free plus non-specifically bound ligand, and the specifically bound ligand) and is described in detail in Section 3.3.2.

6.3.1.2 Reference region model

The candidate models were selected from the models presented in Section 3.3.2, the reference tissue model, the simplified reference model (in which the reversible binding is assumed) and the irreversible binding model (see Section 5.2.2). This kind of analysis was already performed in the monkey study and a comparison with those results should strengthen the choice of the correct model for this ligand.

All these models are based on the assumption that a region exists void of specific binding of the ligand (reference region). In this study cerebellum was considered the reference region.

6.3.2 Time varying model

The data from the tracer only and the co-injection experiments have been analysed with the time varying model presented in Section 3.3.2. The key feature is the time-varying parameter $k_3(t)$

$$k_3(t) = k_{on}\left[B_{\max} - C_s(t) - C_s'(t)\right]$$

where $C_s(t)$ is the concentration of the specifically bound labelled ligand, $C_s'(t)$ is the concentration of the specifically bound unlabelled ligand.

This model is a priori uniquely identifiable from the labelled ligand PET data and the measured plasma concentration of non-metabolised labelled ligand $C_p(t)$. The parameters to be estimated are k_1, k_2, k_{on}, B_{max}, and k_4.

6.4 Parameter estimation

The parameters estimation of all models was carried out using the SAAMII software package (Barrett *et al.*, 1998).

The evaluation of the models was based on the weighted residual plots, the precision of parameter estimates, the comparison of the model predicted vs observed values (see Section 3.5.4).

6.5 Bayesian approach

A Bayesian approach was employed for data where the convergence with the non-linear regression was not achieved. The a priori information (the mean and the standard deviation) was calculated from parameter estimates obtained from the data in which the convergence was reached. This approach assumed that k_2 (the tissue-vascular rate) was not affected by the presence of the cold compound. For the Reference Tissue Model an assumption was also considered that the dissociation rate (k_4) is identical for different treatments.

6.6 Results

The ROI curves expressed as SUV (standardised uptake value), which equals the plasma radioactivity concentration divided by the dose of injected radioactivity normalised to body weight (normalised dose radioactivity), are reported in Appendix A.

The ROI curves confirm that striatum is the region with the highest specific binding. For this reason, we focus our discussion on the striatum results.

6.6.1 Time invariant model

6.6.1.1 Plasma input model

The plasma radioactivity curves expressed as SUV are reported in Figure 26.

The results of metabolite analysis did not permit the plasma radioactivity curves to be corrected. In Appendix C, the table (Table IV) supplied by Uppsala PET Centre with the metabolite analysis for subjects 3825 and 3827 is reported. The unsatisfactory results were probably due to the low levels of radioactivity and the proximity of background noise. Nevertheless we intended to estimate the plasma input function from the plasma radioactivity data without correcting for metabolites. As the pattern of plasma radioactivity shows a growth after thirty minutes it was decided not to consider the last samples (45, 60 and 90 min) for the estimation of the plasma input function. However a reliable estimation of the input function was possible only in a few experiments. Therefore, the results using the estimated plasma radioactivity input function are not reported.

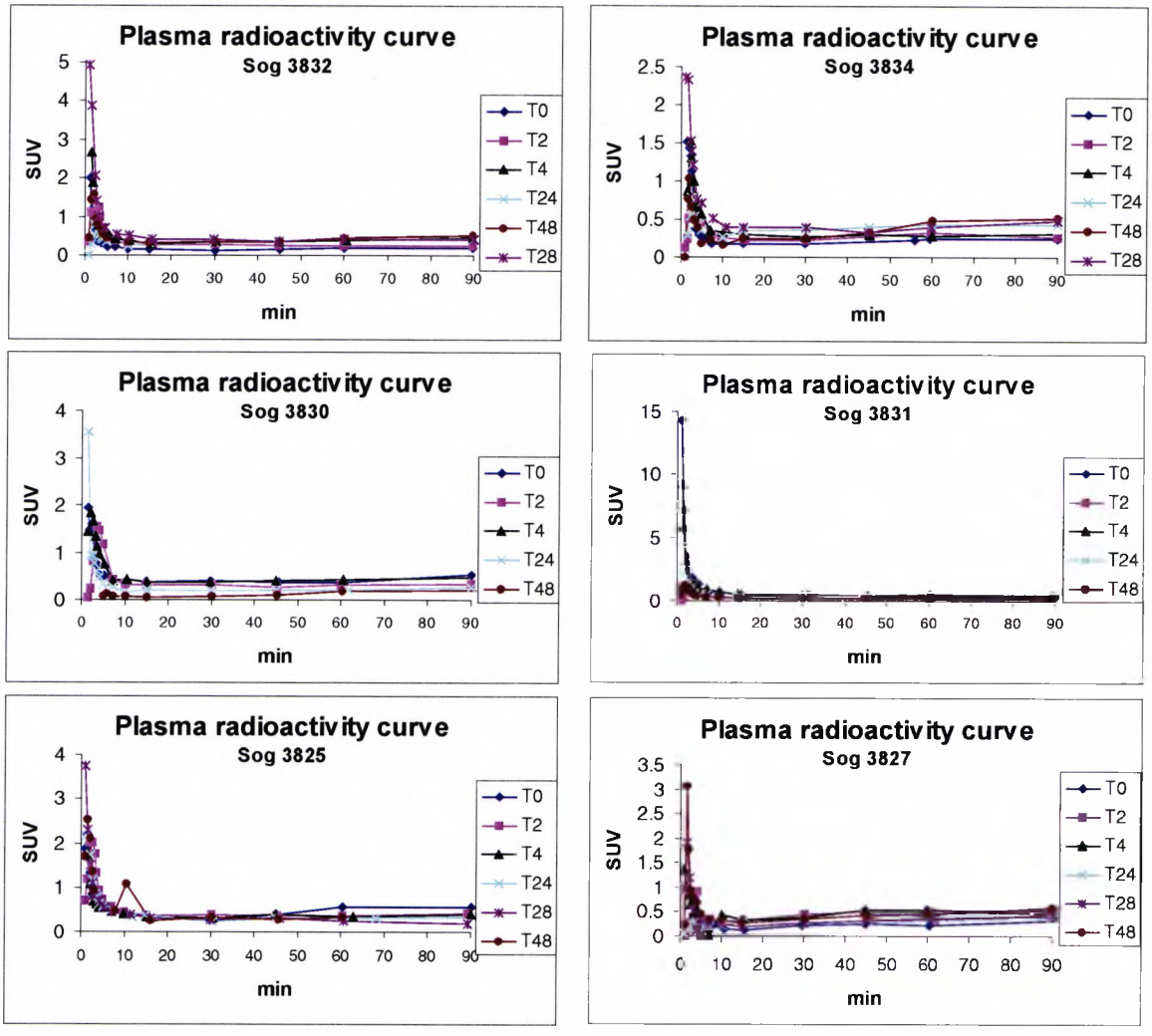

Fig. 26. Plasma radioactivity curves

6.6.1.2 Reference Tissue Model

In Table 6, the number of successful fits are presented; 28 individual fits were executed: 21 data sets reached the convergence with the Simplified Reference Tissue Model (75% success rate), 9 for the Reference Tissue Model (32%), and 11 for the Irreversible Binding Model (39%).

Table 6 **Convergence table** (Numbers of successful fits/total number of fits)

Subject	Simplified Reference Tissue Model	Reference Tissue Model	Irreversible Binding Model
3825	1/5	3/5	2/5
3827	5/5	2/5	2/5
3830	4/4	0/4	2/4
3831	4/4	¼	2/4
3832	4/5	2/5	0/5
3834	3/5	3/5	1/5
TOTAL	**21/28**	**11/28**	**9/28**

Appendix B includes the results of the modelling analysis for striatum. A Bayesian approach was considered for the data sets that failed to converge. The Simplified Reference Tissue Model employed the prior mean and standard deviation (SD) using parameter estimates estimated from other data for the same subject where convergence was reached. The only exception was subject 3825 which converged only with the baseline. The mean and standard deviation were computed using parameter estimates from all subjects.

In the Reference Tissue model and the Irreversible models, due to the small number of successful fittings, it was not possible to estimate prior mean and SD using the parameter estimated for the same subject. The mean and standard deviation were chosen using parameters estimated in all subjects.

Table 7 presents the summary of the Akaike criterion. The Simplified Reference Tissue Model gave the best results.

Table 7 Model selection using the Akaike criterion

Subject	Simplified Reference Tissue Model	Reference Tissue Model	Irreversible Binding Model
3825	5*	0	0
3827	1	2	2
3830	3	1	0
3831	4	0	0
3832	4	1	0
3834	2	2	1
TOTAL	**19**	**6**	**3**

* The number indicates the number of occasions the model performed better than the other two models.

The results of the Reference Tissue Model for other regions of interest are reported in Tables I-III in Appendix C.

The random distribution of weighted residuals and an acceptable precision indicate reliable parameter estimates. The receptor occupancy results are summarised in Table 8.

Table 8 Receptor occupancy

Subj.	Dose		RO (%)			
	Day1	Day2	4 hours	24 hours	28 hours	48 hours
3825	5 mg	5 mg	96 (14)	83 (34)	97 (19)	92 (13)
3827	5 mg	5 mg	98 (34)	86 (35)	98 (24)	89 (65)
3830	0.1 mg	-	87 (35)	-32 (39)		-61(48)
3831	0.1 mg	-	60 (9)	-274 (29)		-171(21)
3832	Placebo	1 mg	38 (28)	45 (29)	94 (32)	52 (39)
3834	0.01mg	1 mg	-8 (26)	9 (26)	95 (24)	47 (28)

Dose of 5 mg

In both subjects, a full receptor occupancy was reached (> 95%) and maintained over 22 hours (> 80 %).

Dose of 1 mg

The results of the receptor occupancy are consistent in the two subjects. A high receptor occupancy (> 90%) was reached after two hours and receptor occupancy close to 50% was estimated at 24 h after the drug injection.

Dose of 0.1 mg

The results are not plausible since receptor occupancy is negative at 28 and 48 h (details in Appendix C). Briefly, the baseline experiments for the two subjects (#3830 and #3831) presented an estimated binding potential lower than at 24 and 48 h. This is more evident for subject 3831 with an estimated binding potential value of 1.053, which is significantly lower than all other estimated values of binding potential for baseline experiments. This result is not consistent with our expectations, i.e. a higher binding potential and consequently higher availability of free receptors for specific binding before the drug infusion. For this reason it is not possible to consider the estimated binding potential from the baseline experiment as the reference value for the estimation of the receptor occupancy.

An alternative way to estimate the receptor occupancy is to use the experiment at 48 h as the reference experiment (see Table 9). In such a case, a complete receptor availability is assumed for specific binding at 46 h after 0.1 mg dose. This assumption seems to be consistent with the estimated binding potential at 24 h for subject 3830. High and similar values of the binding potential at 24 and 48 h suggest that the specific receptors are free. In contrast, the estimated binding potential at 48 h in subject 3831 is unexpectedly lower than that at 24 h for all regions.

Table 9 Receptor occupancy

Subj.	Dose	RO (%)	
		4 hours	24 hours
3830	0.1 mg	92 (35)	18 (39)
3831	0.1 mg	85 (21)	-38 (34)

Dose of 0.01 mg

Only one of the two treated subjects (3832 and 3834) received 0.01mg dose. Results are not physiologically plausible since it is not feasible that after the injected dose of 0.01mg (similar to the tracer amount) receptor occupancy reaches 40%. Moreover for other regions of interest we obtained unreasonable receptor occupancy (details in Appendix B).

6.6.2 Time varying model

For the problems described in Section 6.6.1.1, the analysis based on the time varying model could not be carried out. Thus no reliable results from the models employing the plasma input function were obtained.

6.7 Discussion

An unreliable plasma radioactivity concentration prevented the use of the time varying ligand-receptor model. For the same reason, the plasma input model, which represents the gold standard in ligand-receptor studies, was not applicable. Only the reference tissue models could be used. No comparison between the gold standard plasma input model and the reference tissue models was possible, and consequently the assumption that cerebellum can be used as a reference region was not verified.

The comparison performed for the reference tissue models showed that the Simplified Reference Tissue Model is the most appropriate model to fit the data. This is supported by observations that:

1. the number of data sets reaching convergence is greater for the Simplified Reference Tissue than the other models;
2. the comparison of the results including the analysis with the Bayesian approach provided a better fit for the Simplified Reference Tissue Model:
    - Akaike criterion gave lowest value in 19 data sets for the Simplified Reference Tissue Model; in 6 data sets for the Reference Tissue Model; and in 3 data sets for the Irreversible Binding Model;
    - the goodness of fit demonstrated a better fit for the two reference models (baseline fits are shown in Appendix B).

In addition, the comparison between the Reference Tissue Model and the Irreversible Binding Model using the F test showed that the Reference Tissue Model is better than the Irreversible Binding Model ($P<0.05$) in 19 out of 28 data sets.

The receptor occupancy obtained from the Reference Tissue Model is similar in value as that obtained from the Simplified Reference Tissue Model. The estimates of k_2 are consistent between the two models. These observations suggest that the lack of convergence and poor precision of the estimates of the Reference Tissue Model are related to unstable estimates of k_3 and k_4 parameters. The estimates of BP are robust.

The Reference Tissue Model assumes constant value of receptor occupancy and consequently non-perturbed conditions during the PET experiment. A low dissociation rate supports this assumption for the PET experiment following the drug infusion. However, the results from the co-injection experiment have to be considered only indicative since RO is changing during the PET scan.

A 5 mg drug infusion achieves a complete saturation of the specific receptor sites. This probably decreases receptor occupancy lower than that observed during the lower drug infusion. The experiments after 1 mg drug infusion confirm this assertion: a high receptor occupancy was observed for the 4 h experiments (> 90%) and a relevant decrease of receptor occupancy for the 24 h experiments (> 40%) compared with receptor occupancy after 5 mg dose.

As binding potential for the baseline experiments in the two subjects treated with 0.1 mg could not be estimated, reliable receptor occupancy could not be calculated.

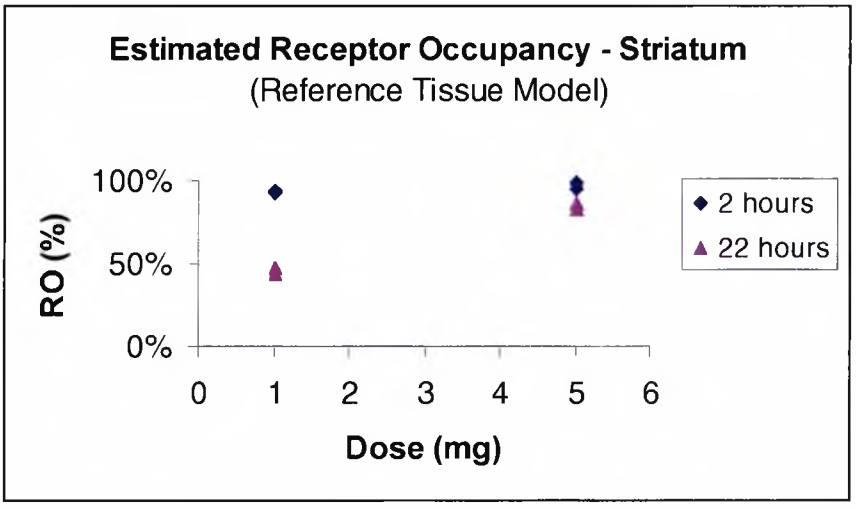

Fig. 27. Estimated receptor occupancy for 1 and 5 mg at 2 and 22 h. The results are obtained using the Reference Tissue Model.

A critical point of this study is related to the validity of the results for the low doses (0.01 and 0.1 mg). In Figure 27, the results for 0.01 and 0.1 mg are not reported since they are not assumed robust.

The data quality remains an important issue requiring further investigations. Probably, due to the low amount of radioactivity in the last part of the experiment, the error associated with the correction for the radioactivity decay may be critical and consequently affect the results. At very low dissociation rate, the last measurements are considered essential for a correct estimation of the binding potential.

The effect of intra-subject variability on receptor occupancy is another issue to be considered. As the estimation of receptor occupancy employs two different experiments, a good reproducibility is necessary for a robust estimation of receptor occupancy. This aspect is more pronounced for the estimation of a low degree of receptor occupancy as the result is obtained as a difference of two similar numbers.

6.8 Conclusion

The principal aim of the present study was to estimate the binding parameters that describe the ligand-receptor interaction. A co-injection experiment was employed to obtain the estimations of k_{on} and B_{max}. However, unreliable plasma radioactivity data prevented the use of an adequate model for estimating these parameters. This finding suggests that complex experiments using a co-injection should be performed only if an accurate profile of plasma radioactivity can be measured.

The results from the Reference Tissue Model facilitate the estimation of binding potential and consequently the extent of receptor occupancy after the drug infusion. The results for 5 mg and 1 mg dose appear robust but the results for lower doses require additional investigations.

These considerations suggest that the Reference Tissue Model, which accounts for a reversible binding, has to be considered the most appropriate model to describe [^{11}C] GR205171 binding. These findings are in agreement with the results obtained in the monkey study, see Chapter 5 (Section 5.2).

7 NON-LINEAR FIXED AND MIXED EFFECT MODELLING APPROACH

7.1 Introduction

In Chapters 5 and 6 the standard modelling methodology, in which any single PET scan is taken as an independent data set, was applied to analyse monkey and human PET data with [^{11}C]GR205171 ligand.

The purpose of this Chapter is to evaluate alternative approaches accounting for intra- and inter-subject variability. One of the major issues to be solved is the estimation of the value and the precision of receptor time-varying occupancy accounting for the variability introduced by complex manipulations necessary to generate the time-activity data and by the intra- (or inter occasion) and inter-subject variability in individual responses.

Examples of abnormal (negative) fractional receptor occupancy based on independent modelling of time-activity data for each subject and for each PET scan time have been reported (Abadie *et al.*, 1996). In addition, a recent study showed that a correct inference about subject responses in a fMRI (functional Magnetic Resonance Imaging) study can be derived through the use of a statistical model which accounts for both intra- and inter-subject variability applying a random-effect modelling approach (McGonigle *et al.*, 2000).

The aim of the present study is to evaluate alternative parameter estimation strategies based on the use of non-linear mixed effect models accounting for intra and inter-subject variability of the time-activity, and the identification of possible sources of this variability using individual covariate measurements. The effective use of the PET measurement technique as an enabling tool for drug development requires the definition of a model linking the brain receptor occupancy with the fluctuations of plasma concentrations. However, the predictive performance of such a model is

strongly related to the accuracy of the estimate of the time varying receptor occupancy values.

The work presented in this chapter has been published (Zamuner *et al.*, 2002). In this work the previous monkey data set (Chapter 5) plus two additional monkey data set were analysed using three different approaches based on the use of non-linear fixed and random effect models.

7.2 Materials and methods

7.2.1 Data

The aim of this study was the *in vivo* evaluation of the binding kinetics of a high affinity NK_1 receptor antagonist, [11C]GR205171, in the monkey brain. The experiments were initially conducted in 5 anaesthetised rhesus monkeys. Furthermore, 2 additional monkeys were included in the same study on a separate occasion. Following a baseline experiment, each monkey received one or two unlabelled ligand followed by a tracer injection. The unlabelled drug was injected at the doses of 0.05 mg/kg and 0.5 mg/kg in the monkey 1, 2, and 3; 0.1 mg/kg in the monkey 4; 1 mg/kg in the monkey 5; 0.001 mg/kg in the monkey 6, and 0.01 mg/kg in the monkey 7. The cerebellum was considered the reference region (RR) without specific receptors and the striatum the region of interest (ROI) according to the information collected during previous autoradiography studies. Each scan lasted approximately 50 minutes for monkey 1, 2, 3, 4, 5 and approximately 90 minutes for monkey 6 and 7. The time activity curves were expressed in SUV (Standardised Uptake Value), which equals the radioactivity concentration divided by dose of injected radioactivity normalised to body weight (normalised dose radioactivity).

7.2.2 Modeling analysis

Time-activity data were analysed using the Simplified Reference Tissue Model, considering the cerebellum as the reference region and the striatum as the region of interest. In the first approach a non-linear fixed effect model was used to analyse

independently the time activity curves collected at each PET scan (Model A). In the second approach all the data collected for the same monkey were simultaneously analysed using a non-linear fixed effects model (Model B). The model was constrained to estimate positive RO. Finally, in the third approach a non-linear mixed effects model was applied (Model C).

The modelling approach using the non-linear mixed effects was based on the assumption that the parameter estimates depend both on fixed effects (kinetic binding parameters) and on experimental conditions according to intra- and inter-subject variability sources. Furthermore a covariate effects analysis was included. The dose of unlabelled ligand was considered a potential covariate explaining the variability observed in the BP parameter value.

7.2.2.1 Model A

A non-linear fixed-effects model (Equation 82) was used to analyze independently the time-activity data collected at each PET scan time as if they come from separate animals

$$\frac{dy}{dt} = (k_2 - \frac{R_1 \cdot k_2}{(1+BP)})C_r(t) - \frac{k_2}{(1+BP)}y$$
$$C_t(t) = y + R_1 \cdot C_r(t) \qquad (82)$$

where C_t and C_r are the tracer concentrations in ROI and in RR respectively, BP is the binding potential, R_1 is the ratio of the delivery in ROI compared to that in RR (ratio of influx), and k_2 is the efflux rate constant from ROI. The fractional receptor occupancy value at scan time i ($\%RO_i$) was further derived from the primary model parameters using the binding potential value estimated at the baseline (BP_0) and the one estimated at the i^{th} PET scan time (BP_i) as

$$\%RO_i = 100\frac{BP_0 - BP_i}{BP_0} \qquad (83)$$

7.2.2.2 Model B

All the time-activity data collected in a monkey were simultaneously analysed using a non-linear fixed-effects approach and the Model B (Equation 84). All parameters were considered as fixed-effect parameters. R_1 and k_2 were assumed to have a typical value for each monkey constant across PET scan times. R_1 and k_2 were estimated using all the measurements at the different times, BP_0 was estimated using only baseline data while $\%RO_i$ was estimated using the measurements at time i. The model was constrained to estimate positive $\%RO_i$ values using a model re-parameterisation. The receptor occupancy (%RO) was constrained to be equal to 0 at baseline and to assume values ranging between 0 and 100% at the different PET scan times

$$\begin{aligned} \frac{dy}{dt} &= (k_2 - \frac{R_1 \cdot k_2}{(1+BP)})C_r(t) - \frac{k_2}{(1+BP)}y \\ BP &= BP_0 - \frac{\%RO_i \cdot BP_0}{100} \\ C_t(t) &= y + R_1 \cdot C_r(t) \end{aligned} \qquad (84)$$

The parameters estimated in the Model B are BP_0, R_1, k_2, and $\%RO_i$ [i = 1, number of PET scans (including baseline) – 1].

7.2.2.3 Model C

The non-linear mixed-effects approach was applied using the structural model defined by equation 85. All data for each monkey and each scan time were jointly analysed accounting for intra (or inter occasion) - and inter- monkey variability. The modelling approach (Model C) was based on the assumptions that: (a) typical tracer kinetic and binding parameters exist for each monkey (fixed-effect) and (b) these parameters may vary across monkey and experimental conditions within the same monkey according to two variability sources: an Inter-Occasion Variability (IOV) and Inter-Individual Variability (IIV). IIV was estimated as a first level random-effect parameter while occasion-specific departure of the parameter from the individual typical values (IOV) was accounted by a second level random-effect model component

$$\frac{dy}{dt} = (k_2 - \frac{R_1 \cdot k_2}{(1+BP)})C_r(t) - \frac{k_2}{(1+BP)}y$$
$$C_t(t) = y + R_1 \cdot C_r(t) \qquad (85)$$

7.2.2.4 Model for IIV and IOV

Denoting the ith subject average parameter value P_i, and its value at the jth occasion P_{ij}, a general model for IOV was

$$\begin{aligned} P_i &= f(P^*, \eta_i) \\ P_{ij} &= g(P_i, k_{ij}) \end{aligned} \qquad (86)$$

where P^* is a typical value of P in the population, and η_i and k_{ij} are assumed to be independently, normally distributed parameters with zero mean and variance ω^2 and π^2, respectively. The η represents the inter individual difference (IIV) and the k represents the inter occasion difference within an individual (IOV). The following exponential models were evaluated to describe IIV and IOV variability

$$\begin{aligned} P_{ij} &= P^* \cdot e^{(\eta_i + k_{ij})} \\ \eta_i &\approx N(0, \omega^2) \\ k_{ij} &\approx N(0, \pi^2) \end{aligned} \qquad (87)$$

Using this approach, the model parameters were partitioned into fixed effects (R_1, k_2, BP), random effects (ωR_1, ωk_2 and ωBP), and the residual error (σ). All the parameters (fixed and random) were estimated using all the collected measurements. R_1, k_2 and BP were assumed to vary across PET scan times taking values from two distributions having typical values equal to R_1^*, k_2^* and BP^* with a dispersion proportional to ωR_1, ωk_2 and ωBP to account for IIV, and to πR_1, πk_2 and πBP to account for IOV variance component.

7.2.2.5 Model for residual error

The residual error of the time-activity measurements was modelled using either the additive or the proportional model. This error term component represents the residual departure of the model from the observations and contains contributions from unexplained variability, the measurement error, and the model misspecification for the dependent variable.

7.2.2.6 Covariate effects

The dose of unlabelled ligand was expected to affect BP values estimated on different occasions. Therefore, the dose of unlabelled ligand was considered as a covariate potentially explaining the variability observed in the BP fixed-effect parameter value. The procedure adopted to investigate the influence of the covariate was based on the analysis of the plot of the individual Bayesian parameter estimates vs. the covariate values (Maitre *et al.*, 1991) and on the log-likelihood ratio test. The exponential (Model C-b, Equation 88) and the sigmoid (Model C-c, Equation 89) models were investigated as potentially explanatory models

$$BP_{ij} = BP_0 \cdot e^{-Dose_{ij} \beta} \tag{88}$$

$$BP_{ij} = BP_0 - \frac{Emax \cdot Dose_{ij}}{ED_{50} + Dose_{ij}} \tag{89}$$

where BP_0 is the binding potential at baseline, BP_{ij} is the binding potential at i^{th} scan for j^{th} subject, β is a slope factor, Emax represents the maximum BP reduction, and ED_{50} the dose giving 50% of the maximum BP reduction.

The retained model was included as a second stage model in the equation 85. The predictive accuracy of the individual Bayesian estimates of the time activity data was evaluated by comparing the scatter plot of individual predictions vs. the observed data with the unitary slope reference line.

7.2.3 Data analysis

All analyses were performed using the first-order estimate method as implemented in NONMEM Version V (Beal and Sheiner, 1992). Furthermore, using the population parameter the Bayesian individual estimates of kinetic parameters were estimated. Minimising the objective function provided by NONMEM is equivalent to maximising the likelihood of data. Hypothesis testing was performed by comparing the changes in the objective function (OF) when the value of one or more parameters have been fixed in the regression model. The difference in OF values is asymptotically distributed as χ^2 with a degree of freedom equal to the difference in the number of parameters between the two regression models. Any reduction in OF greater than 3.84 and 5.99 (χ^2, $p<0.05$ with 1 and 2 *df*) was considered to be significant and the parameter(s) concerned retained in the model according to the log-likelihood ratio test (Dobson, 1983).

7.3 Results

The parameters estimated using the fixed-effect modelling approach (Model A) are shown in Table 10. The computational algorithm failed to reach convergence for monkey 4 at baseline and at scan 1, and for monkey 5 at scan 1 probably due to the variability of the time-activity data. Furthermore, an inconsistent negative value for receptor occupancy was estimated in monkey 6.

Table 10 Parameter values estimated using Model A

Monkey		R_I	k_2	BP	%RO
1	Baseline	0.840	0.0349	2.620	0
	Scan 1	1.360	0.3270	0.209	92
	Scan 2	1.050	0.0354	0.300	88
2	Baseline	0.778	0.0290	4.550	0
	Scan 1	0.778	0.0405	0.418	91
	Scan 2	0.848	0.1100	0.109	98
3	Baseline	0.863	0.0245	3.340	0
	Scan 1	0.905	0.0418	0.234	93
	Scan 2	1.000	0.0651	0.221	93
4	Baseline	*	*	*	-
	Scan 1	*	*	*	-
5	Baseline	1.070	0.0341	3.860	0
	Scan 1	*	*	*	-
6	Baseline	1.040	0.0433	0.848	0
	Scan 1	0.938	0.0151	1.020	-20
7	Baseline	1.090	0.0323	1.710	0
	Scan 1	1.010	0.0076	0.932	45

* Non-linear regression procedure failed to reach convergence
- Parameter not estimated

In Model B, all time-activity observations collected in the same monkey at different scan times were simultaneously analysed using a re-parameterised model where the %RO value was fixed to 0 at baseline and to a value ranging between 0 and 100% at the different scan times. The parameters estimated using this modelling approach are shown in Table 11.

Table 11 Parameter values estimated using Model B

Monkey	R_I	k_2	BP_0	$\%RO_1$	$\%RO_2$
1	1.100	0.0142	119.00	100	100
2	0.830	0.0302	2.97	83	88
3	0.946	0.0217	2.95	87	80
4	0.613	0.0211	282.00	100	
5	1.090	0.0246	16.80	98	
6	0.968	0.0429	0.93	63	
7	1.030	0.0392	1.59	84	

$\%RO_1$, $\%RO_2$: receptor occupancy estimated at the first and second scan time

Two sets of analyses were conducted using the non-linear mixed effects to evaluate the influence of the additive and the proportional error model. The analysis database

included 7 monkey with 17 time-activity curves and a total of 267 measurements. The results, shown in Table 12, indicate that the proportional error model significantly improved OF values for all the modelling approaches used.

Table 12 **Non-linear mixed effects modelling: comparison of the objective function values estimated using an additive and a proportional error model assumption**

	Model C-a	Model C-b	Model C-c
Proportional error model	-643.112	-647.658	-687.345
Additive error model	-622.654	-630.683	-663.933

The fixed and random parameter values estimated with the Models C-a, C-b, and C-c using the proportional error model are shown in Table 13. The results of this analysis indicate that the fixed influx/efflux parameter R_1 and k_2 estimated from the four models have similar values with the exception of k_2 in Model C-c which shows a higher value.

Table 13 **Non-linear mixed effects modelling: fixed and random effects parameter values** (The ICV, IIV, IOV and residual error variability are expressed as CV%)

Parameters	Model C-a	Model C-b	Model C-c
R_1	0.982	0.981	1.000
k_2	0.0171	0.0196	0.0268
BP	1.19	β = 2.19 B0 = 1.23	E0 = 3.31 Emax = 3.05 ED50 = 0.0000323
ωR	15	15	16
$\omega k2$	< 1	< 1	< 1
ωBP	< 1	< 1	< 1
πR_1	11	12	11
πk_2	35	33	< 1
πBP	182	145	56
σ	8	8	7
OF	-643.112	-647.658	-687.345
ΔOF	0	4.546	44.233
Probability		df = 1 P < 0.05	df = 2 P < 0.01

The comparison of random effects estimates indicates that IOV variability seems to represent the most important component of the total variability and that the inclusion of the Emax model, as a second stage regression model, significantly ($P < 0.01$) explains the observed variability of BP as a function of the unlabelled drug dose administered at the different scan times. The overall evaluation of the fit obtained with Model C-c is illustrated by an excellent agreement between individual predictions vs. observed %RO values with the unitary slope reference line (Figure 28).

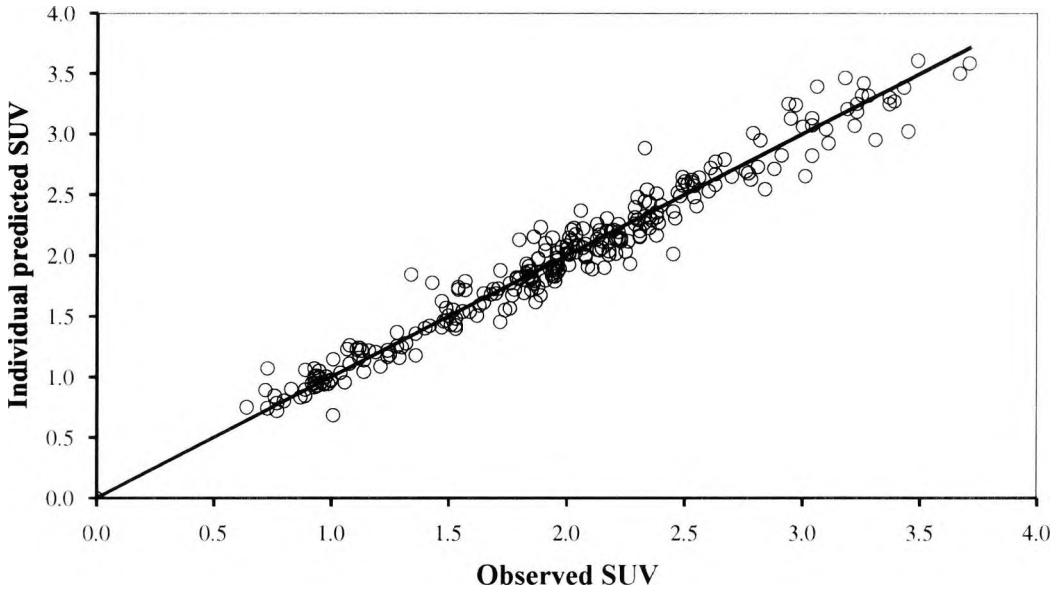

Fig. 28. Individual predicted versus observed time-activity data (SUV) with the reference unitary slope line (continuous line).

7.4 Discussion

PET offers unique possibilities to investigate physiology, metabolism, pharmacokinetic, pharmacodynamic, and modes of action of drugs from animal and human studies. Several methods have been proposed for the analysis and the quantification of *in vivo* ligand-receptor interactions from PET data even if no universally "best" method has been recognised (Slifstein and Laruelle, 2001). In any case, the modelling approach based on the arterial plasma input function appears as the method of choice (Van Waarde, 2000). However, in the absence of arterial input function, mainly due to technical problems in properly identifying and measuring metabolite concentrations, the reference tissue methods remain, at the moment, a preferred modelling strategy despite the limitations and the known problems associated with this approach. In the present study, the Simplified Reference Tissue Model (STRM) has been selected according to statistical and goodness of fit criteria. At variance from the graphical method, which provides biased parameter estimates, SRTM usually supplies well identified but, at times, underestimated parameter values.

A reliable estimate of the time-varying fraction of receptor occupancy integrated with the drug pharmacokinetic properties will enable researchers to build predictive models necessary to optimise the drug development process. Monte Carlo simulations have demonstrated that ignoring the presence of the inter-occasion variability may lead to biased and more variable parameter estimates (Karlsson and Sheiner, 1993; Lalonde, 1999) in pharmacokinetic/pharmacodynamic studies. For this reason, similar problems are expected in the analysis of PET experiments due to the repeated measure structure of the time-activity data and the complex mathematical models used to describe the response.

The presence of intra- and inter-subject variability can be detected by inspecting the changes over time of the time-activity data measured in RR following the same tracer injection. By definition, RR is expected to be drug receptor free, therefore the variability observed in the time-activity kinetics in this region is assumed to reflect only inter- and intra-subject variability. This can be quantified by the distribution property of the area under the time-activity curve estimated using the linear trapezoidal rule from 0 to 50 minutes (mean = 82.7, min = 42.1, max = 110.4, S.D. = 19.2, CV% = 23.4). Some of this variation can be linked to experimental conditions associated with the PET technology (such as equipment calibration and tuning, procedures to collect and process data, sensitivity and detection limits, etc.) or to physiological processes associated with individual behaviour. Non-linear mixed effect modelling approaches seems appropriate to improve estimate of the receptor occupancy accounting for the different sources of variability.

The evaluation of the different modelling approaches revealed that one of the major limitations of Model A is related to the underlying assumption which considers each time-activity curve as a measurement coming from a separate individual. This assumption aggregates the within subject and the measurement error variability into an overall measurement noise, causing an overestimation of measurement error. The consequences of this assumption were non-feasible parameter estimates such as a negative receptor occupancy and, in some cases, the inability to reach convergence.

This finding is in agreement with previously reported observations (Abadie, 1996; Parsey, 2000).

To overcome these limitations, Model B was proposed. In this model the whole set of observations collected at different scan times on each monkey was simultaneously fitted and the model was constrained to estimate positive %RO values. Furthermore, R_1 and k_2 were estimated on all individual data, assuming that these values remain constant in the same monkey, while the observations at the baseline and at different scan times were used to estimate BP_0 and the %RO. Using this approach we did not observe any computational problem or any inconsistency in the estimated parameter values. However, two major limitations persist: (a) R_1 and k_2 values are not constant over time for an individual but they may change over time, (b) this approach does not account for intra-individual variability which was, again, lumped into the measurement noise.

Finally, three mixed effect models were investigated. The first Model C-a only accounted for IIV and IOV while Model C-b and Model C-c included two alternative second stage models to explain variability in BP as a function of the dose of the unlabelled drug. Comparison of the different models indicates that the mixed effects approach with a primary model partitioning the variance in term of IIV and IOV and a second stage model relating the changes of the binding potential to the dose of the unlabelled drug with an Emax model is definitely the preferred approach. However, the limited number of subjects (7 monkeys) and the limited number of occasions for subjects (3 occasions in 3 monkeys and 2 occasions in 4 monkeys) suggests that the estimate of each variance term component must be cautiously interpreted even if the overall database used in the analysis (267 observations) was sufficiently large to allow a proper parameter estimation. In any case, the contribution of IOV to the overall variance remains larger than that of IIV indicating the presence of an important intra-subject variability in the time-activity data collected during a PET experiment in the same subject. In addition, the relative error affecting the receptor occupancy seems inversely proportional to its value: the lower the value, the higher the discrepancy between %RO values estimated with the different methods as reported in Table 14.

This observation indicates that the influence of the estimation procedure may become a critical factor for the appropriate evaluation of this parameter in particular at low %RO values (i.e. < 50%). These findings may be of particular interest in the analysis of experiments designed for the evaluation of receptor occupancy kinetic profiles over time where several PET scans are collected in the same individual and where the extent of intra-subject variability may introduce artefact and/or bias in the evaluation of the results.

Table 14 Brain receptor occupancy (%) estimated using fixed and mixed effect modelling approach

Monkey	Scan	Model A	Model B	Model Cc
1	1	92	100	92
	2	88	100	91
2	1	91	83	86
	2	98	88	93
3	1	93	87	86
	2	93	80	85
4	1	*	100	97
5	1	*	98	95
6	1	-20	63	50
7	1	45	84	85

* The non-linear regression procedure failed to reach convergence

7.5 Conclusion

In conclusion, the non-linear mixed effects modelling represents a valid alternative analysis approach mainly because it accounts for the repeated-measurement structure of the data and supplies an estimate of the different variability components on the parameter values. In addition, this approach allows integration of a second stage regression model to investigate the sources of variability in terms of concomitant measurements (covariates). In our example only dose was included in this second stage model. However this approach can be easily extended to account for other factors such as demographic, pathophysiological, and genetic factors which could be used to investigate sources of variability in brain receptor occupancy.

8 PK/PD MODELLING

8.1 Introduction

In the previous chapters different PET models have been developed to estimate receptor-ligand parameters and to evaluate RO after administration of the cold compound.

The main purpose of the following chapter is to introduce a PK/PD approach to relate receptor occupancy to plasma levels (Fitzgerald *et al.*, 2000). RO as observed in the IV human study changes with the plasma concentration of the drug. RO estimated in the IV study with the Simplified Reference Tissue model (Chapter 6) was used in this PK/PD modelling work.

This simulation study forecasts the expected receptor occupancy of GR205171 in striatum and cortex after single oral dose of 5 mg and repeated administrations of 1, 5 and 10 mg once a day during one week. The percentage of brain occupancy and the GR205171 plasma concentrations after IV administration of 1 and 5 mg were taken from a previous study. A three-compartment model best fitted the PK data. The brain occupancy was considered as a surrogate pharmacodynamic effect of GR205171 and a sigmoid E_{max} model (Hill equation) best fitted the brain receptor occupancy using the plasma concentration as a predictor variable (Keller *et al.*, 2002).

To obtain an estimate of the PK inter-individual variability, a PK population analysis was carried out employing plasma concentrations estimated at the lowest oral dose available in a previous study (single oral dose of 30 mg collected in 18 subjects).

Finally, the integration of the plasma-concentration/brain-occupancy model and the predicted oral concentrations allowed the brain striatum receptor occupancy after single administration of 5 mg and repeated administration (once a day) of 1, 5 and 10 mg during one week treatment with GR205171 to be forecasted.

8.2 Pharmacokinetic modelling after IV dosing

The GR205171 plasma concentrations following 1 and 5 mg IV dosing were collected in four healthy volunteers in a previous study, which investigated distribution and binding characteristics of NK1 receptors in the brain using PET.

In the study, the first two subjects (3825 and 3827) received 5 mg GR205171 as an infusion over 2 minutes on two separate occasions at a 1 day interval. The other two subjects (3832 and 3834) received 0.1 mg on day one (PK not available) and 1 mg on day 2.

A three-compartment open model with zero-order input rate over 2 min was used to fit the data (Equation 90). The PK model was simultaneously fitted to all available drug concentrations. The NONMEM (version V) package was used. The appropriateness of the model and the consistency of the estimated parameters were evaluated by comparing the Bayesian individual predictions with the observed concentrations as reported in Figure 29. The model is described by a set of differential equations

$$\begin{aligned}
\frac{dC_1(t)}{dt} &= \frac{R}{V} + k_{21} \cdot C_2(t) + k_{31} \cdot C_3(t) - (k + k_{13} + k_{12}) \cdot C_1(t) \\
\frac{dC_2(t)}{dt} &= k_{12} C_1(t) - k_{21} C_2(t) \\
\frac{dC_3(t)}{dt} &= k_{13} C_1(t) - k_{31} C_3(t)
\end{aligned} \tag{90}$$

where R is the infusion rate (mg/h), C_i the concentration of i-th compartment (C_1 represents the plasma compartment), V (L) the volume of the central compartment, k the elimination rate (h^{-1}), and k_{ij} the constant transfer rate (h^{-1}) from the i-th to the j-th compartment.

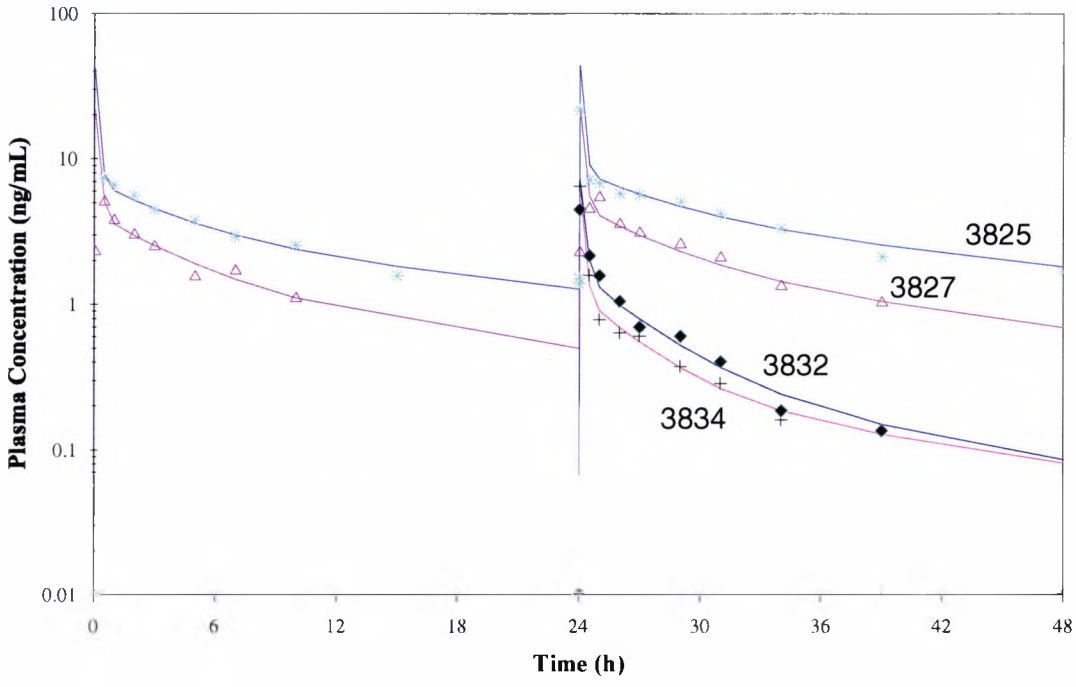

Fig. 29. Bayesian individual fit to the GR205171 concentrations in two subjects (3825 and 3827) receiving an IV dose of 5 mg (day 1 and 2) and two subjects (3832 and 3834) on 1 mg on day 2.

The individual parameters are reported in Table 15.

Table 15 PK parameter estimates

PK parameters	3825	3827	3832	3834
k: elimination rate (h^{-1})	0.448	0.503	0.765	0.923
k_{12}: central to peripheral1 rate (h^{-1})	4.938	3.865	2.771	3.574
k_{21}: peripheral1 to central rate (h^{-1})	1.170	1.170	1.170	1.170
V: volume of central compartment (10^3 L)	0.106	0.208	0.130	0.140
k_{13}: central to peripheral2 rate (h^{-1})	0.594	0.458	0.346	0.617
k_{31}: peripheral2 to central rate (h^{-1})	0.114	0.091	0.082	0.084

8.3 Pharmacodynamic modelling

Table 16 reports the NK1 receptor percentage occupancy in striatum and cortex as estimated by the modelling approach based on the simplified reference tissue method.

A direct PK/PD approach was used to model the brain occupancy kinetics as a function of the plasma drug concentration, considering the brain occupancy as a surrogate pharmacodynamic effect of GR205171. A sigmoid E_{max} model (Hill equation) best fitted the striatum and cortex occupancy at the doses of 1 and 5 mg using the plasma concentration as the predictor variable.

The PD model included three parameters, EC_{50} (the predicted plasma concentration producing 50% of receptor occupancy), γ (the slope factor), and E_{max} (the maximal attainable effect) which was fixed at 100%

$$RO = 100 \cdot \frac{C^{\gamma}}{EC_{50}{}^{\gamma} + C^{\gamma}} \qquad (91)$$

Since PK concentrations are not available at certain time points of PET scans, the predicted plasma concentration was used to drive the PD model. According to Figure 30 a good agreement between individual prediction vs. observed plasma concentrations was obtained.

Table 16 % NK1 receptor occupancy in striatum and cortex

	Dose	Time	Subj. 3827	Subj. 3825	Mean
Striatum	5 mg	2 h 22 h 26 h 46 h	98% 86% 98% 89%	96% 83% 97% 92%	97% 84% 97% 90%
Cortex	5mg	2 h 22 h 26 h 46 h	100% 93% 96% 95%	95% 95% 98% 93%	97% 94% 97% 94%
			Subj. 3832	Subj. 3834	
Striatum	1 mg	2 h 22 h	95% 47%	94% 52%	94% 49%
Cortex	1 mg	2 h 22 h	99% 91%	97% 84%	98% 87%

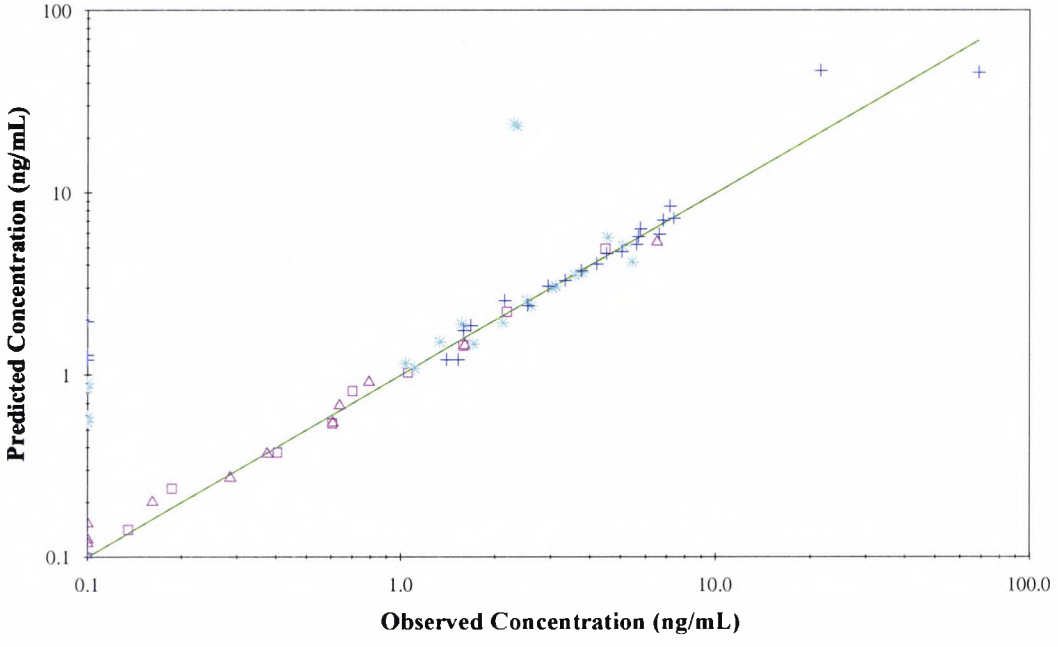

Fig. 30. Individual predicted versus observed plasma concentration with the reference unitary slope line (continuous line).

Table 17 reports the estimated PD parameters.

Table 17 Estimated PD population parameters

Parameter	Striatum		Cortex	
	mean	IIV (CV)	mean	IIV (CV)
EC_{50} (ng/mL)	0.133	64	0.00429	< 1
γ (unitless)	1.130	< 1	0.58100	17

The fit to the receptor occupancy is shown in Figures 31 and 32 for striatum and cortex, respectively.

The PD model was evaluated by comparing the predicted occupancy using the estimated concentrations at 2 and 22 h with observed occupancy after the administration of 1 mg and 5 mg IV. The graphs reported in Figures 33 and 34 show the predicted sigmoid E_{max} model response which relates the GR205171 plasma concentration to %RO in striatum and cortex together with %RO observed at the doses of 1 and 5 mg IV.

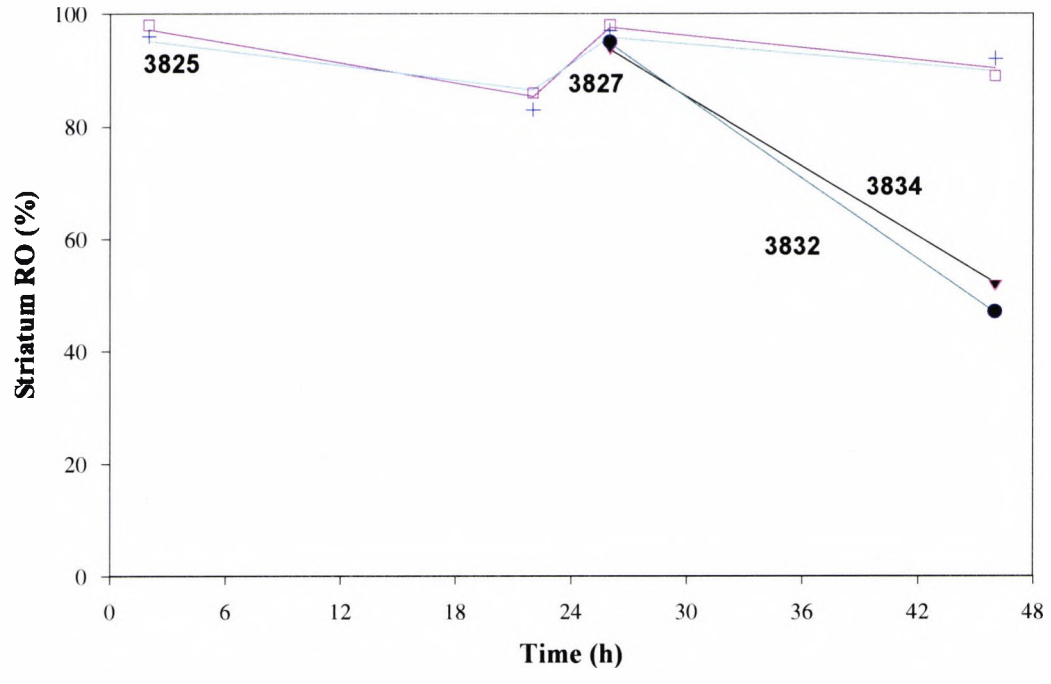

Fig. 31. % Receptor occupancy fit in striatum

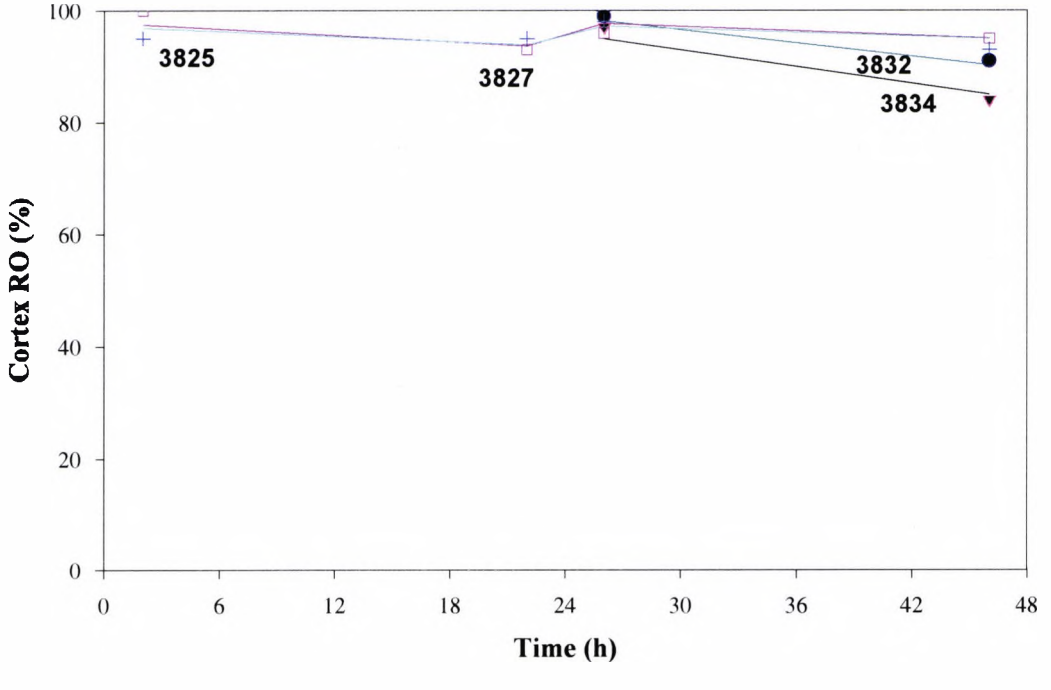

Fig. 32. % Receptor occupancy fit in cortex

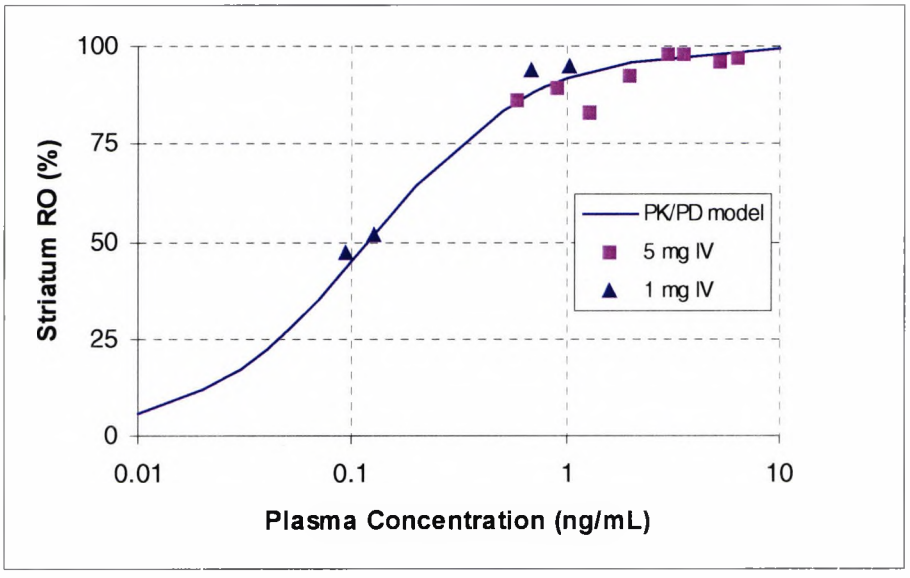

Fig. 33. Predicted NK1 receptor occupancy in striatum as a function of GR205171 plasma concentrations using the population PD model

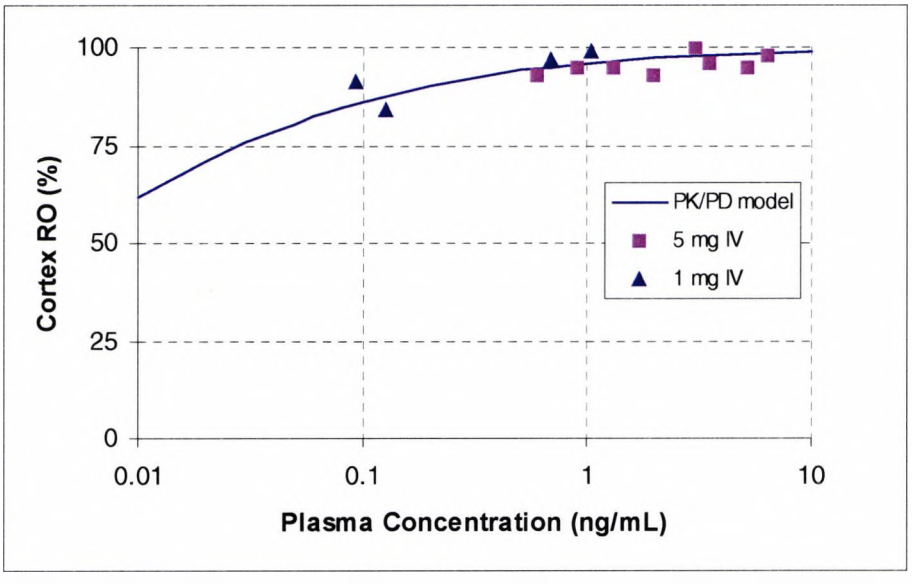

Fig. 34. Predicted NK1 receptor occupancy in cortex as a function of GR205171 plasma concentrations using the population PD model

8.4 Population pharmacokinetic modelling after oral dosing

The PK/PD model used to relate plasma concentration to RO accounts only for the PD variability. The limited number of subjects in the IV study did not allow the PK variability to be estimated. In order to introduce the PK variability and to forecast plasma profiles after oral administration, PK data from previous studies after oral administration were considered.

A PK population analysis was carried out using plasma concentrations estimated at the lowest oral dose in a previous study (a single oral dose of 30 mg in 18 subjects). The concentrations normalised to a dose of 5-mg were used in the analysis assuming that linear kinetics exist for doses ranging between 1 to 30 mg. A two compartment model with a first-order input rate and an absorption lag time was used to fit the data using the NONMEM program with the first order conditional estimation option. Figure 35 displays the individual observations with the mean population curve and the 95% confidence interval. The population model parameters (mean values, inter-individual variability, and residual variability) were used to predict the expected concentrations after the administration of an oral dose of 1, 5, and 10 mg.

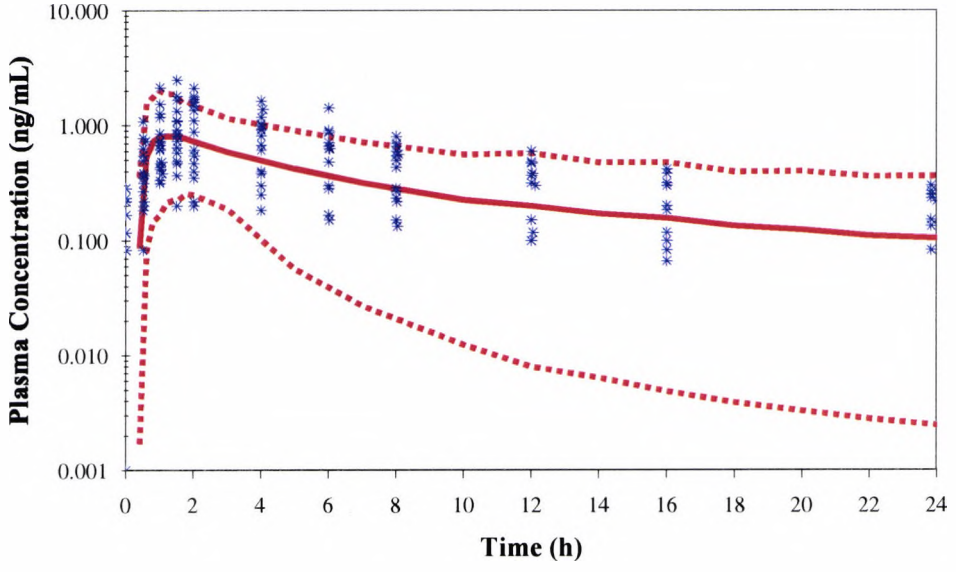

Fig. 35. GR205171 population oral model fit to the individual observations, the mean population curve (solid line) and the 95% confidence intervals (dotted lines) after the administration of an oral dose of 5 mg.

The population PK parameters and inter-individual variability are reported in Table 18 where V represents the central volume, Q the intercompartmental clearance, V_{SS} the volume of distribution at steady state [k = CL/V, k_{12} = Q/V and k_{21} = Q/(V_{SS}-V), k_a the absorption rate, T_{lag} the lag time, and F the bioavalability].

Table 18 **Population model parameters** (mean values, inter-individual variability[a])

	Value	**IIV** (CV)
CL/F (L/h)	650	91
V/F (L)	4880	56
Q/F (L)	296	< 1
V_{SS}/F (L)	3090	< 1
k_a (1/h)	2.83	95
T_{lag} (h)	0.407	8

[a] expressed as coefficient of variation

8.5 Simulated brain receptor occupancy

The integration of the plasma-concentration / brain-occupancy model and the predicted oral concentrations allowed the brain striatum and cortex receptor occupancy to be forecasted after repeated administration of 1, 5, and 10 mg once a day during one week's treatment with GR205171. The simulated mean curves and a 95% confidence interval for % brain receptors occupancy were estimated using a Monte Carlo approach based on the generation of 400 individual kinetic profiles. The simulated brain receptor occupancy accounted both for the inter-individual variability of the population PK model and of the PD model.

Figures 36 to 39 display the simulated plasma concentration profiles, and the expected striatum and cortex receptor occupancy after the oral administration of 1, 5, and 10 mg once a day during one week.

The estimated average receptor occupancy after one week's oral treatment was 25% for 1 mg, 55% for 5 mg, and 65% for 10 mg the striatum, and 85% for 1 mg, 89% for 5 mg, and 90% for 10 mg in the cortex.

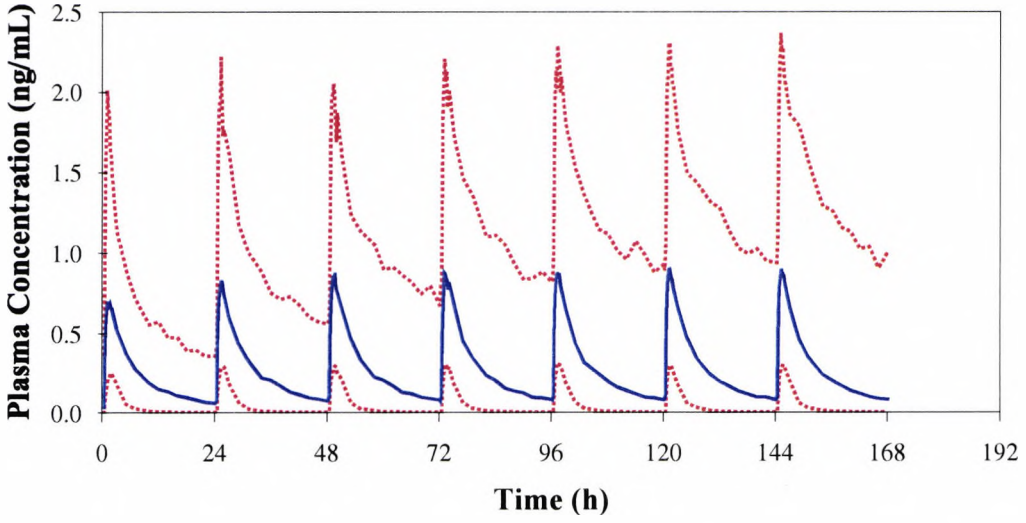

Fig. 36. GR205171 predicted average plasma concentrations with a 95% confidence interval after oral administration of 5 mg.

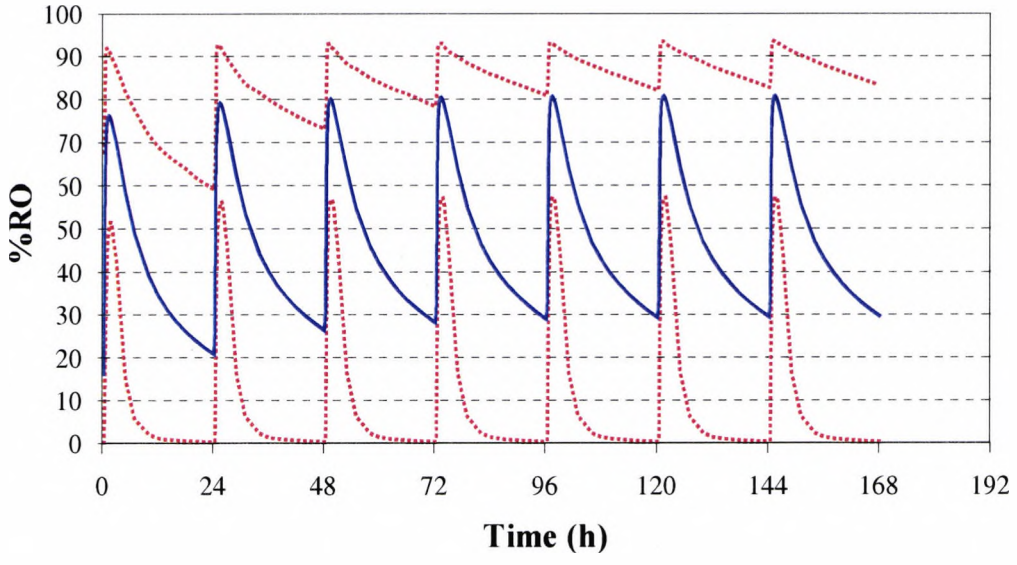

Fig. 37. Predicted average %RO in the striatum with a 95% confidence interval after a 5 mg oral dose.

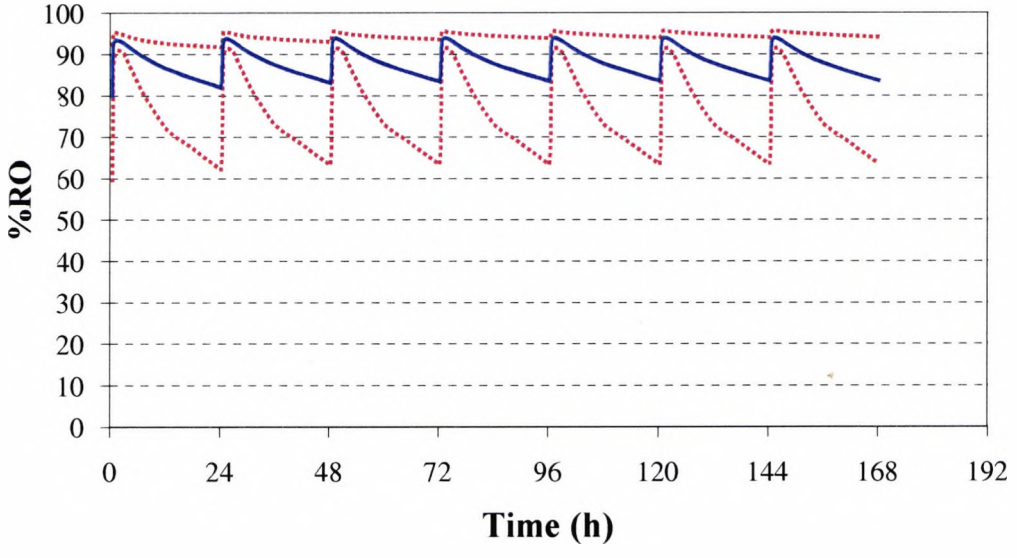

Fig. 38. Predicted average %RO in the cortex with a 95% confidence interval after a 5mg oral dose.

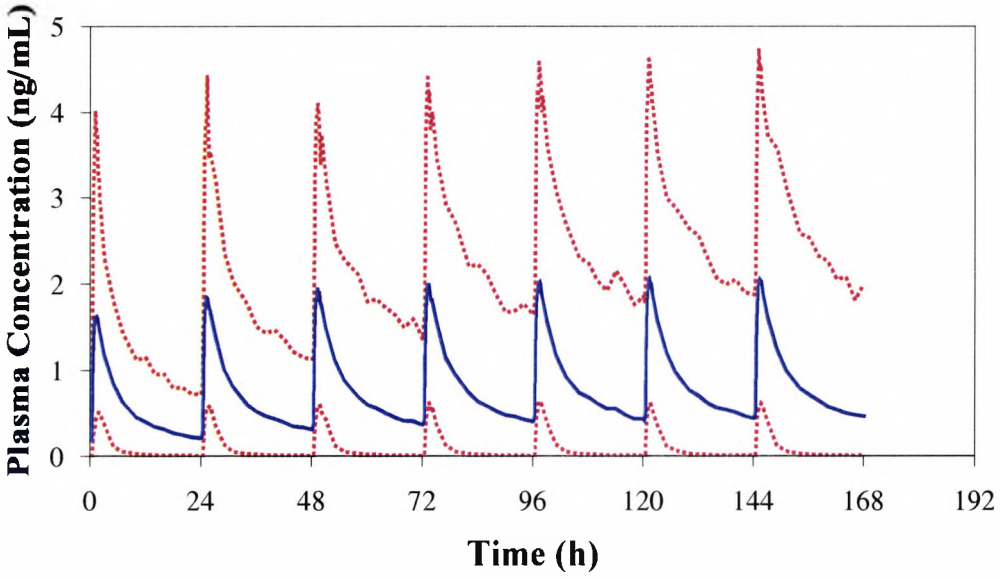

Fig. 39. GR205171 predicted average plasma concentrations with a 95% confidence interval after an oral administration of 10 mg.

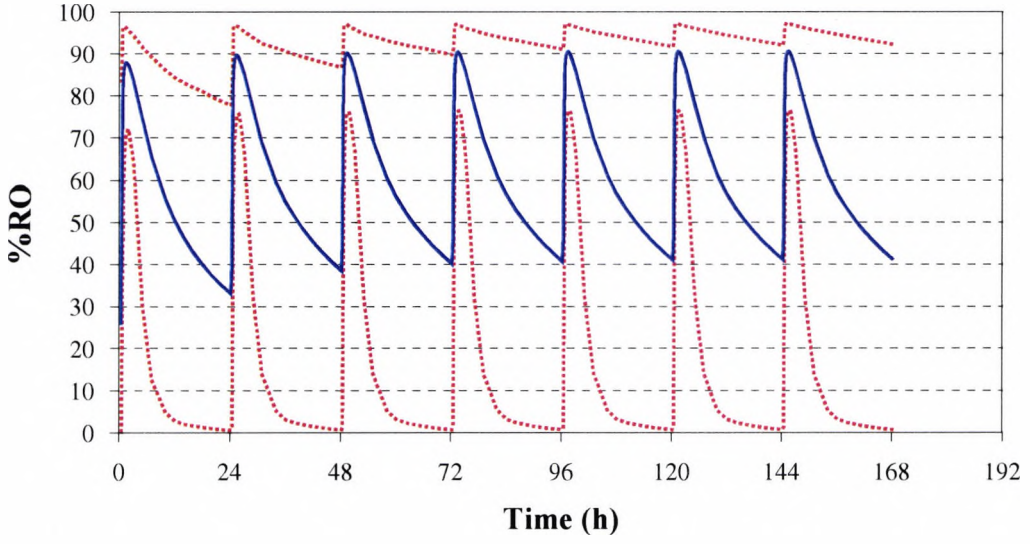

Fig. 40. Predicted average %RO in the striatum with a 95% confidence interval after a 10 mg oral dose.

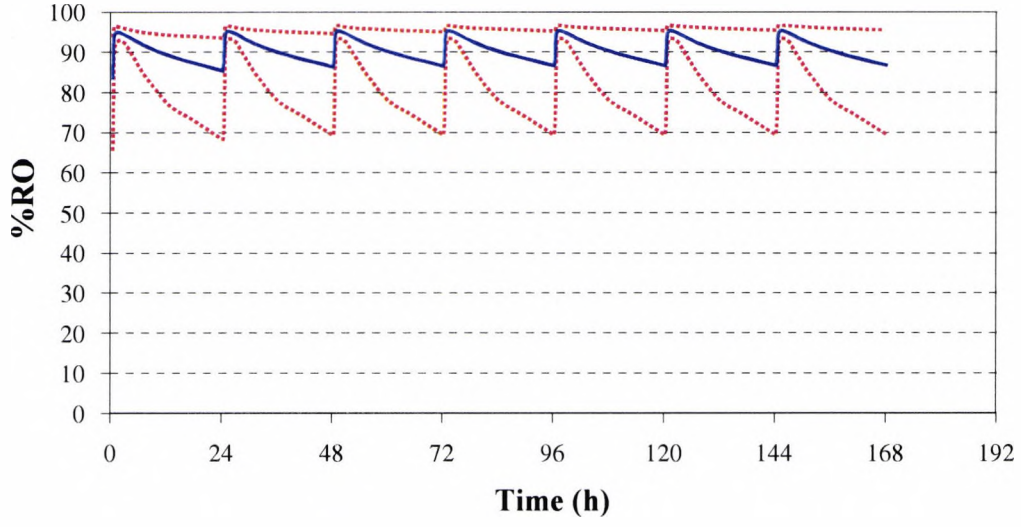

Fig. 41. Predicted average %RO in the cortex with a 95% confidence interval after a 10 mg oral dose.

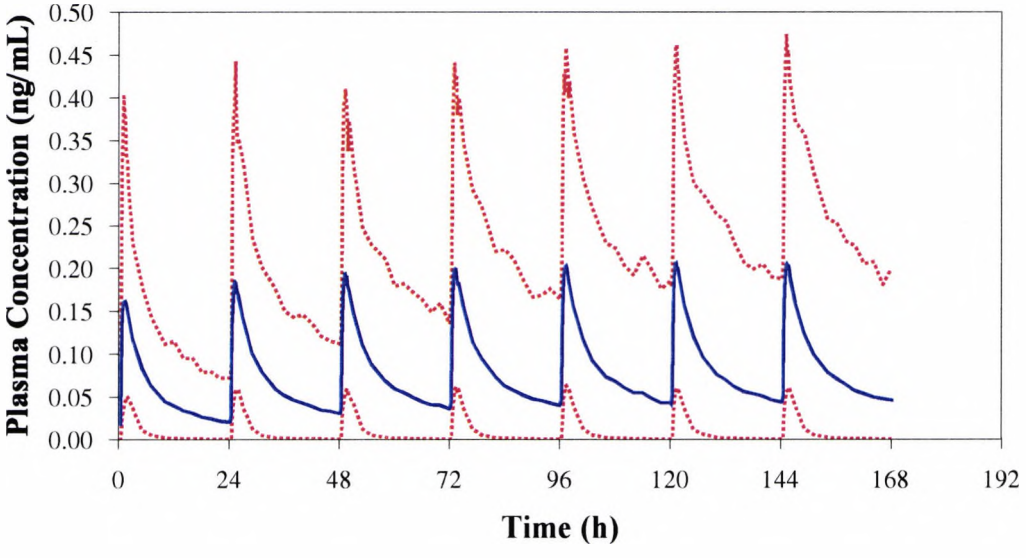

Fig. 42. GR205171 predicted average plasma concentrations with a 95% confidence interval after an oral administration of 1 mg.

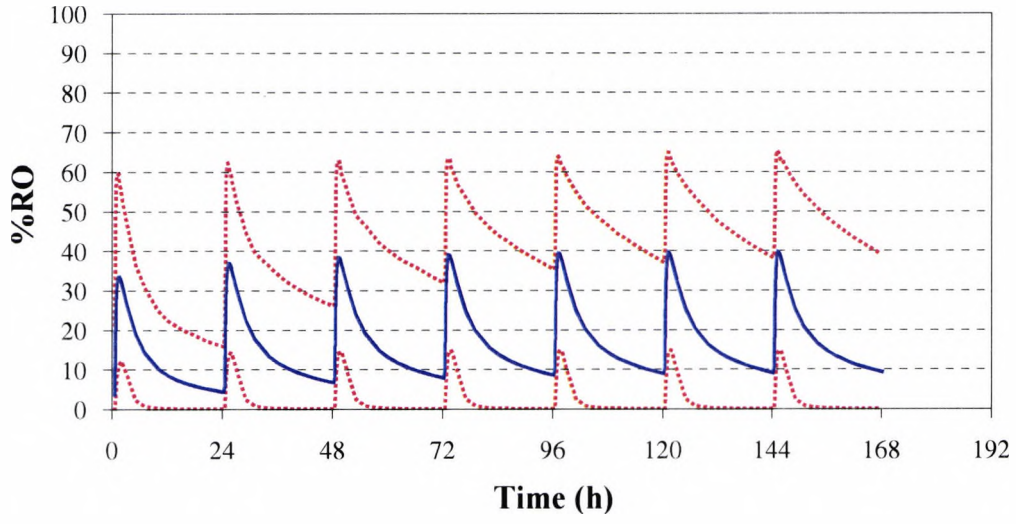

Fig. 43. Predicted average %RO in the striatum with a 95% confidence interval after a 1 mg oral dose.

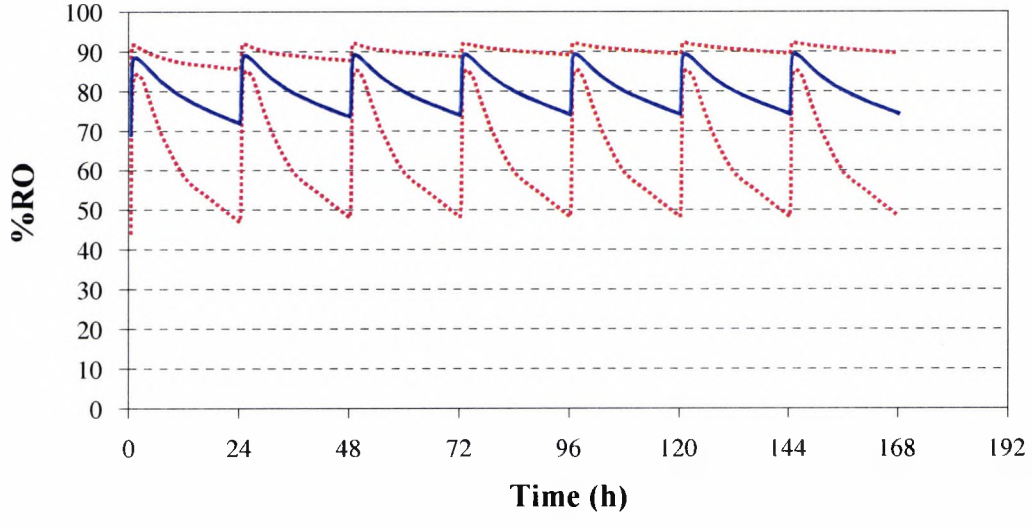

Fig. 44. Predicted average %RO in the cortex with a 95% confidence interval after a 1 mg oral dose.

8.6 Discussion

The present study was carried out to predict the expected brain receptor occupancy for various oral doses and dosage regimens.

A PK/PD approach was introduced to establish the relationship between RO and plasma concentration. In the PET field, according to our knowledge, relating plasma concentration to RO is a novel approach. However, the lack of information at lower doses and consequently concentrations did not allow a robust PK/PD model to be established.

A direct sigmoidal model linking plasma concentration to RO was used. No delay due to the brain penetration and receptor binding was considered. The penetration property of the compound established in the pre-clinical species (data not reported) justifies the assumption of a fast equilibrium between plasma and brain concentrations. Moreover, the evaluation of receptor occupancy on two occasions after dosing does not permit the presence of a hysteresis loop between plasma concentration and RO to be evaluated.

The PD model was built using plasma concentrations and RO data available in the PET study in four subjects with three doses. In order to introduce PK variability, a different population PK analysis was considered. Finally, using the plasma/RO relationship obtained from the PET study (PD model) and the PK population study, a simulation study forecast brain occupancy for various oral dose administrations.

The simulations gave receptor occupancy profiles for different doses and administration regimens. A relationship between the dose, the plasma concentration, and the NK1 receptor occupancy using GR205107 was established. The main goal of this approach is to provide a framework for the prediction of NK1 RO to achieve optimal therapeutic effect in the treatment of the target disease.

8.7 Conclusions

The simulated mean curves and the 95% confidence intervals for % brain receptor occupancy have been estimated using a Monte Carlo approach based on the generation of 400 individual kinetic profiles. The inter-individual variability of both the PK and PD model has been considered.

Due to limited data (few plasma levels to build the PD model), the predictions need to be independently validated.

9 EVALUATION OF THE PREDICTIVE PERFORMANCE OF THE PK/PD MODEL

9.1 Introduction

In the previous chapter a new approach relating PK to receptor occupancy has been developed. The main objective of this investigation is to evaluate the performance of the PK/PD model using new PK and RO data obtained from an oral GR205171 dose study.

The major benefit of relating PK concentration to RO is in cost reduction and acceleration of the drug development. The PET technique facilitates the investigation of the brain-receptor binding process, but the generation of this information is quite expensive. Consequently, the PK/PD approach could improve our understanding of the relationship between PK information and efficacy outcome.

Formally, model precision and bias have to be established employing newly observed data to assess the predictive model performance (Sheiner and Beal, 1981). Due to the limited number of measured RO in the GR205171 oral study, this procedure is not applicable. The predictive performance of the PK/PD model is evaluated by assessing the percentage of observed RO within the estimated confidence interval.

The first part of this chapter describes the estimation of receptor occupancy using the reference tissue methods, while the second part evaluates the predictive capabilities of the PK/PD model.

9.2 PET oral study

9.2.1 Experimental protocol

This study was conducted in 8 healthy male volunteers. Subjects received a PET scan using ^{11}C-GR205171 prior to and 4 hours after the first oral dose of GR205171. 5mg GR205171 once a day was initially investigated in four subjects, then 5 mg twice a day was used in four additional subjects.

The first four subjects on day 1 following the baseline PET scan with ^{11}C- GR205171 received 5mg GR205171 (oral administration), then at 4 hours post dose a second PET scan using ^{11}C- GR205171 was conducted. Each subject received an oral dose every day for 7 days, and two PET scans were conducted on day 7, one before and the other 4 hours after the last oral dose, see details in Table 19.

Table 19 Study design protocol

Study Procedure	Day 1 Predose	Day 1	Day 1 3hrs	Day 1 4hrs	Day 2	Day 3	Day 4	Day 5	Day 6	Day 7 Predose	Day 7	Day 7 3hrs	Day 7 4hrs	Day 8
Oral Dosing		X			X	X	X	X	X		X			
PET scan	X			X						X			X	
PK blood	X		X	X	X			X	X	X		X	X	X

9.2.2 PET

Two equal whole body PET cameras, Siemens ECAT EXACT HR+ were used in the project. These systems generate 63 contiguous slices with a distance of 2.5 mm between planes and an in-plane resolution of 4 mm. The time series which are acquired depend on the tracer and are defined by the camera control program. For evaluation of PET images, regions of interest are outlined on the images.

Each scan lasted approximately 90 minutes and involved the capture of 24 sequential frames (1 x 1 min, 4 x 0.5 min, 4 x 1 min, 4 x 2 min, 8 x 5 min, 2 x 10 min, and 1 x 15 min).

9.2.3 Blood sampling for assay of GR205171

5ml blood samples for the analysis of unlabelled GR205171 were taken at the following times:

- Day 1 and 7; prior to dosing and at 30 min, 1, 1.5, 2, 3, 4, 5, 6, 8, 10, 12 and 24 hour post dose
- Days 5 and 6 prior to dosing.

9.2.4 Model analysis

Based on the results from monkey and IV human studies, all data from PET experiments were analysed using the Simplified Reference Tissue Model (Lammertsma and Hume 1996) presented in Section 3.3.2.

This model approach relies on the absence of specific binding of the ligand in the reference region. It is assumed that the distribution volume of the free ligand is the same in the reference region (cerebellum) and in any other region of interest.

The model equation is described by the expression:

$$C_t(t) = R_1 C_r(t) + \left[k_2 - \frac{R_1 k_2}{1 + BP} \right] C_r(t) \otimes \exp\left[\frac{-k_2 t}{1 + BP} \right] \qquad (92)$$

where $C_t(t)$ and $C_r(t)$ are, respectively, tracer concentrations from a region of interest and the reference tissue; R, k_2 and BP (binding potential) are the estimated parameters; and $\otimes$ is the convolution operator.

The model was numerically identified by non-linear least squares and the SAAMII (Barrett *et al.*, 1998) software package was used. The evaluation of model results is based on the weighted residual plots and the precision of the parameter estimates (expressed as percent CV).

The percent receptor occupancy (%RO) is calculated using the estimated binding potential from baseline (BP) and after unlabelled administration (BP') experiments:

$$RO\% = \frac{BP\text{-}BP'}{BP} \times 100 \qquad (93)$$

9.3 RO estimation

Tables 20-23 report the results for receptor occupancy in two regions of interest (striatum and occipital cortex).

Tables 20-21 report the results of 5mg and 2x5 mg treatments in striatum. Tables 22-23 report the results of 5mg and 2x5 mg treatments in occipital cortex.

In Appendix D the results of the individual fitting are shown. Three data sets (all associated with the occipital cortex) did not reach convergence.

Table 20 Receptor occupancy in striatum (5 mg)

Subj.	RO (%)		
	Day 1 4h after 1st dose	**Day 7** Pre-dose (24h post dosing)	**Day 7** 4h after 7th dose
4235	82	57	73
4236	56	22	54
4237	93	75	94
4238	93	20	81
MEAN (SD)	**81 (17)**	**44 (27)**	**76 (17)**

Table 21 Receptor occupancy in striatum (2x5 mg)

Subj.	RO (%)		
	Day 1 4h after 1st dose	**Day 7** Pre-dose (24h post dosing)	**Day 7** 4h after 7th dose
4239	97	98	98
4240	92	55	58
4241	73	26	70
4242	73	64	81
MEAN (SD)	**84 (13)**	**61 (30)**	**77 (17)**

Table 22 Receptor occupancy in oc. cortex (5 mg)

Subj.	RO (%)		
	Day 1 4h after 1st dose	**Day 7** Pre-dose (24h post dosing)	**Day 7** 4h after 7th dose
4235	95	55	94
4236	92	64	90
4237	100	90	99
4238	100	73	95
MEAN (SD)	**97 (4)**	**71 (15)**	**95 (4)**

Table 23 Receptor Occupancy in oc. cortex (2x5 mg)

Subj.	RO (%)		
	Day 1 4h after 1st dose	**Day 7** Pre-dose (24h post dosing)	**Day 7** 4h after 7th dose
4239	100	99	99
4240	86	NA	87
4241	91	NA	89
4242	87	82	NA
MEAN (SD)	**91 (6)**	**91 (12)**	**92 (6)**

NA: Not available due to lack of algorithm convergence

9.4 Assessment of predictive performance of the PK/PD model

A simulation was run to assess both 5 and 2x5 mg oral dose results (brain receptor occupancy after 5 mg twice a day was not included in the previous simulations). In total, 400 simulated individual kinetic profiles were generated using a Monte Carlo approach employing PK and PD values reported in Tables 17 and 18.

The number of observed RO within the predicted 95% confident interval was used to evaluate the predictive performance of the PK/PD model. The simulated profiles with observed RO are plotted in Figures 45-48.

In Figure 45 and 46 the simulated and observed %ROs after 5 mg are plotted. The simulated brain receptor occupancy accounts for the inter-individual variability in PK and PD parameters. The predictive accuracy of the PK/PD model was excellent in striatum where all observed receptor occupancies were within the confidence interval. A good predictive accuracy was observed in the cortex region where 10 out of 12 observed RO were within the 95% confidence interval.

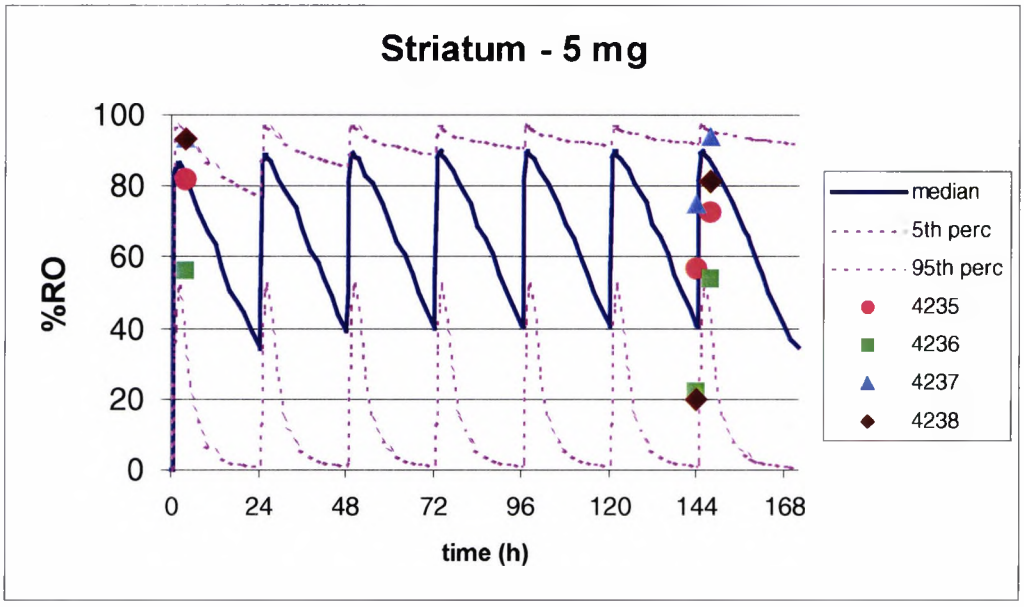

Fig. 45. Median %RO prediction in striatum with a 95% confidence interval and observed %RO after a 5-mg dose

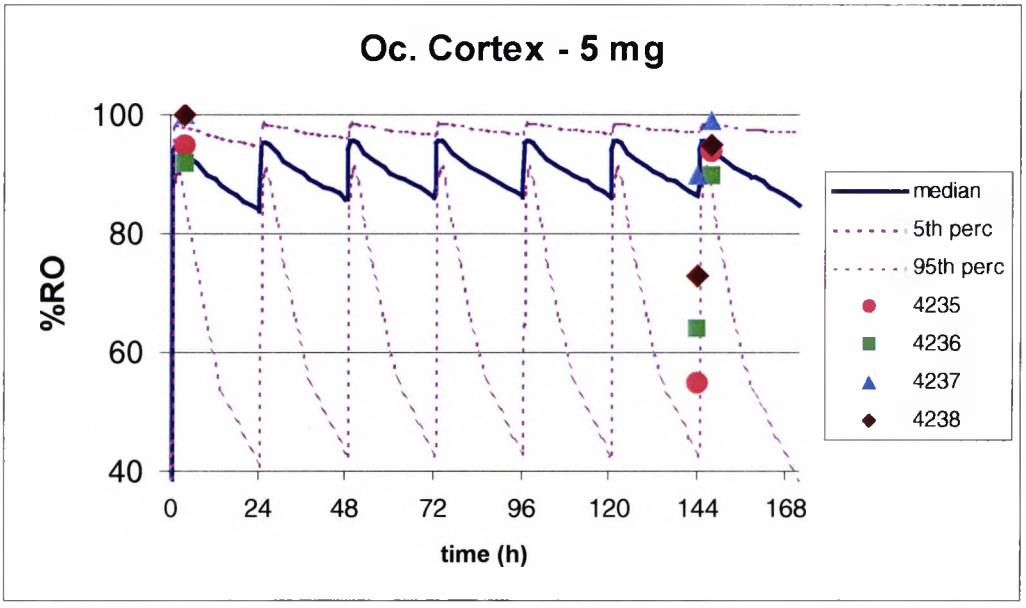

Fig. 46. Median %RO prediction in occipital cortex with a 95% confidence interval and observed %RO after a 5-mg dose

Figures 47 and 48 show the simulated and observed %RO after 5 mg twice a day. A good prediction of the brain receptor occupancy was obtained. Only one observed RO out of all striatum and cortex data was outside the confidence interval (%RO for subject 4239 after 2 hour).

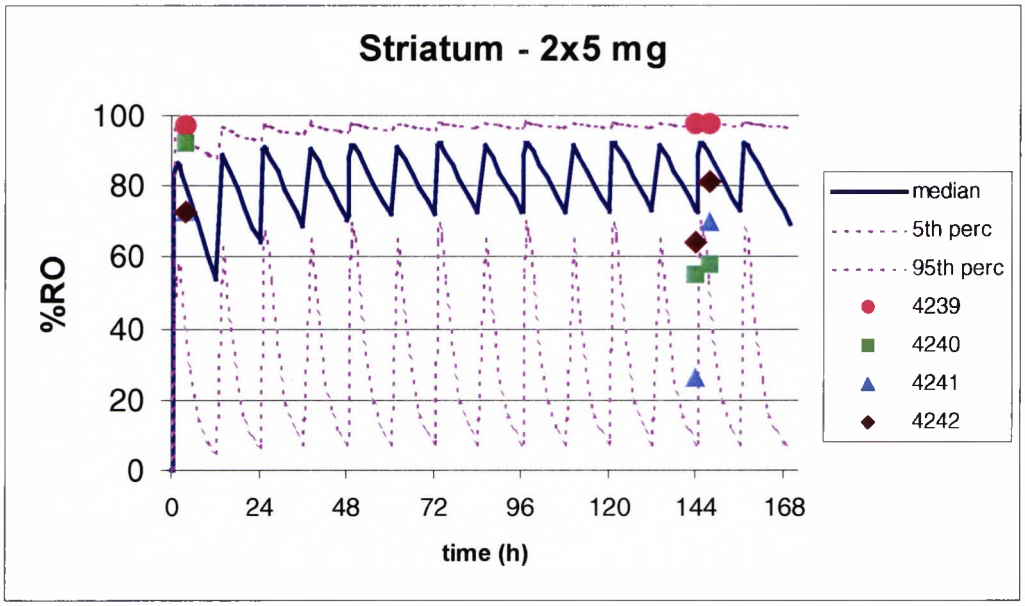

Fig. 47. Median %RO prediction in striatum with a 95% confidence interval and observed %RO after a 5-mg dose twice a day

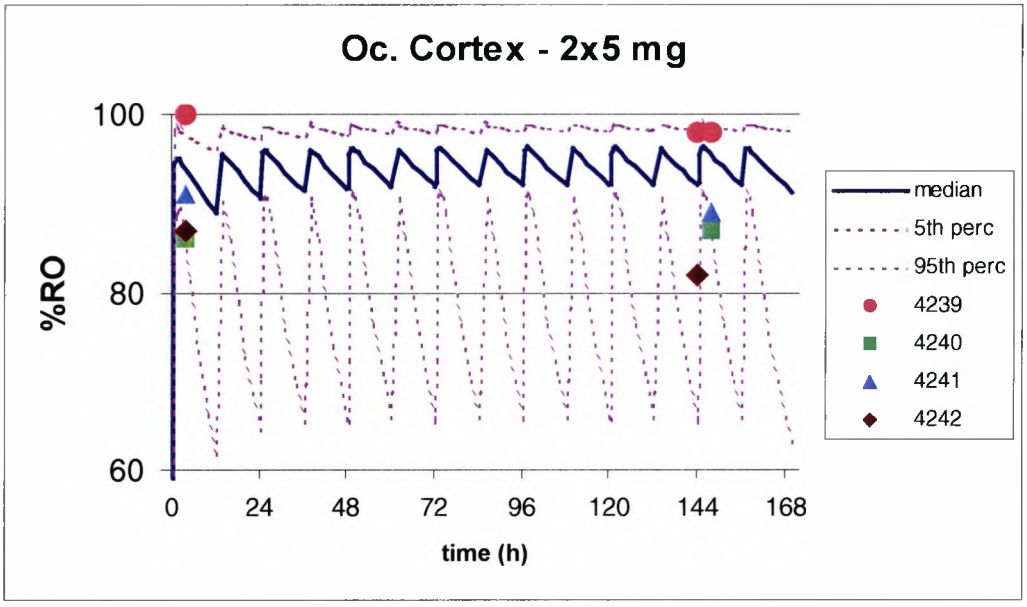

Fig. 48. Median %RO prediction in occipital cortex with a 95% confidence interval and observed %RO after a 5-mg dose twice a day

The number of observed RO within the 95% confidence interval is summarised in Table 24.

Table 24 Evaluation of the predictive performance of the PK/PD model

Region	Dose (mg)	Number RO within CI / Total number of RO	% Accuracy
Striatum	5	12/12	100%
	2x5	11/12	92%
Cortex	5	10/12	83%
	2x5	8/9	89%

9.5 Discussion

High values of receptor occupancy are attained after treatment with both 5 mg and 2x5 mg. In Table 25 the average receptor occupancy and SD among the four subjects receiving the same drug treatment are summarised. Similar results for 5mg and 2x5 mg dosing at 4 hours after drug administration are obtained, whereas 2x5 mg dosing gave an increased RO at 24 hour post dose.

The striatum presents a lower level of RO than occipital cortex especially for the 24 hour post dose experiment. This is in agreement with previous results.

Table 25 Summary of observed receptor occupancy

		% RO (SD)		
Region of Interest	Dose	**Day 1** 4h after 1st dose	**Day 7** Pre-dose (24h post dose on day 6)	**Day 7** 4h after 7th dose
Striatum	5 mg	**81 (17)**	**44 (27)**	**76 (17)**
	2x5 mg	**84 (13)**	**61 (30)**	**77 (17)**
Oc. Cortex	5 mg	**97 (4)**	**71 (15)**	**95 (4)**
	2x5 mg	**91 (6)**	**91 (12)**	**92 (6)**

The main objective of this chapter was to evaluate the prediction of the PK/PD model with independent data. The PK/PD model was assessed by comparing the model predicted RO with values observed in a separate experiment employing 5mg and 2x5 mg dosing. Figures 45-48 show a good agreement between the predictions and

observations. According to the results presented in Table 24 almost all estimated RO after oral dosing are within the estimated 95% confidence interval. These findings validate the PK/PD model based predictions.

The principal limitations of the proposed approach originate from questionable accuracy of the inter-subject variability due to the low number of intravenous PK profiles (4 subjects) used to describe the receptor occupancy vs concentration and the linear kinetic assumption for doses from 1 to 30 mg used to generate the oral PK profile.

This simulation framework has provided the opportunity to assess the approximate levels of occupancy of central NK1 receptor for different doses. In this way, the dose selection strategy for clinical trials with a therapeutic indication in patients can be provided in rational way.

This approach is useful, especially when the therapeutic window is quite narrow, to increase the drug effect by increasing the dose level. With the knowledge of plasma-receptor occupancy relationship it is possible to establish the trough plasma level giving the fully receptor blockage (usually %RO > 90%) and consequently define the relationship between dose and RO (Hargreaves, 2002). This enables the dose to be increased while reducing the possible adverse events related to the compound. Moreover, it is also possible to establish whether absence of therapeutic action in a clinical trial is due to an inadequate receptor blockage rather than an indication that the target receptor pathway is not directly involved in the studied disease.

9.6 Conclusion

The main objective of this chapter was to evaluate the predictive performance of the PK/PD model presented in the previous chapter. The wider aim was to evaluate a methodology that allows RO from PK concentrations to be forecasted.

RO after oral administration of GR205171 was estimated. Two different dosage regimens (5 mg once a day and 5 mg twice a day for 7 days) were evaluated and PET scans on day 1 and day 7 were performed. According to the findings of the IV human study, a reference approach was applied. High levels of RO were estimated in all regions of interest.

Despite several limitations principally due to the low number of PK and PET experiments employed to build up the PK/PD model, the approach was able to predict with accuracy the RO range after oral administration.

10 DISCUSSION AND CONCLUSION

10.1 Overall discussion

Positron Emission Tomography (PET) is an imaging technology used to measure the distribution and kinetics of a positron-emitting isotope in in-vivo tissue. Due to its inherent quantitative biochemical nature, PET is in the extraordinary position to reveal the molecular mechanisms of human disease and to facilitate the development of new drugs.

PET utilises compounds labelled with generally short-lived, positron emitting radionuclides. These tracer compounds are injected intravenously and are distributed, bound, and eliminated according to the biological properties of the native compound. After a positron has been emitted from the tracer, it annihilates and produces two high-energy gamma rays that are readily detected by the surrounding detector system. The raw data thus collected are reconstructed and a time series of tomographic images is generated. The images show the quantitative distribution and time course of the tracer in contiguous planes. The most commonly used positron emitting nuclide is ^{11}C, with a half-life of 20 minutes. The half-life of ^{11}C allows tracer kinetics to be recorded during a time window of about 60-90 minutes.

The principal aim of this PhD thesis was to characterise the NK-1 receptor PET ligand [^{11}C]GR-205171, a high affinity and selective NK1-receptor antagonist labelled with ^{11}C in the Uppsala University PET Centre (Bergstom *et al.*, 2000), and to test whether [^{11}C]GR-205171 is sufficiently robust and sensitive to provide reliable information about NK-1 receptor occupancy using positron emission tomography (PET).

[^{11}C]GR-205171, a radioactive, brain-penetrant tracer that binds to the NK1 receptor permits real-time evaluation of receptor occupancy in living animals and humans via modeling interpretation of PET imaging. PET studies in monkeys and humans showed that, after both IV and oral doses, [^{11}C]GR-205171 can be displaced by

pharmacological doses of NK-1 antagonists, and therefore may be a suitable radioligand to investigate the degree and duration of receptor occupancy.

In order to provide interpretation on receptor-ligand interaction from PET measurements, different methods have been used (Mintum *et al.*, 1984; Wong *et al.*, 1986; Perlmutter *et al.*, 1986; Lammertsma *et al.*, 1996; Lammertsma and Hume, 1996; Delforge *et. al.*, 1993). The general description of receptor-ligand interaction must account for the free-ligand penetration through the blood brain barrier (BBB) and the ligand receptor binding in the tissue. Many factors are involved in these processes: the BBB penetration, the presence of metabolites, non-specific binding, the affinity and selectivity of specific binding.

An experiment in the non-steady state, which includes a simultaneous administration of labelled and unlabelled ligand (co-injection or displacement experiment), is necessary to estimate affinity (K_D) and receptor density (B_{max}), and to obtain quantitative information on receptor occupancy. At variance with this approach, a simple tracer experiment leads to a (pseudo) steady state condition, which does not permit the parameters K_D and B_{max} to be estimated but allows estimations of aggregated parameters, i.e. the potential binding (BP), representing the ratio B_{max}/K_D. The percent receptor occupancy (%RO) is then estimated using the binding potential computed before (BP) and after treatment (BP') experiment as %RO=100*(BP-BP')/BP.

Three different methods were used to describe the kinetics of [^{11}C]GR-205171. A time varying model was used to estimate K_D and B_{max} from a co-injection (simultaneous injection of labelled and unlabelled ligand) (Delforge et. al, 1990; Delforge et. al, 1993). The design of this trial permits the achievement and simultaneous analysis of different values of receptor occupancy. The second method uses the arterial concentration of the tracer corrected for metabolites as an input function (Mintum et al., 1984; Perlmutter et al., 1986). The third method is based on a region void of specific receptors acting as the reference region (Lammertsma *et al.*, 1996; Lammertsma and Hume, 1996).

Unfortunately, due to technical problem, it was not possible to correct properly the arterial blood concentrations for the metabolites. Consequently models using this input function (also the time varying approach) could not be applied. Therefore, the [^{11}C]GR-205171 signal was quantified using the reference tissue model that relies on the presence of a region without specific NK1 receptor (confirmed by cerebellum-autoradiography in monkey).

The absence of the arterial concentration corrected for metabolites represents the weakness of this work. The full validation of the present approach should include the comparison with the arterial methodology.

We tested for both the reversibility and irreversibility of receptor–ligand binding during the 90 min of PET experiments. Considering reversibility, we assumed that it was possible to estimate both the association (k_3) and dissociation (k_4) rate constants of the ligand-receptor interaction. For this purpose, the Reference and the Simplified Reference Tissue Models were used. In the irreversible scenario, we assumed an irreversible binding ($k_4 = 0$) using a modified version of the Reference Tissue Model. The statistical criteria indicated that the Simplified Reference Tissue Model (STRM) was the most appropriate model to describe the time-activity curves and provided precise estimates of model parameters.

Alternative parameter estimation strategies based on the use of non-linear mixed effect models accounting for intra- and inter-subject variability of the time-activity curves and for the identification of possible sources of this variability using individual covariate measurements were developed in this thesis. A major limitation of the standard estimation approaches is related to the underlying assumption that each time-activity curve comes from a separate individual. To overcome these limitations the mixed effect models were investigated including also dose in a second stage.

Despite the limited number of subjects and the limited number of occasions, the non-linear mixed effects modelling represents a valid alternative analysis approach because

it accounts for the repeated-measurement structure of the data and supplies an estimate of the different variability components of the parameter values.

An important objective in the clinical development of any novel CNS therapy is the establishment of a clear relationship between the dose or plasma level of the drug and the receptor occupancy achieved. The present methodology can be used to guide dosing in efficacy studies, as the achievement of adequate receptor occupancy in proof-of-concept studies is a prerequisite for adequate assessment of efficacy hypotheses. PET imaging data, together with plasma drug levels can be used to examine the dose-receptor occupancy relationship in successful clinical studies.

In the last part of the thesis, the relationship between dose, plasma concentration, and NK1 receptor occupancy using the GR205171 was examined. The goal of this PK/PD analysis was to provide a framework for prediction of NK1 receptor occupancy required to achieve optimal therapeutic effect of the target disease. In fact, according to the plasma-receptor occupancy link (sigmoidal model) it was possible to determine plasma levels giving the full receptor blockage and consequently to define the relationship between dose and the RO profile.

The PK/PD relationship was established using PET data after GR205171 IV administration and a forecasted RO profile after different oral dose treatments. Finally, the predictive performance of the PK/PD model was independently validated using data from PET studies after oral administration of GR205171.

10.2 Achievement of objectives

The main objective of this thesis was to define the appropriate model for GR205171 tracer and to calculate receptor occupancy in monkey and human brain. This objective was met but, due to lack of arterial radioactivity only models relying on the presence of a region without specific receptor were implemented. This did not allow the reference tissue models with the models using the arterial radioactivity as an input function to be compared. We introduced novel methodological approaches for

parameter estimation in the PET field, the Bayesian and the non-linear mixed effect approaches.

The definition of a relationship between plasma drug concentration and receptor occupancy was an important achievement of this work. The demonstration of quantitative relationships between drug binding *in vivo* and plasma concentration data allowed an RO profile after different dose regimens to be forecasted. The predictive performance of the PK/PD model was independently validated employing new PET data.

10.3 Future work

The full characterisation of an appropriate model for GR205171 tracer should include the comparison with the arterial methodology in order to increase confidence in the results and to ascertain that no other factors, such as changes in cerebral blood flow or saturation of the metabolic activity, affect the estimation of receptor occupancy.

A simulation study to understand the impact of bias on the estimation of receptor occupancy with 90 minutes PET scan should be implemented for GR205171.

REFERENCES

Abadie P, Rioux P, Scatton B, Zarifian E, Barré L, Patat A, Baron JC. Central benzodiazepine receptor occupancy by zolpidem in the human brain as assessed by positron emission tomography. *Eur J Pharmacol.*1996; **295**:35-44.

Aboagye EO, Price PM, Jones T. In vivo pharmacokinetics and pharmacodynamics in drug development using positron-emission tomography. *Drug Discov Today.* 2001 **6**:293-302.

Barrett PHR, Bell BM, Cobelli C, Golde H, Schumitzky A, Vicini P, Foster DM. SAAMII: simulation, analysis, and modeling software for tracer and pharmacokinetic studies. *Metabolism.* 1998, **47**:484-492.

Beal SL, Scheiner LB. *NONMEM Users Guide*, NONMEM Project Group, USCF, San Francisco, CA, 1992.

Bergstom M, Fasth KJ, Kilpatrick G, Ward P, Cable KM, Wipperman M.D, Sutherland DR, Langstrom B. Brain uptake and receptor binding of two [^{11}C]labelled selective high affinity NK1-antagonists, GR203040 and GR205171-PET studies in Rhesus Monkey. *Neuropharmacology.* 2000; **39**:664-70.

Delforge J, Syrota A, Bottlaender M, Varastet M, Loc'h C, Bendriem B, Crouzel C, Brouillet E, Maziere M. Modelling analysis of [^{11}C]Flumazenil kinetics studied by PET: application to a critical study of the equilibrium approaches. *J Cereb Blood Flow Metab.* 1993; **13**:454-468.

Delforge J, Syrota A, Mazoyer BM. Identifiability analysis and parameter identification of an in vivo ligand-receptor model from PET data. *IEEE Trans Biomed Eng.* 1990; **37**:653-61.

Dobson J. An Introduction to Statistical Modelling. Chapman and Hall, New York, 1983.

Farde L. PET in neuropsychiatric drug development. In: Comar D eds. *PET for drug development and evaluation.* Dordrech: Kluwer Accademic Publisher, 1995; 51-92.

Farde L. The advantage of using positron emission tomography in drug research. *Trends Neurosci.* 1996; **19**:211-14.

Fitzgerald PB, Kapur S, Remington G, Roy P, Zipursky RB. Predicting haloperidol occupancy of central dopamine D2 receptors from plasma levels. *Psychopharmacology.* 2000; **149**:1-5.

Grasby PM. Imaging strategies in depression. *J Psychopharmacol.* 1999; **13**:346-351.

Halldin C, Gulyas B, Farde L. PET studies with carbon-11 radioligands in neuropsychopharmacological drug development. *Curr Pharm Des.* 2001; **7**:1907-29.

Hargreaves R. Imaging substance P receptors (NK1) in the living human brain using positron emission tomography. *J Clin Psychiatry.* 2002; **63 Suppl 11**:18-24.

Hoffman EJ, Phelps ME. Positron Emission Tomography: Principles and quantitation. In: Phelps ME, Maziotta J, Schelbert H, eds. *Positron Emission Tomography and Autoradiography: Principles and Applications for the Brain and Heart.* New York: Raven Press, 1986; 237-286.

Karlsson MO, Sheiner LB. The importance of modeling interoccasion variability in population pharmacokinetic analyses. *J Pharmacokin Biopharm.* 1993; **21**:735-750.

Keller F, Giehl M, Czock D, Zellner D. PK-PD curve-fitting problems with the Hill equation? Try one of the 1-exp functions derived from Hodgkin, Douglas or Gompertz. *Int J Clin Pharmacol Ther.* 2002; **40**:23-9.

Kramer MS, Cutler N, Feighner J, et al. Distinct mechanism for antidepressant activity by blockade of central substance P receptors. *Science.* 1998; **281**:1640-1645.

Lalonde RL, Ouellet D, Kimanani EK, Potvin D, Vaughan LM, Hill MR. Comparison of different methods to evaluate population dose-response and relative potency: importance of interoccasion variability. *J Pharmacokin Biopharm.* 1999; **27**:67-83.

Lammertsma AA, Bench CJ, Hume SP, Osman S, Gunn K, Brooks DJ, Frackowiak RS. Comparison of methods for analysis of clinical [^{11}C]raclopride studies. *J Cereb Blood Flow Metab.* 1996; **16**:42-52.

Lammertsma AA, Hume SP. Simplified reference tissue model for PET receptor studies. *Neuroimage.* 1996; **4**: 153-8.

Ludden TM, Beal SL, Sheiner LB. Comparison of the Akaike Information Criterion, the Schwarz criterion and the F test as guides to model selection. *J Pharmacokin Biopharm* 1994; **22**:431-445.

Mackay D. Concentration-response curves and receptor classification: Null method or operational model? *Trends Pharmacol Sci.* 1988; **9**: 202-205.

Maitre PO, Buhrer M, Thomson D, Stanski DR. A three-step approach combining Bayesian regression and NONMEM population analysis: Application to Midazolam. *J Pharmacokin Biopharm.* 1991; **19**:377-384.

Mazoyer BM, Huesman RH, Budinger TF, Knittel BL. Dynamic PET data analysis. *J Comput Assist Tomogr.* 1986; **10**:645-53.

McGonigle DJ, Howseman AM, Athwal BS, Friston KJ, Frackowiak RSJ, Holmes AP. Variability in fMRI: An examination of intersession differences. *Neuroimage.* 2000; **11:**708-734.

Mintum MA, Raichle ME, Kilbourn ME, Wooten GF, Welch MJ. A quantitative model for the in vivo assessment of drug binding sites with PET. *Ann Neurol.* 1984; **15**:217-227.

Nutt D. Substance-P antagonists: A new treatment for depression? *Lancet.* 1998; **352**:1644-1646.

Paans AM, Vaalburg W. Positron Emission Tomography in Drug Development and drug Evaluation. *Curr Pharm Des.* 2000; **6**:1583-1591.

Paans AM, van Waarde A, Elsinga PH, Willemsen AT, Vaalburg W. Positron emission tomography: the conceptual idea using a multidisciplinary approach. *Methods.* 2002; **27**:195-207.

Parsey RV, Slifstein M, Hwang DR, Abi-Dargham A, Simpson N, Mawlawi O, Guo NN, Van Heertum R, Mann JJ, Laruelle M. Validation and reproducibility of measurements of 5-HT_{1A} receptor parameters with [*carbonyl*-^{11}C]WAY-100635 in humans: Comparison of arterial and reference tissue input function. *J Cereb Blood Flow Metab.* 2000; **20**:1111-1133.

Perlmutter JS, Larson KB, Raichle ME, Markham J, Mintun MA, Kilbourn MR, Welch MJ. Strategies for in vivo measurement of receptor binding using positron emission tomography. *J Cereb Blood Flow Metab.* 1986; **6**:154-69.

Phelps ME, Maziotta J, Schelbert H, eds. *Positron Emission Tomography and Autoradiography: Principles and Applications for the Brain and Heart.* New York: Raven Press, 1986.

Qume M. Overview of ligand-receptor binding techniques. *Methods Mol Biol.* 1999; **106**:3-23.

Rupniak NM, Kramer MS. Discovery of the antidepressant and anti-emetic efficacy of substance P receptor (NK1) antagonists. *Trends Pharmacol Sci.* 1999; **20**:485-90.

Saria A. The tachykinin NK1 receptor in the brain: pharmacology and putative functions. *Eur J Pharmacol.* 1999; **375**:51-60.

Sheiner LB, Beal SL. Evaluation of methods for estimating population pharmacokinetics parameters. I. Michaelis-Menten model: routine clinical pharmacokinetic data. *J Pharmacokin Biopharm.* 1980; **8**:553-71.

Sheiner LB, Beal SL. Some suggestions for measuring predictive performance. *J Pharmacokin Biopharm.* 1981; **9**:503–512

Sheiner LB, Beal SL. Evaluation of methods for estimating population pharmacokinetic parameters. III. Monoexponential model: routine clinical pharmacokinetic data. *J Pharmacokin Biopharm.* 1983; **11**:303-19.

Sheiner LB, Ludden TM. Population pharmacokinetics/dynamics. *Annu Rev Pharmacol Toxicol.* 1992; **32**:185-209.

Slifstein M, Laruelle M. Models and methods for derivation of in vivo neuroreceptor parameters with PET and SPECT reversible radiotracers. *Nucl Med Biol.* 2001; **28**:595-608.

Stephenson RP. A Modification of Receptor Theory. *Brit J Pharmacol.* 1956; **11**,379.

Van Waarde A. Measuring receptor occupancy with PET. *Current Pharm Design.* 2000; **6**:1593-1610.

Wong DF, Gjedde A, Wagner HN Jr, Dannals RF, Douglass KH, Links JM, Kuhar MJ. Quantification of Neuroreceptors in the living human brain. II. Inhibition studies of receptor density and affinity. *J Cereb Blood Flow Metab.* 1986; **6**:147-53.

Wong DF, Gjedde A, Wagner HN Jr. Quantification of neuroreceptors in the living human brain. I. Irreversible binding of ligands. *J Cereb Blood Flow Metab.* 1986; **6**:137-46.

Young AB, Frey KA, Agranoff BW. Receptor Assays: In Vitro and In Vivo. In: Phelps ME, Maziotta J, Schelbert H, eds. *Positron Emission Tomography and Autoradiography: Principles and Applications for the Brain and Heart.* New York: Raven Press, 1986;73-111.

Zamuner S, Gomeni R, Bye A. Estimate the time varying brain receptor occupancy in PET imaging experiments using non-linear fixed and mixed effect modeling approach. *Nucl Med Biol.* 2002; **29:**35-43.

APPENDIX

Appendix A

In this Appendix the standard uptake value (SUV) for each PET scan in the IV human study is reported. The SUV curve represents a normalised activity profile in a selected region of interest measured and reconstructed by the PET system during the scan.

Different PET scans were performed for each subject: a baseline experiment, a co-injection experiment and a series of experiments after the unlabelled drug administration (5 mg, 1 mg, 0.1, mg, and 0.01 mg).

In all figures the Cerebellum and Striatum profiles (upper part) and all the drawn regions of interest profiles (lower part) are illustrated.

Data Plots

Dose: 5 mg

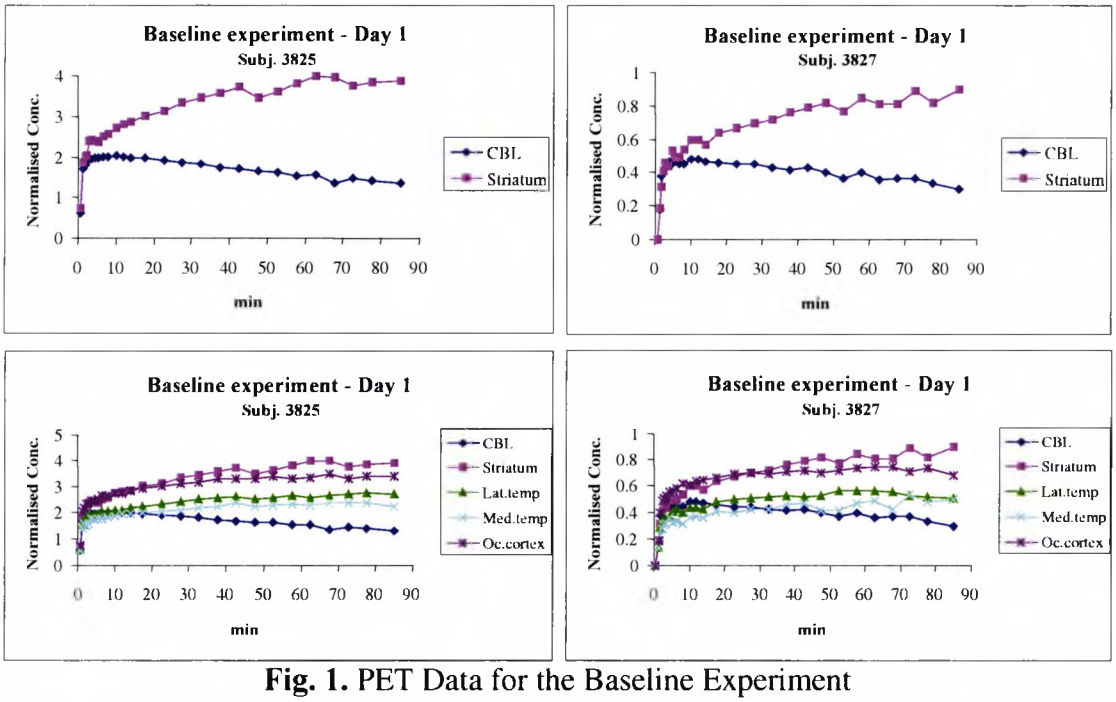

Fig. 1. PET Data for the Baseline Experiment

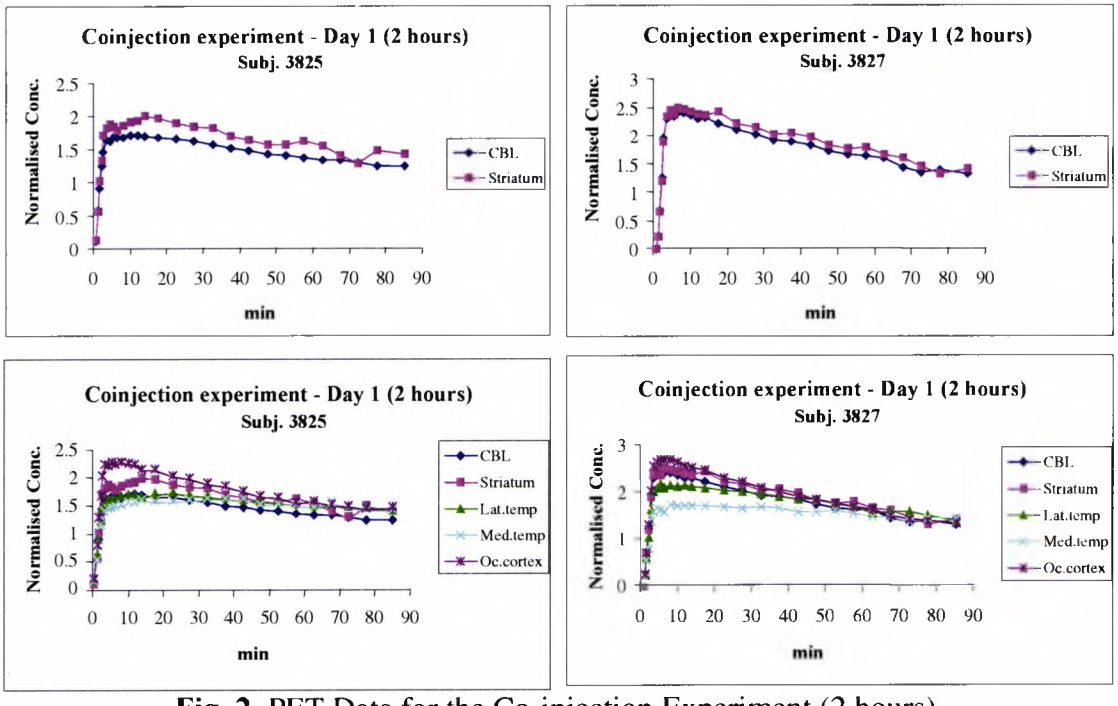

Fig. 2. PET Data for the Co-injection Experiment (2 hours).

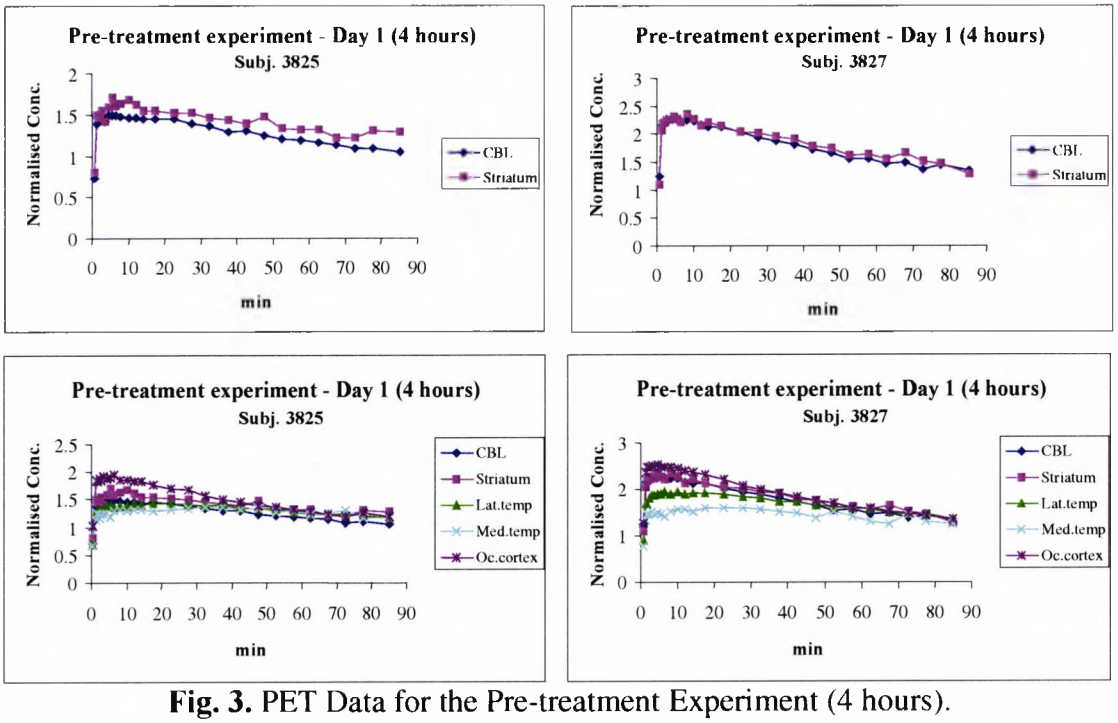

Fig. 3. PET Data for the Pre-treatment Experiment (4 hours).

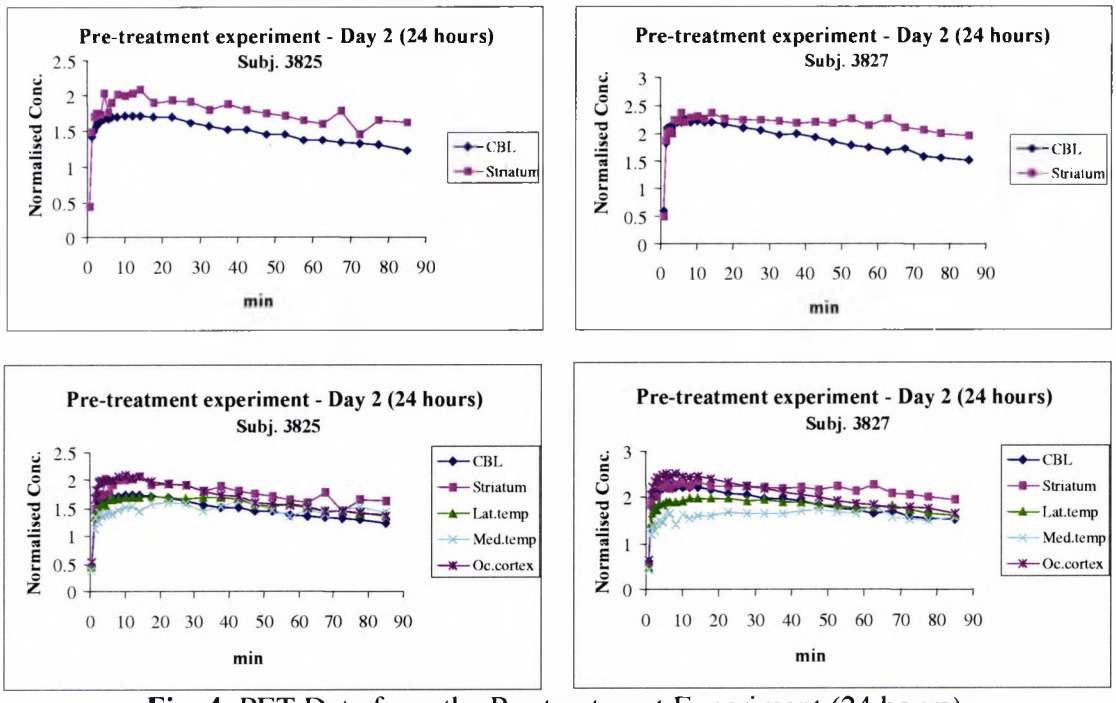

Fig. 4. PET Data from the Pre-treatment Experiment (24 hours).

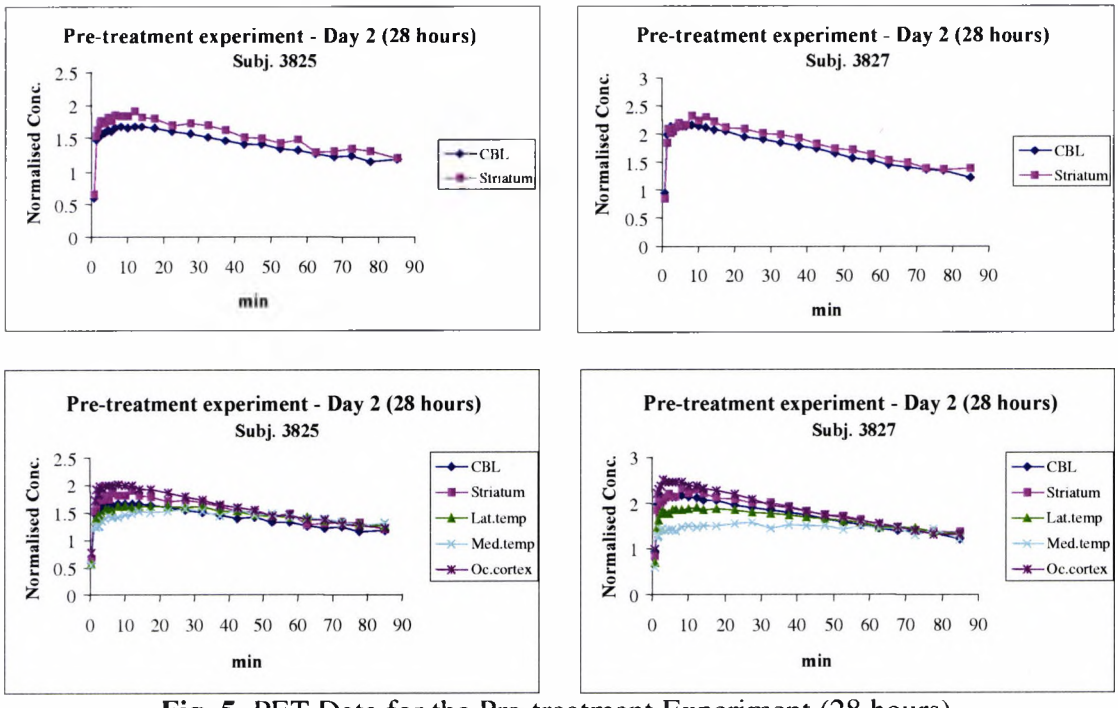

Fig. 5. PET Data for the Pre-treatment Experiment (28 hours).

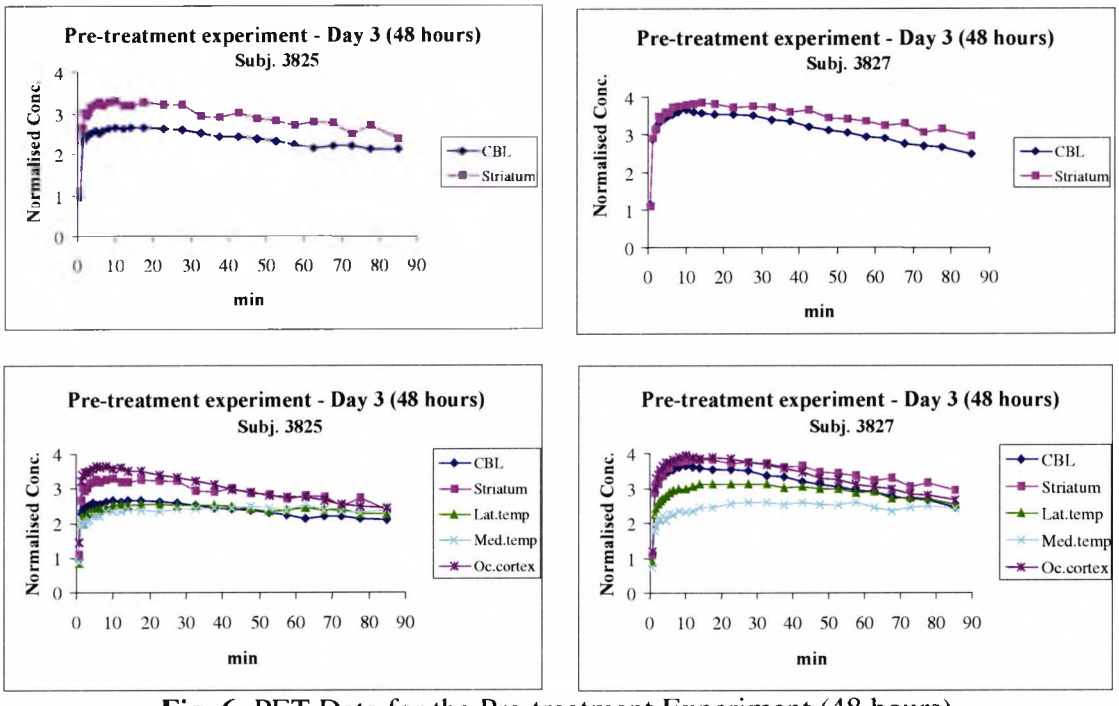

Fig. 6. PET Data for the Pre-treatment Experiment (48 hours).

Dose: 0.1 mg

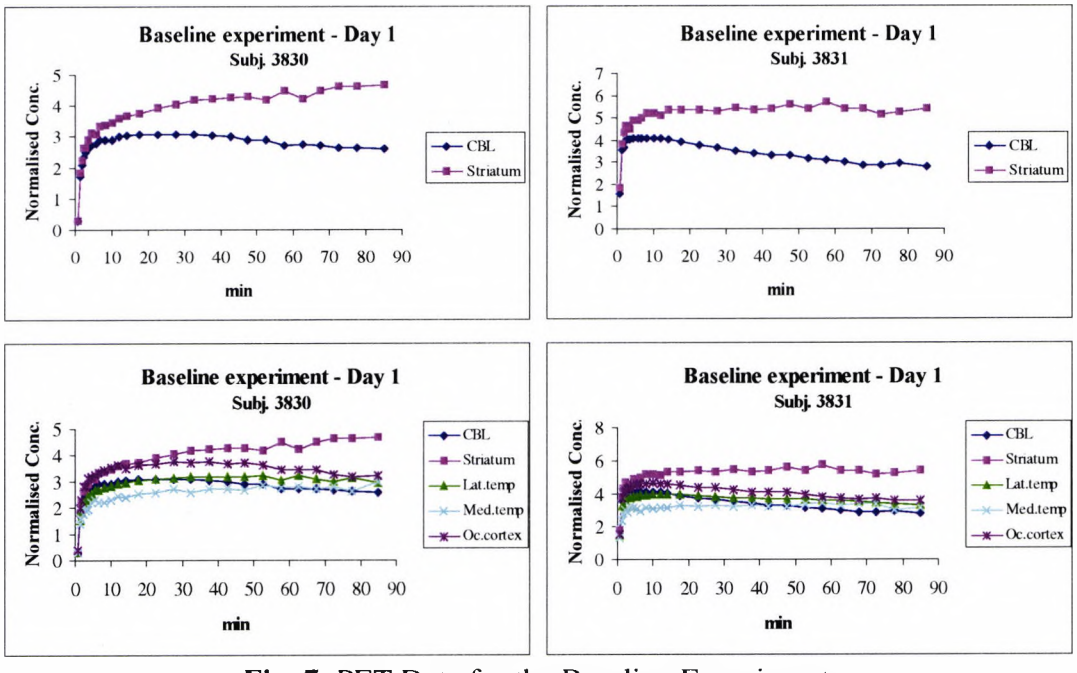

Fig. 7. PET Data for the Baseline Experiment.

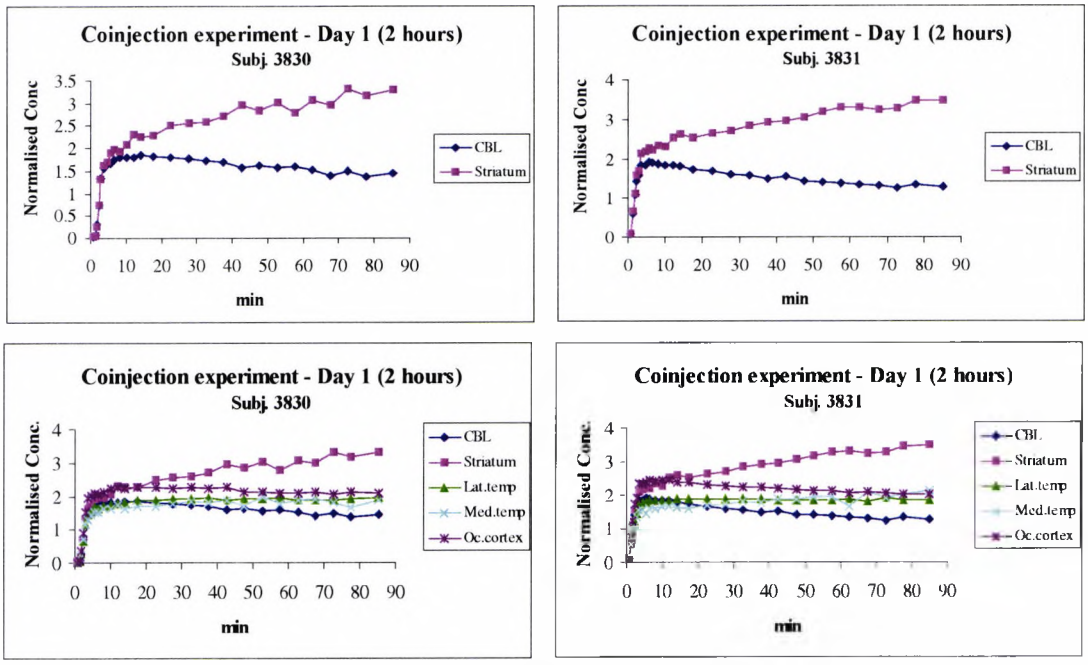

Fig. 8. PET Data for the Co-injection Experiment (2 hours).

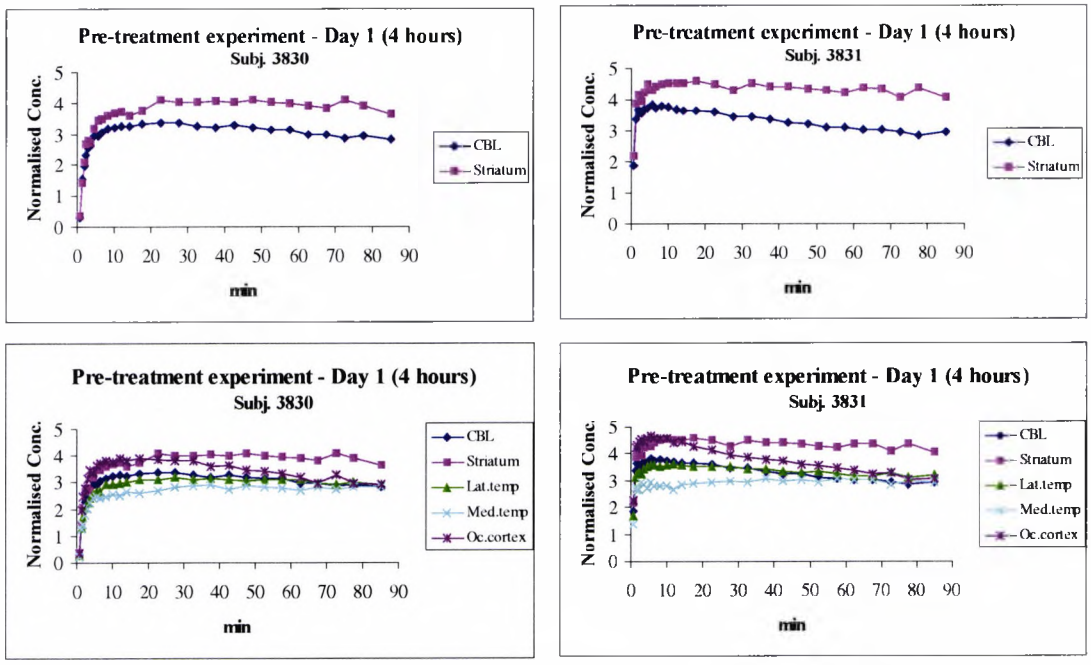

Fig. 9. PET Data for the Pre-treatment Experiment (4 hours).

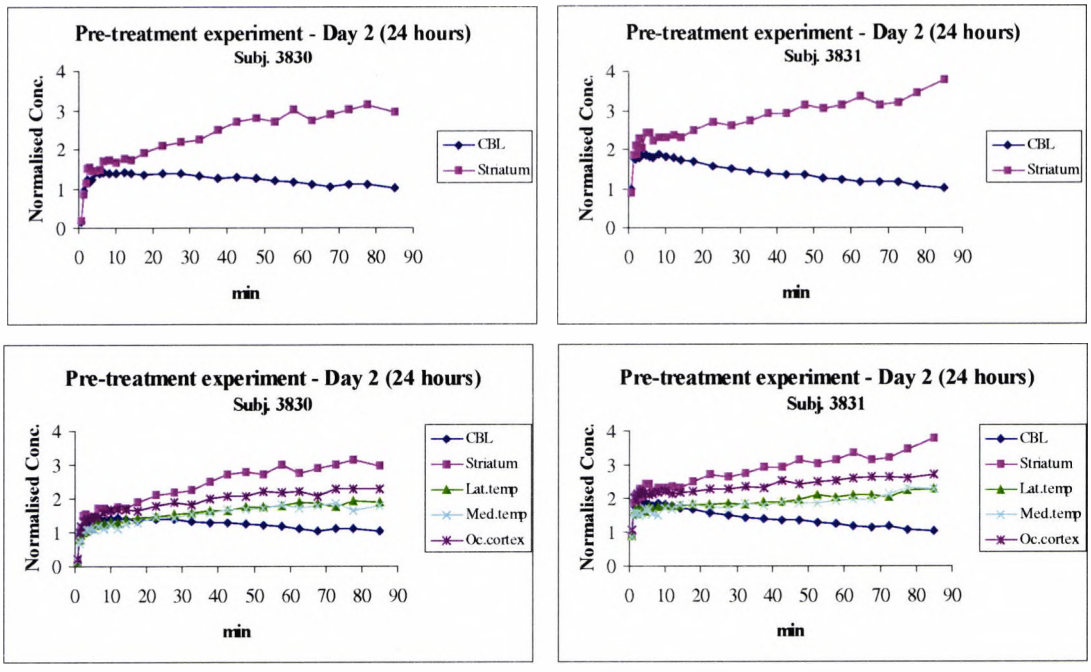

Fig. 10. PET Data for the Pre-treatment Experiment (24 hours).

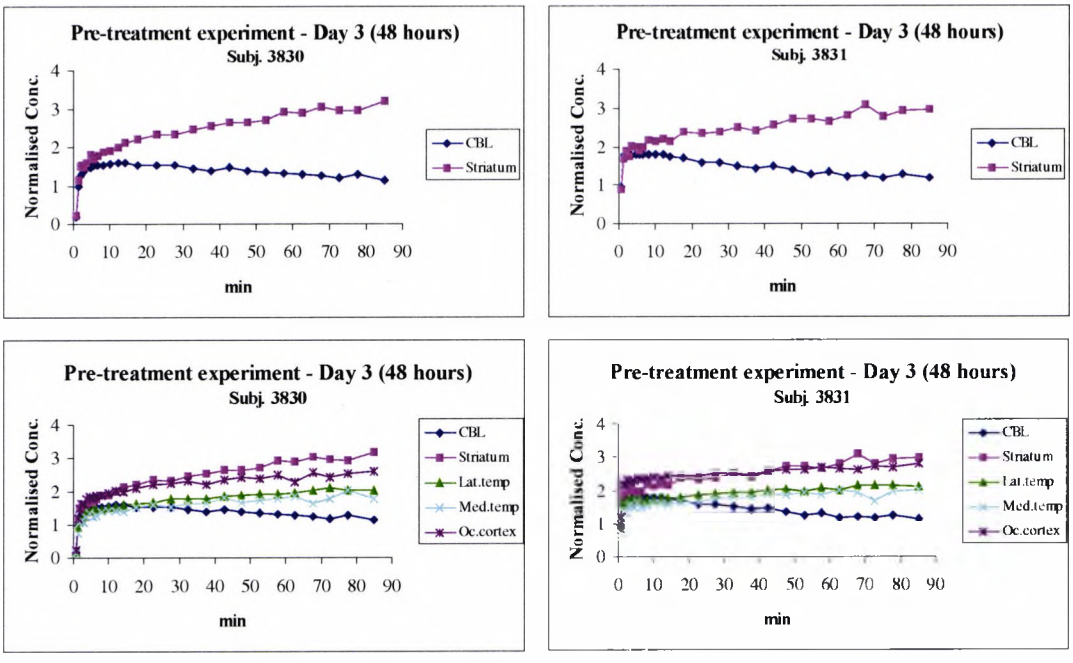

Fig. 11. PET Data for the Pre-treatment Experiment (48 hours).

Dose: 0.01 and 1 mg

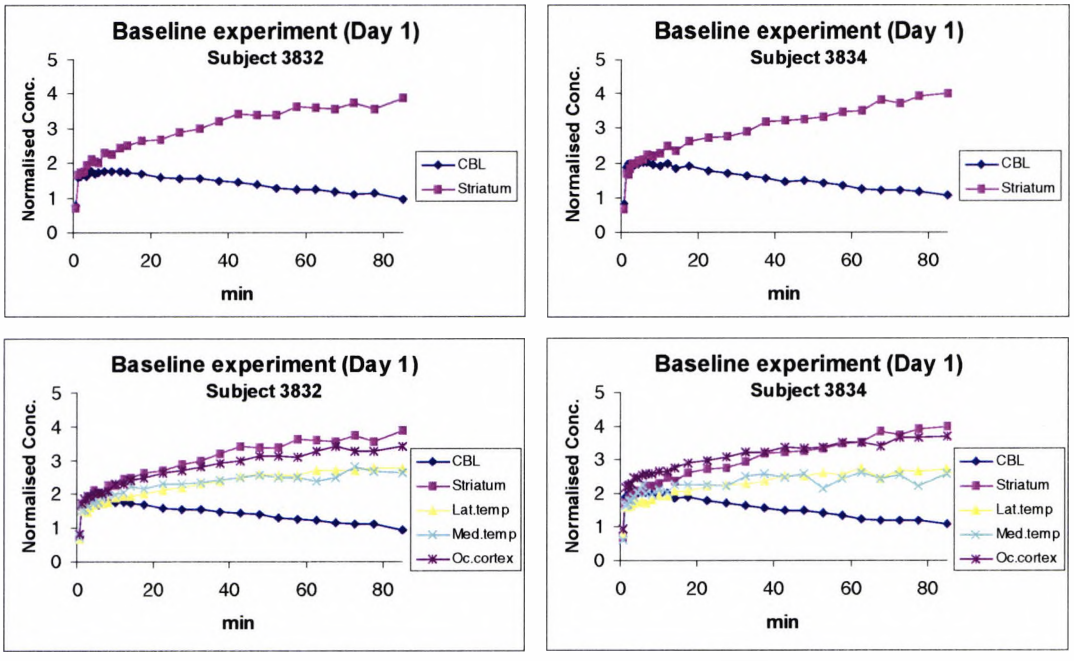

Fig. 12. PET Data for Baseline Experiment.

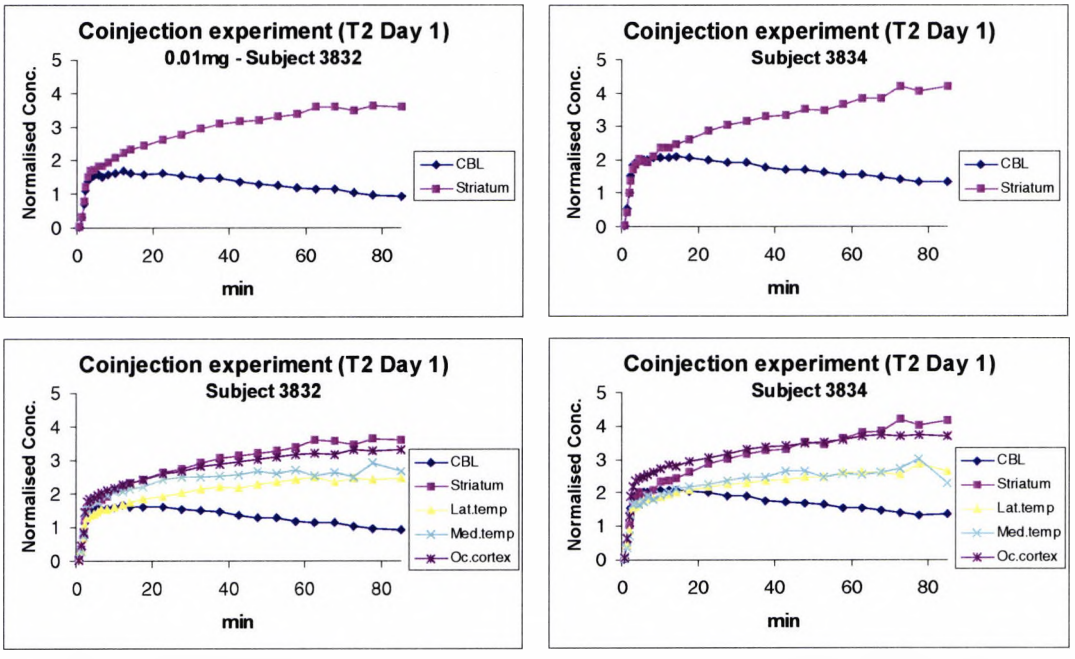

Fig. 13. PET Data for the Co-injection Experiment at 2 hours with 0.01 mg (subj. 3832) and placebo (subj. 3834).

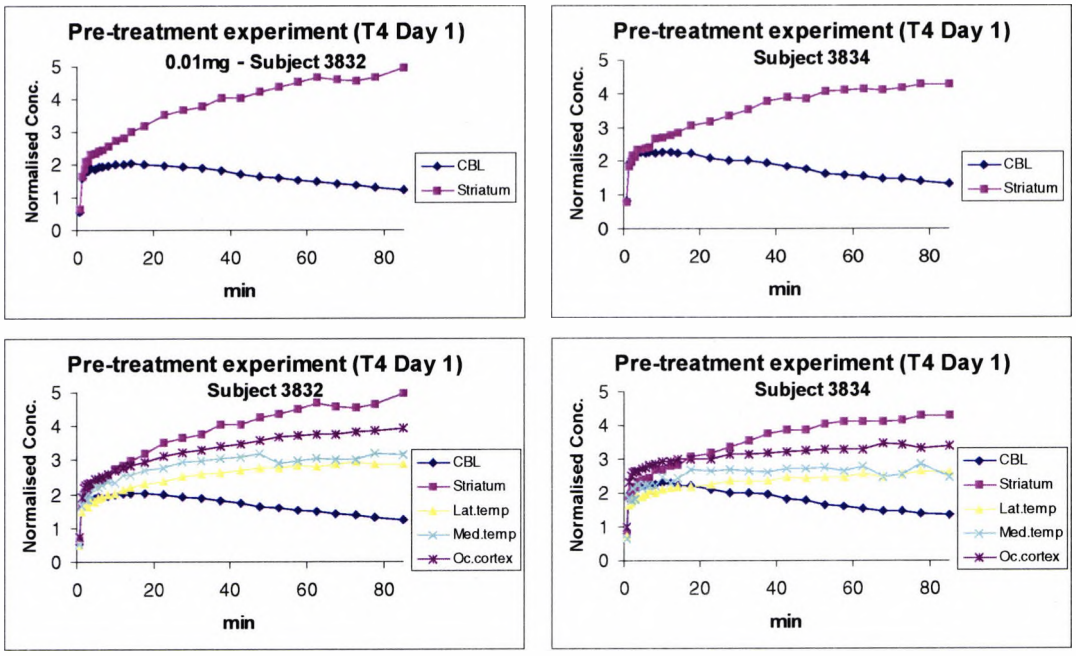

Fig. 14. PET Data for the Pre-treatment Experiment at 4 hours after 0.01 mg (subj. 3832) and placebo (subj. 3834).

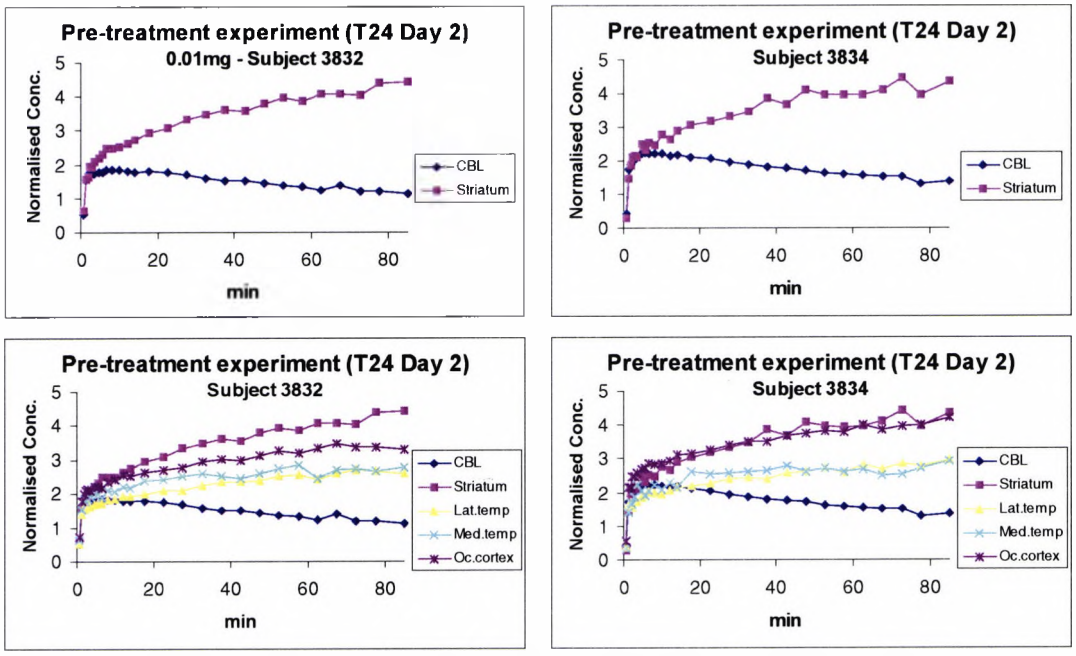

Fig. 15. PET Data for the Pre-treatment Experiment at 24 hours after 0.01 mg (subj. 3832) and placebo (subj. 3834).

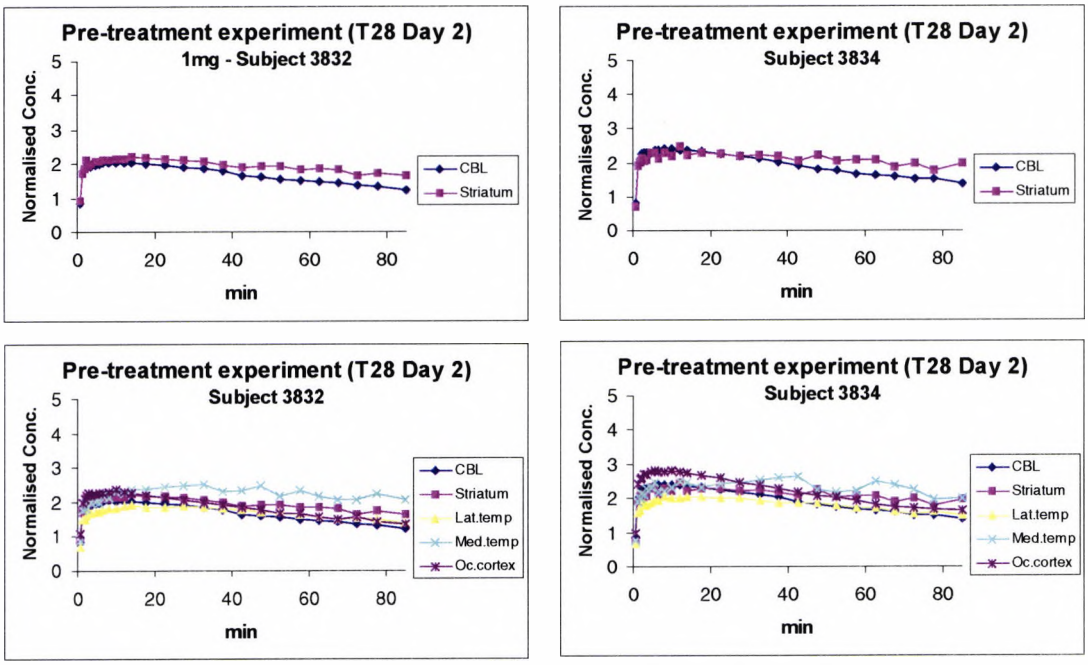

Fig. 16. PET Data for the Pre-treatment Experiment 28 after 1 mg (28 hours).

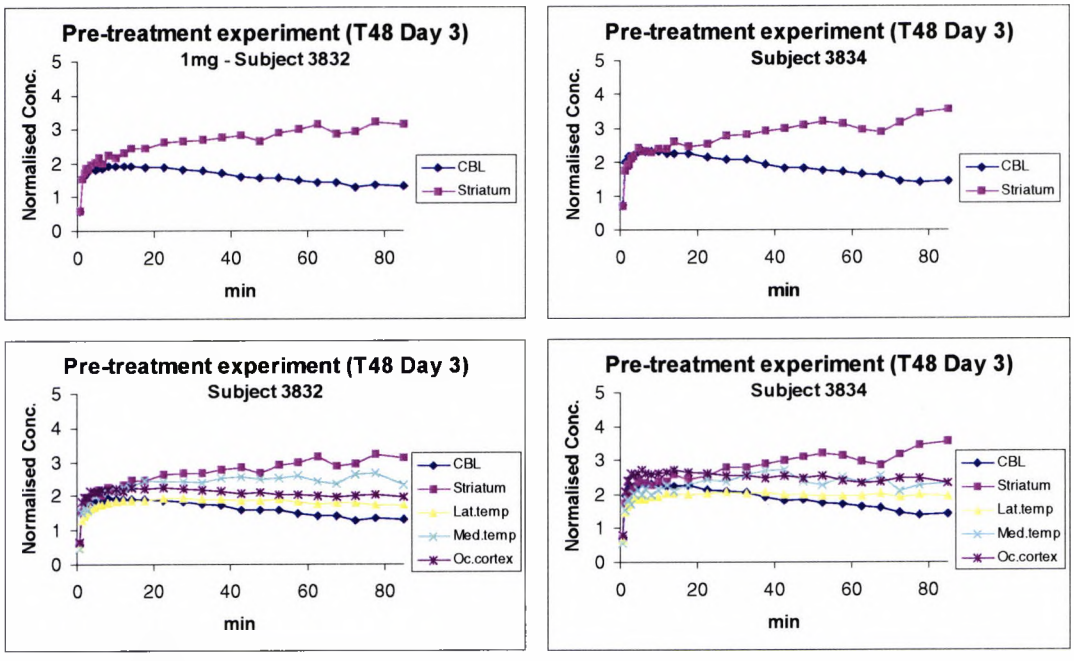

Fig. 17. PET Data for the Pre-treatment Experiment 28 after 1 mg (48 hours).

Appendix B

In this Appendix the modelling results for the three proposed versions of the reference tissue approach in the intravenous human study are presented. Only the Striatum data were analysed.

To perform the modelling analysis the SAAM II software was used. A Bayesian approach was employed for all the sets of data where the convergence was not reached.

A comparison among the three models based on AIC criteria, F test and predicted vs observed regression line with the unitary slope and zero intercept line is presented.

Also the fitting and the weighted residuals plot are included for baseline experiments.

Subject 3825

Simplified Reference Tissue Model

Subj. 3825	R	CV(%)	k_2 (min^{-1})	CV(%)	BP	CV(%)	RO
Baseline	1.097	3	0.043	9	2.299	9	
T4	1.071	1	0.031[a]	40	0.101	11	96%
T24	1.099	2	0.015[a]	61	0.380	33	83%
T28	1.109	1	0.028[a]	43	0.068	16	97%
T48	1.248	2	0.030[a]	41	0.188	9	92%

[a] estimated by a Bayesian approach (0.032±0.012)

Irreversible model

	R	CV(%)	k_2 (min^{-1})	CV(%)	k_3 (min^{-1})	CV(%)	RO
Baseline	1.430	24	0.813[b]	61	0.021	4	
T4	1.091	2	0.018	90	0.003	38	84%
T24	1.130	2	0.002[b]	33	0.081	148	-280%
T28	1.103	1	0.005	90	0.000[a]		100%
T48	1.237	2	0.002	135	0.000[a]		100%

[a] fixed to zero by the algorithm
[b] estimated by a Bayesian approach (0.5±0.5)

Reference Tissue Model

	R		k2		k3		k4		BP		RO
Baseline	1.120	8	0.044	17	0.908	411	0.397	408	2.286	10	
T4	1.092	2	0.021	87	0.003	37	0.000[a]				
T24	1.146	2	0.025[b]	49	0.016	43	0.044	52	0.375	23	84%
T28	1.109	21	0.028[b]	44	0.677	1.3^{E+05}	10.000	1.3^{E+05}	0.068	26	97%
T48	NC		NC		NC		NC				

[a] fixed to zero by the algorithm
[b] estimated by a Bayesian approach (0.033±0.012)

AKAIKE CRITERIA

Subj. 3825	Reference Tissue Model	Simplified Reference Tissue Model	Irreversible Model	Best Model
Baseline	-0.7194	-0.7542	0.3934	S.R.T
T4	-1.5428	-1.7800	-1.5798	S.R.T
T24	-1.2715	-1.2757	-1.2005	S.R.T
T28	-1.5092	-1.5437	-1.5033	S.R.T
T48	N.C.	-0.7659	-0.5961	S.R.T

Comparison between Irreversible (k_4=0) and the reversible binding model

	Akaike criteria		F Test	
	Irreversible	Reference	Value	Prob.
Baseline	0.3934	-0.7194	204.81	P<0.05
T4	-1.5798	-1.5428	0.35	NS
T24	-1.2005	-1.2715	-1.77	NS
T28	-1.5033	-1.5092	-1.23	NS
T48	-0.5961	N.C.		

Subject 3827

Simplified Reference Tissue Model

Subj. 3827	R	CV(%)	k_2 (min^{-1})	CV(%)	BP	CV(%)	RO
Baseline	1.000	4	0.032	15	2.747	22	
T4	0.978	2	0.039	58	0.058	25	98%
T24	0.969	2	0.019	36	0.385	26	86%
T28	0.899	5	0.326	45	0.061	9	98%
T48	1.022	1	0.011	79	0.303	61	89%

Irreversible model

	R	CV(%)	k_2 (min^{-1})	CV(%)	k_3 (min^{-1})	CV(%)	RO
Baseline	0.934	23	0.996[a]	51	0.018	3	
T4	0.785	21	2.290	124	0.001	11	96%
T24	0.890	10	0.760[a]	61	0.003	5	82%
T28	0.828	23	1.644	175	0.001	14	95%
T48	0.983	7	0.827[a]	63	0.002	5	89%

[a] estimated by a Bayesian approach (0.5±0.5)

Reference Tissue Model

	R	CV(%)	k_2	CV(%)	k_3	CV(%)	k_4	CV(%)	BP	CV(%)	RO
Baseline	1.006	4	0.032	15	2.848	106	1.038[a]	104	2.744	22	
T4	0.980	2	0.039	61	0.063	101	1.094[a]	99	0.058	26	98%
T24	0.866	15	1.018	130	0.004	16	0.009	56	0.507	41	82%
T28	0.895	8	0.541	114	0.017	171	0.283	173	0.061	10	98%
T48	1.024	1	0.010	81	0.333	118	1.087[a]	99	0.307	63	89%

[a] estimated by a Bayesian approach (1±1)

AKAIKE CRITERIA

Subj. 3827	Reference Tissue Model	Simplified Reference Tissue Model	Irreversible Model	Best Model
Baseline	-1.9130	-1.9001	-1.5778	R.T
T4	-1.3401	-1.4638	-1.5648	I.
T24	-1.0795	-0.9980	-0.9749	S.R.T
T28	-1.3681	-1.3307	-1.0967	R.T
T48	-1.0154	-1.0489	-0.7620	S.R.T

Comparison between Irreversible (k_4=0) and the reversible binding model

	Akaike criteria		F Test	
	Irreversible	Reference	Value	Prob.
Baseline	-1.5778	-1.9130	27.22	P<0.05
T4	-1.5648	-1.3401	-4.15	NS
T24	-0.9749	-1.0795	4.00	NS
T28	-1.0967	-1.3681	19.70	P<0.05
T48	-0.7620	-1.0154	20.24	P<0.05

Subject 3830

Simplified Reference Tissue Model

Subj. 3830	R	CV(%)	k_2 (min^{-1})	CV(%)	BP	CV(%)	RO
Baseline	1.092	1	0.014	19	2.350	34	
T4	1.060	2	0.047	24	0.306	6	87%
T24	0.988	4	0.037	12	3.112	18	-32%
T48	0.029	15	1.072	3	2.837	25	-21%

Irreversible model

	R	CV(%)	k_2 (min^{-1})	CV(%)	k_3 (min^{-1})	CV(%)	RO
Baseline	1.252	15	0.767[a]	64	0.010	4	
T4	1.207	16	0.593[a]	83	0.005	8	53%
T24	1.196	19	0.855[a]	59	0.022	4	-123%
T48	1.372	18	0.911[a]	54	0.019	3	-92%

[a] estimated by a Bayesian approach (0.5±0.5)

Reference Tissue Model

	R	CV(%)	k_2	CV(%)	k_3	CV(%)	k_4	CV(%)	BP	CV(%)	RO
Baseline	1.095	1	0.014	19	2.500	108	1.061[a]	102	2.356	35	
T4	1.068	2	0.048	24	0.325	101	1.062[a]	101	0.306	6	87%
T24	1.113	6	0.091	167	0.061	145	0.025	143	2.458	8	-4%
T48	1.104	5	0.031	25	0.442	209	0.163	195	2.711	27	-15%

[a] estimated by a Bayesian approach (1±1)

AKAIKE CRITERIA

Subj. 3830	Reference Tissue Model	Simplified Reference Tissue Model	Irreversible Model	Best Model
Baseline	-1.2172	-1.3394	-0.0414	S.R.T
T4	-0.8285	-0.9316	0.1741	S.R.T.
T24	-0.9495	-0.8876	-0.3762	R.T
T48	-1.0823	-1.1121	-0.3942	S.R.T

Comparison between Irreversible (k_4=0) and the reversible binding model

	Akaike criteria		F Test	
	Irreversible	Reference	Value	Prob.
Baseline	-0.0414	-1.2172	249.82	P<0.05
T4	0.1741	-0.8285	177.36	P<0.05
T24	-0.3762	-0.9495	47.92	P<0.05
T48	-0.3942	-1.0823	65.45	P<0.05

Subject 3831

Simplified Reference Tissue Model

Subj. 3831	R	CV(%)	k_2 (min^{-1})	CV(%)	BP	CV(%)	RO
Baseline	1.123	2	0.035	12	1.004	7	
T4	0.717	2	0.017	23	0.098	57	90%
T24	1.068	3	0.033	14	3.937	28	-292%
T48	1.008	2	0.027	11	2.622	17	-161%

Irreversible model

	R	CV(%)	k_2 (min^{-1})	CV(%)	k_3 (min^{-1})	CV(%)	RO
Baseline	1.310	21	0.733[a]	68	0.011	6	
T4	1.289	21	0.531	145	0.006	9	47%
T24	1.097	18	0.950[a]	54	0.023	4	-108%
T48	0.942	16	1.042[a]	49	0.016	3	-44%

[a] estimated by a Bayesian approach (0.5±0.5)

Reference Tissue Model

	R	CV(%)	k_2	CV(%)	k_3	CV(%)	k_4	CV(%)	BP	CV(%)	RO
Baseline	1.128	9	0.035	18	1.915	2160	1.907	2160	1.004	7	
T4	1.139	5	0.038	28	0.442	697	1.057	696	0.418	7	58%
T24	1.074	3	0.033	15	3.996	111	1.013[a]	107	3.945	29	-293%
T48	1.013	2	0.028	12	2.854	101	1.088[a]	99	2.624	18	-161%

[a] estimated by a Bayesian approach (1±1)

AKAIKE CRITERIA

Subj. 3831	Reference Tissue Model	Simplified Reference Tissue Model	Irreversible Model	Best Model
Baseline	-0.4593	-0.4949	0.8671	S.R.T
T4	-0.7512	-0.9993	0.5923	S.R.T.
T24	-0.6004	-0.6948	-0.0871	S.R.T
T48	-0.9569	-1.0654	-0.4420	S.R.T

Comparison between Irreversible (k_4=0) and the reversible binding model

	Akaike criteria		F Test	
	Irreversible	Reference	Value	Prob.
Baseline	0.8671	-0.4593	341.12	P<0.05
T4	0.5923	-0.7512	348.32	P<0.05
T24	-0.0871	-0.6004	48.24	P<0.05
T48	-0.4420	-0.9569	24.45	P<0.05

Subject 3832

Simplified Reference Tissue Model

Subj. 3832	R	CV(%)	k_2 (min^{-1})	CV(%)	BP	CV(%)	RO
Baseline	1.049	3	0.035	9	5.496	21	
T4	1.107	2	0.037	6	5.909	16	-8%
T24	1.097	3	0.041	8	5.008	15	9%
T28	0.994	1	0.025[a]	17	0.295	10	95%
T48	1.029	2	0.023	14	2.896	26	47%

[a] estimated by a Bayesian approach (0.036±0.005)

Irreversible model

	R	CV(%)	k_2 (min^{-1})	CV(%)	k_3 (min^{-1})	CV(%)	RO
Baseline	1.110	19	1.050[a]	49	0.026	3	
T4	1.400	20	0.926	54	0.029	3	-9%
T24	1.284	23	0.979	52	0.030	4	-12%
T28	1.047	6	0.762[a]	67	0.003	4	88%
T48	1.108	14	0.985[a]	52	0.015	3	44%

[a] estimated by a Bayesian approach (0.5±0.5)

Reference Tissue Model

	R		k2		k3		k4		BP		RO
Baseline	1.054	3	0.035	9	5.722	106	1.037[a]	104	5.517	21	
T4	1.112	2	0.037	7	5.952	108	1.007[a]	107	5.909	16	-7%
T24	1.103	3	0.041	8	5.074	108	1.013[a]	107	5.010	16	9%
T28	1.050	1	0.034[a]	16	0.011	24	0.033	35	0.341	13	94%
T48	1.033	2	0.023	15	2.918	111	1.007[a]	107	2.896	27	48%

[a] estimated by a Bayesian approach (1±1) for k_4 and (0.036±0.005) for k_3

AKAIKE CRITERIA

Subj. 3832	Reference Tissue Model	Simplified Reference Tissue Model	Irreversible Model	Best Model
Baseline	-0.8020	-0.8961	-0.1537	S.R.T
T4	-0.9220	-1.0229	0.1442	S.R.T
T24	-0.7105	-0.8070	0.1881	S.R.T
T28	-1.5414	-1.3684	-1.2411	R.T
T48	-0.9282	-1.0327	-0.4613	S.R.T

Comparison between Irreversible (k_4=0) and the reversible binding model

	Akaike criteria		F Test	
	Irreversible	Reference	Value	Prob.
Baseline	-0.1537	-0.8020	71.84	P<0.05
T4	0.1442	-0.9220	207.04	P<0.05
T24	0.1881	-0.7105	139.26	P<0.05
T28	-1.2411	-1.5414	9.93	P<0.05
T48	-0.4613	-0.9282	43.31	P<0.05

Subject 3834

Simplified Reference Tissue Model

Subj. 3834	R	CV(%)	k_2 (min^{-1})	CV(%)	BP	CV(%)	RO
Baseline	0.915	2	0.031	8	5.763	27	
T4	0.935	1	0.036	4	3.383	7	41%
T24	0.934	3	0.042	9	2.841	11	51%
T28	0.871	2	0.022[a]	19	0.352	17	94%
T48	0.859	4	0.022[a]	16	2.793	34	52%

[a] estimated by a Bayesian approach (0.036±0.005)

Irreversible model

	R	CV(%)	k_2 (min^{-1})	CV(%)	k_3 (min^{-1})	CV(%)	RO
Baseline	0.779	9	0.810	32	0.023	2	
T4	0.940	15	1.051[a]	47	0.022	2	8%
T24	0.800	27	1.041[a]	48	0.022	3	5%
T28	0.917	3	0.048	35	0.005	15	80%
T48	0.921	7	0.142	41	0.015	8	36%

[a] estimated by a Bayesian approach (0.5±0.5)

Reference Tissue Model

	R		k2		k3		k4		BP		RO
Baseline	0.918	2	0.031	8	6.081	107	1.053[a]	103	5.777	27	
T4	0.957	4	0.037	8	0.818	181	0.244	178	3.351	7	42%
T24	0.941	3	0.042	9	3.104	99	1.092[a]	99	2.842	11	51%
T28	0.925	2	0.034[a]	16	0.007	31	0.008	122	0.875	95	85%
T48	0.966	4	0.033[a]	16	0.049	31	0.016	56	3.041	34	47%

[a] estimated by a Bayesian approach (1±1) for k_4 (0.036±0.006) for k_3

AKAIKE CRITERIA

Subj. 3832	Reference Tissue Model	Simplified Reference Tissue Model	Irreversible Model	Best Model
Baseline	-1.1290	-1.2521	-1.2653	I.R
T4	-1.3230	-1.3573	-0.3415	S.R.T
T24	-0.5048	-0.5932	-0.0003	S.R.T
T28	-1.1001	-0.8443	-0.8174	R.T
T48	-0.4505	-0.3487	-0.3917	R.T

Comparison between Irreversible (k_4=0) and the reversible binding model

	Akaike criteria		F Test	
	Irreversible	Reference	Value	Prob.
Baseline	-1.2653	-1.1290	-0.63	NS
T4	-0.3415	-1.3230	138.79	P<0.05
T24	-0.0003	-0.5048	47.77	P<0.05
T28	-0.8174	-1.1001	-0.01	NS
T48	-0.3917	-0.4505	-2.01	NS

Figures

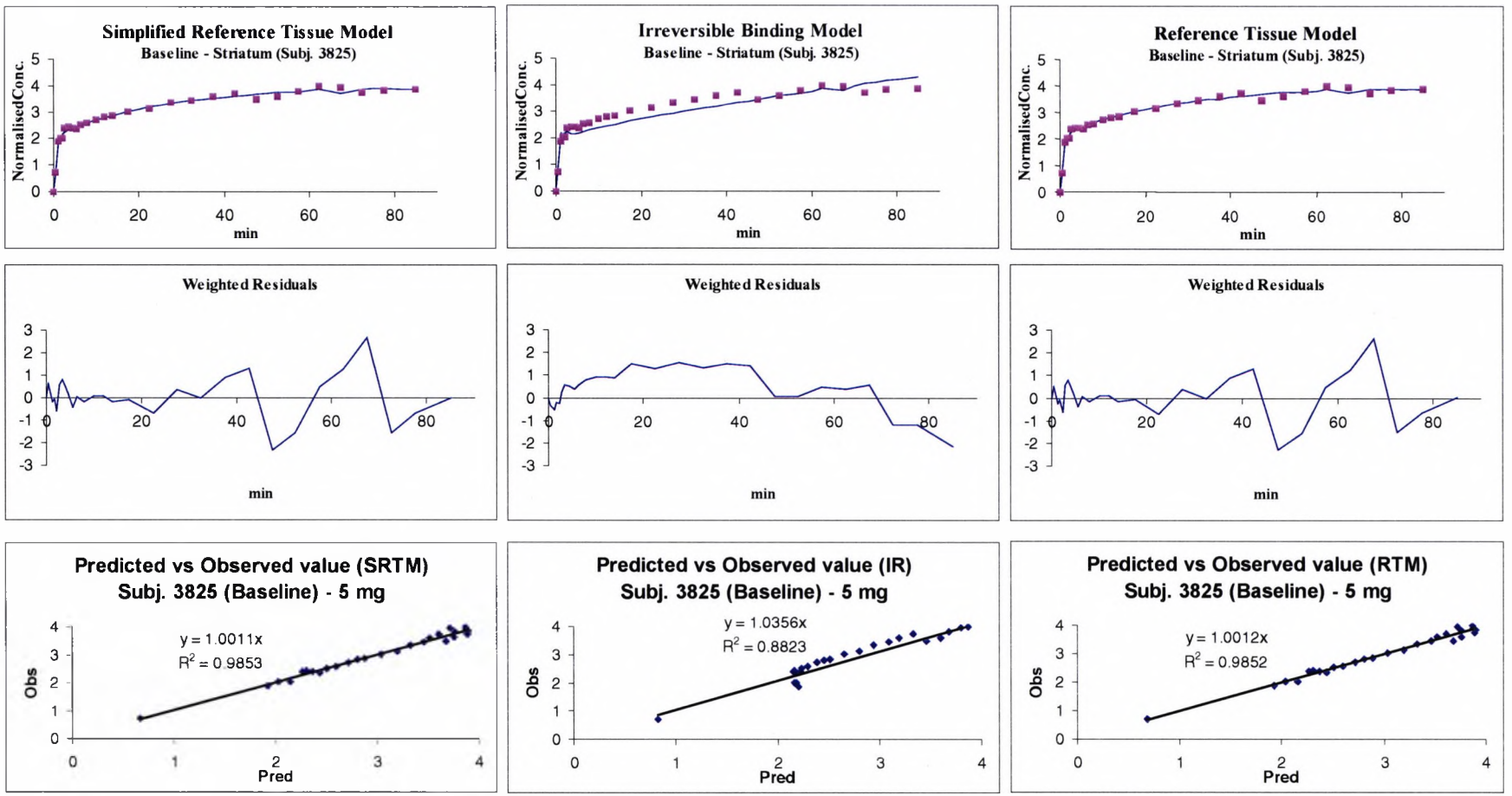
Simplified Reference Tissue Model
Baseline - Striatum (Subj. 3825)
NormalisedConc.
min
Irreversible Binding Model
Baseline - Striatum (Subj. 3825)
NormalisedConc.
min
Reference Tissue Model
Baseline - Striatum (Subj. 3825)
NormalisedConc.
min
Weighted Residuals
min
Weighted Residuals
min
Weighted Residuals
min
Predicted vs Observed value (SRTM)
Subj. 3825 (Baseline) - 5 mg
y = 1.0011x
R2 = 0.9853
Obs
Pred
Predicted vs Observed value (IR)
Subj. 3825 (Baseline) - 5 mg
y = 1.0356x
R2 = 0.8823
Obs
Pred
Predicted vs Observed value (RTM)
Subj. 3825 (Baseline) - 5 mg
y = 1.0012x
R2 = 0.9852
Obs
Pred

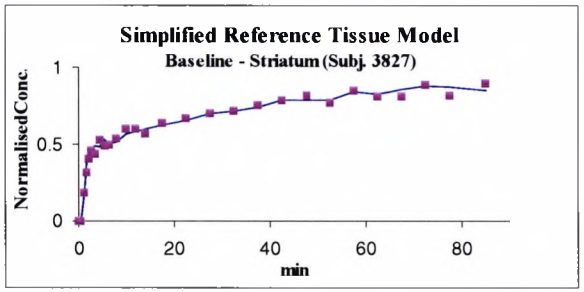
Simplified Reference Tissue Model
Baseline - Striatum (Subj. 3827)
NormalisedConc.
min

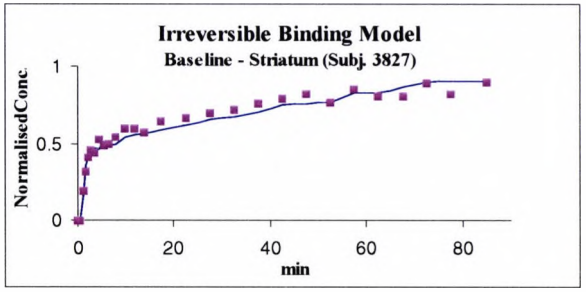
Irreversible Binding Model
Baseline - Striatum (Subj. 3827)
NormalisedConc.
min

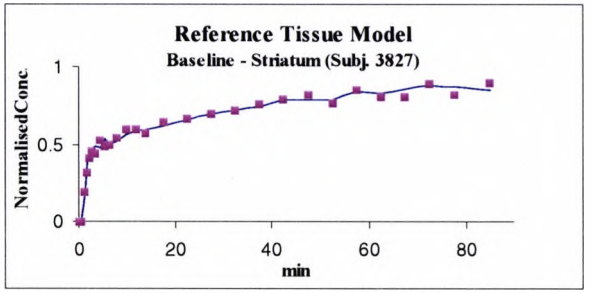
Reference Tissue Model
Baseline - Striatum (Subj. 3827)
NormalisedConc.
min

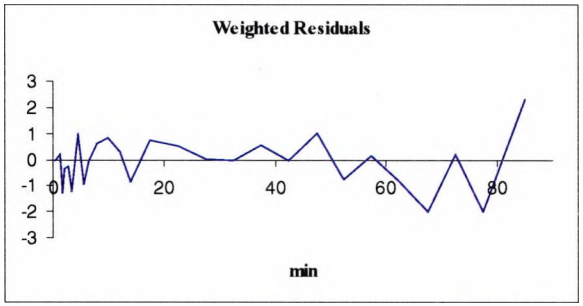
Weighted Residuals
min

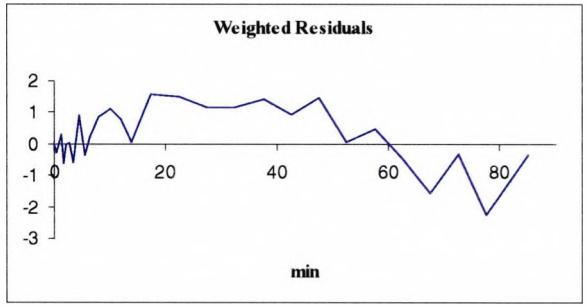
Weighted Residuals
min

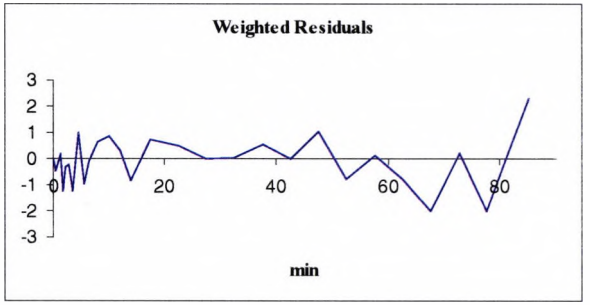
Weighted Residuals
min

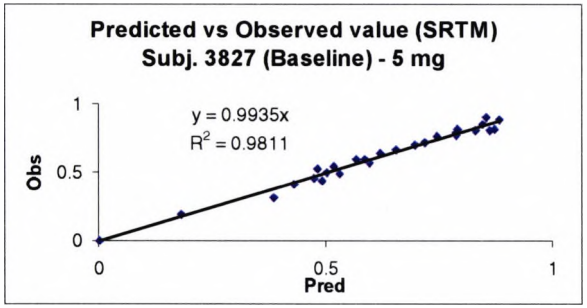
Predicted vs Observed value (SRTM)
Subj. 3827 (Baseline) - 5 mg
y = 0.9935x
R2 = 0.9811
Obs
Pred

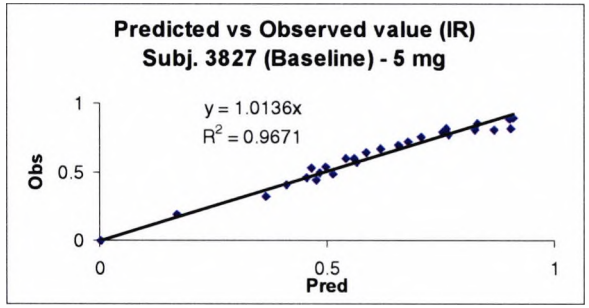
Predicted vs Observed value (IR)
Subj. 3827 (Baseline) - 5 mg
y = 1.0136x
R2 = 0.9671
Obs
Pred

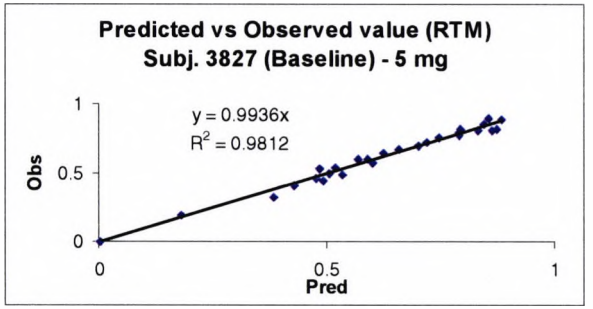
Predicted vs Observed value (RTM)
Subj. 3827 (Baseline) - 5 mg
y = 0.9936x
R2 = 0.9812
Obs
Pred

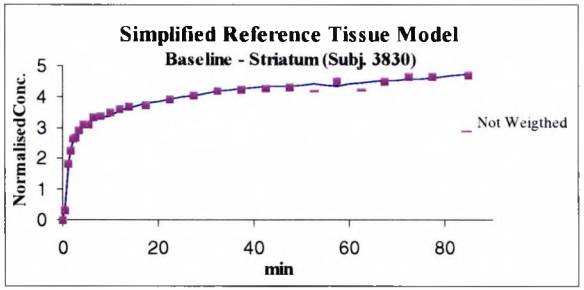
Simplified Reference Tissue Model
Baseline - Striatum (Subj. 3830)
NormalisedConc.
Not Weigthed
min

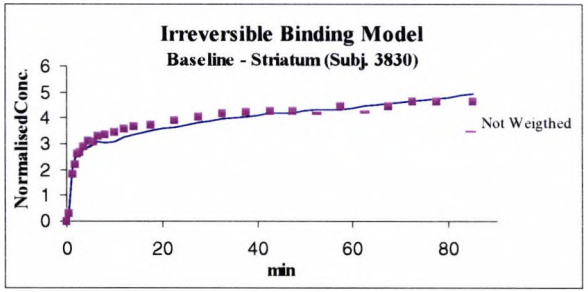
Irreversible Binding Model
Baseline - Striatum (Subj. 3830)
NormalisedConc.
Not Weigthed
min

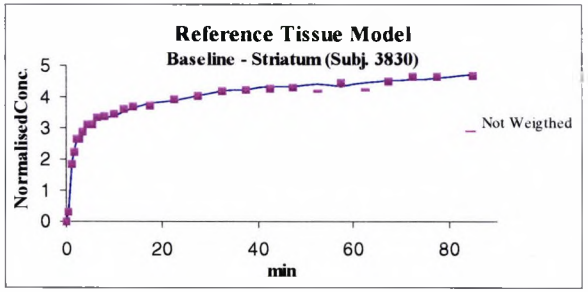
Reference Tissue Model
Baseline - Striatum (Subj. 3830)
NormalisedConc.
Not Weigthed
min

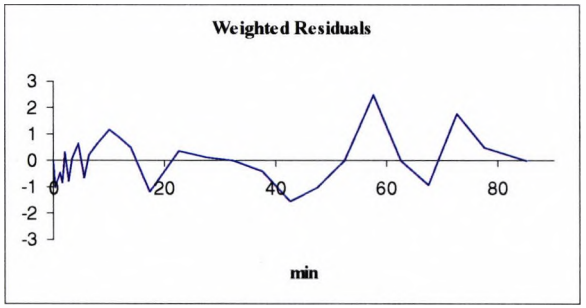
Weighted Residuals
min

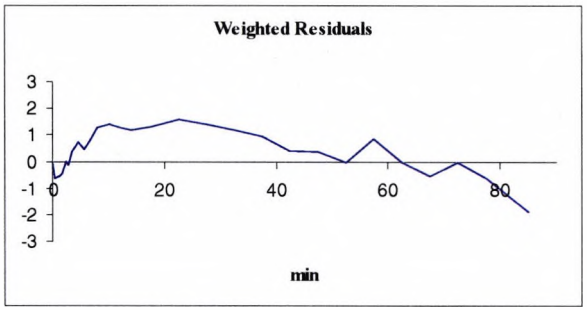
Weighted Residuals
min

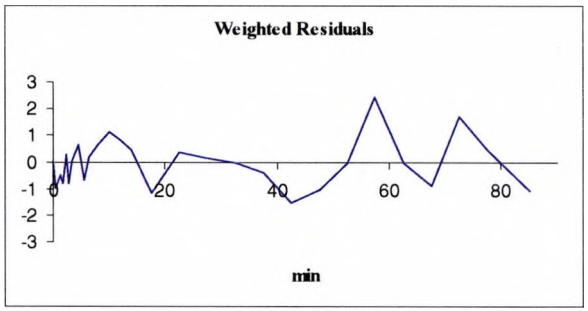
Weighted Residuals
min

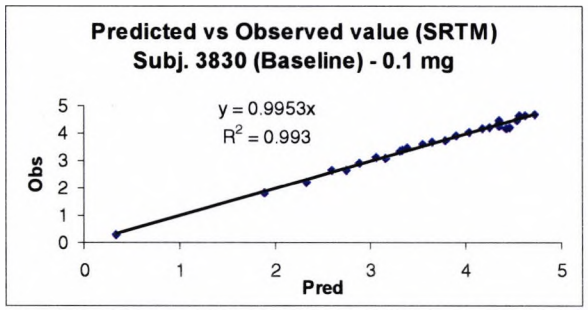
Predicted vs Observed value (SRTM)
Subj. 3830 (Baseline) - 0.1 mg
y = 0.9953x
R2 = 0.993
Obs
Pred

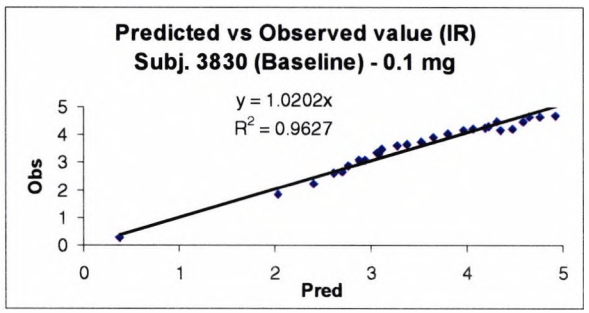
Predicted vs Observed value (IR)
Subj. 3830 (Baseline) - 0.1 mg
y = 1.0202x
R2 = 0.9627
Obs
Pred

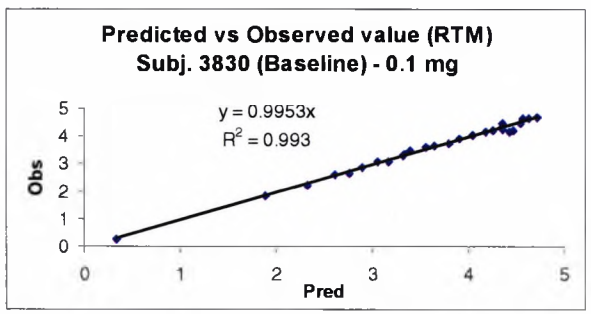
Predicted vs Observed value (RTM)
Subj. 3830 (Baseline) - 0.1 mg
y = 0.9953x
R2 = 0.993
Obs
Pred

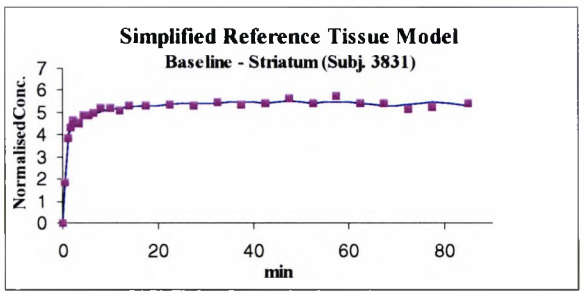
Simplified Reference Tissue Model
Baseline - Striatum (Subj. 3831)
NormalisedConc.
min

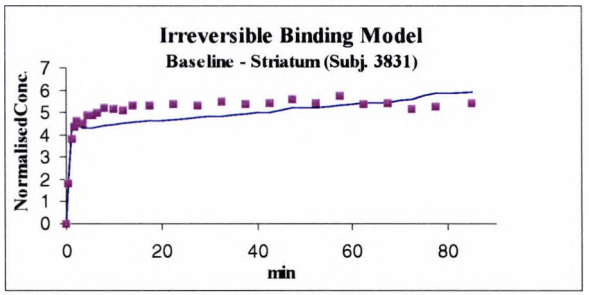
Irreversible Binding Model
Baseline - Striatum (Subj. 3831)
NormalisedConc.
min

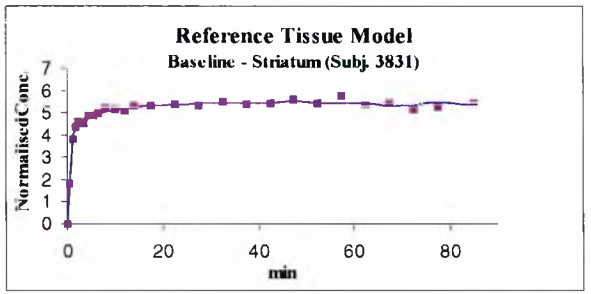
Reference Tissue Model
Baseline - Striatum (Subj. 3831)
NormalisedConc.
min

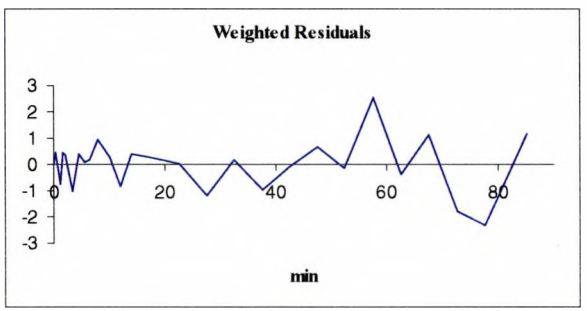
Weighted Residuals
min

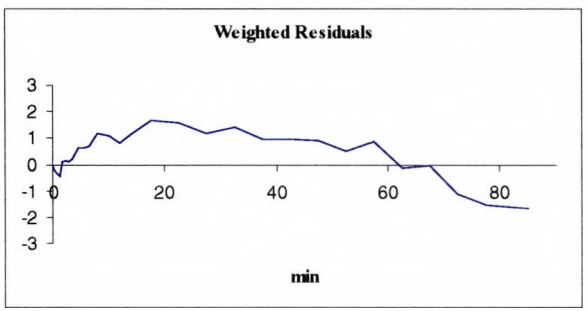
Weighted Residuals
min

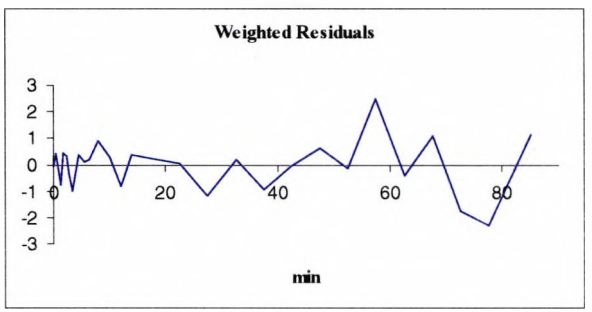
Weighted Residuals
min

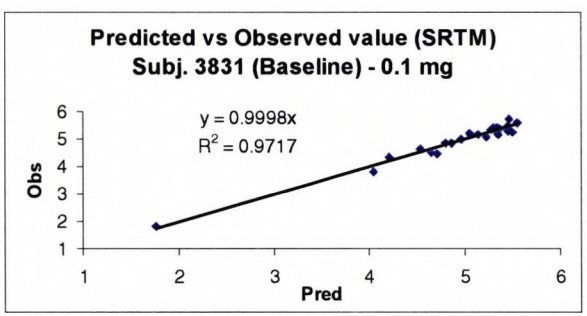
Predicted vs Observed value (SRTM)
Subj. 3831 (Baseline) - 0.1 mg
y = 0.9998x
R2 = 0.9717
Obs
Pred

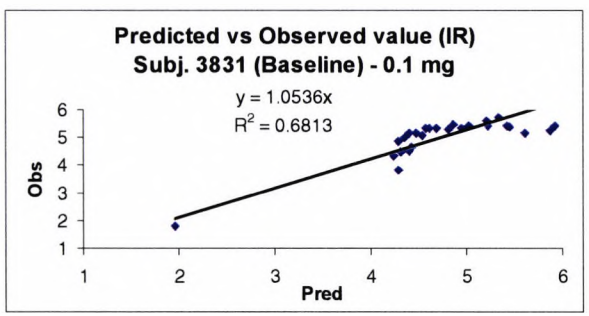
Predicted vs Observed value (IR)
Subj. 3831 (Baseline) - 0.1 mg
y = 1.0536x
R2 = 0.6813
Obs
Pred

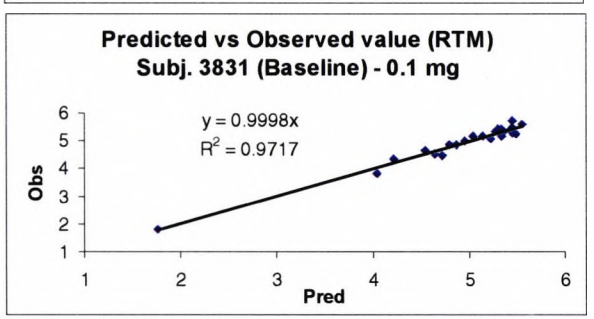
Predicted vs Observed value (RTM)
Subj. 3831 (Baseline) - 0.1 mg
y = 0.9998x
R2 = 0.9717
Obs
Pred

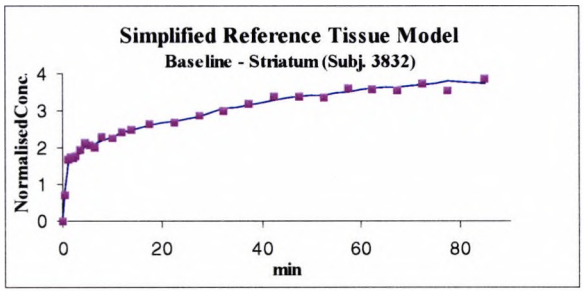
Simplified Reference Tissue Model
Baseline - Striatum (Subj. 3832)
NormalisedConc.
min

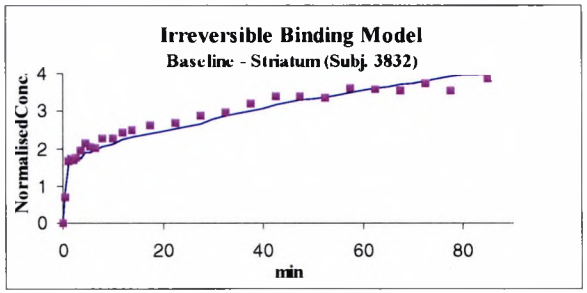
Irreversible Binding Model
Baseline - Striatum (Subj. 3832)
NormalisedConc.
min

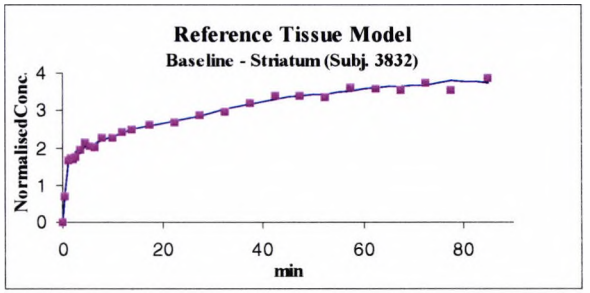
Reference Tissue Model
Baseline - Striatum (Subj. 3832)
NormalisedConc.
min

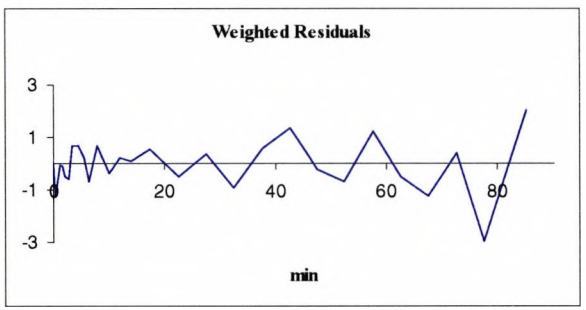
Weighted Residuals
min

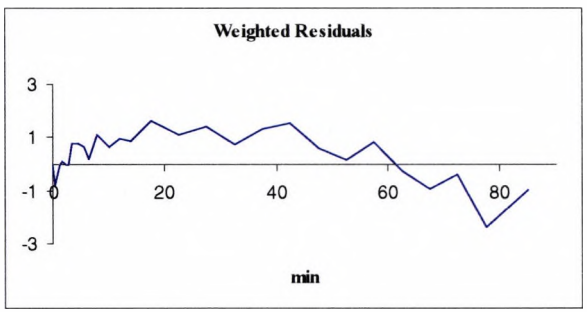
Weighted Residuals
min

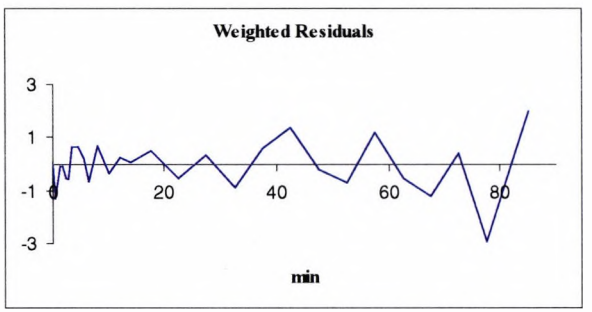
Weighted Residuals
min

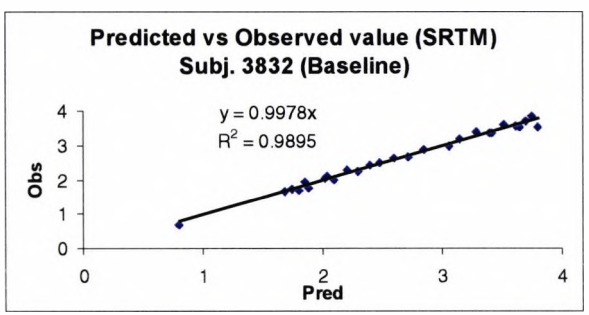
Predicted vs Observed value (SRTM)
Subj. 3832 (Baseline)
y = 0.9978x
R2 = 0.9895
Obs
Pred

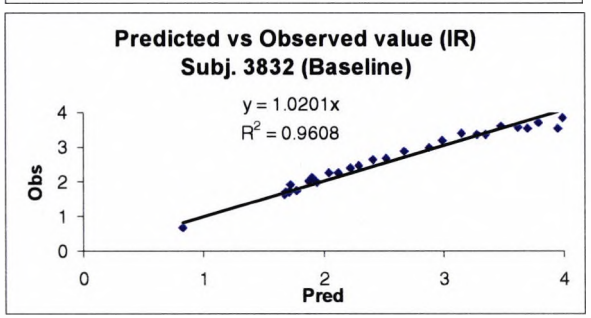
Predicted vs Observed value (IR)
Subj. 3832 (Baseline)
y = 1.0201x
R2 = 0.9608
Obs
Pred

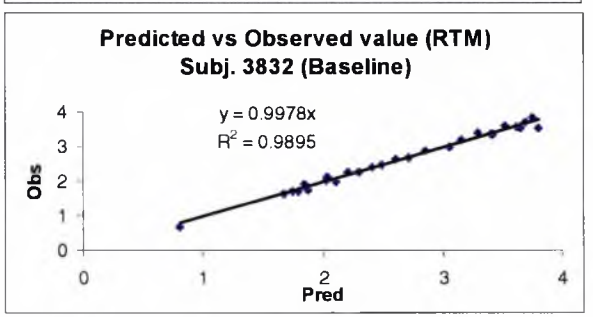
Predicted vs Observed value (RTM)
Subj. 3832 (Baseline)
y = 0.9978x
R2 = 0.9895
Obs
Pred

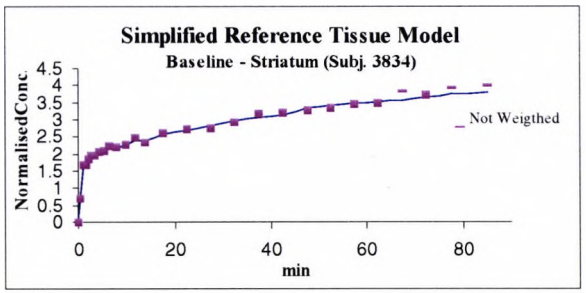
Simplified Reference Tissue Model
Baseline - Striatum (Subj. 3834)
NormalisedConc.
Not Weigthed
min

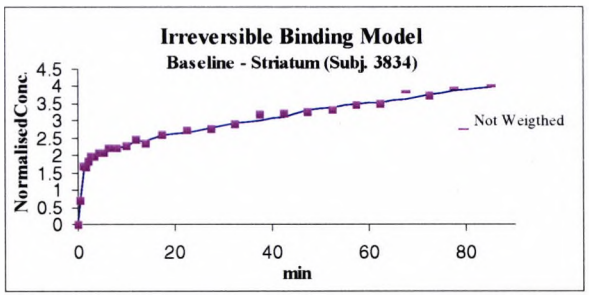
Irreversible Binding Model
Baseline - Striatum (Subj. 3834)
NormalisedConc.
Not Weigthed
min

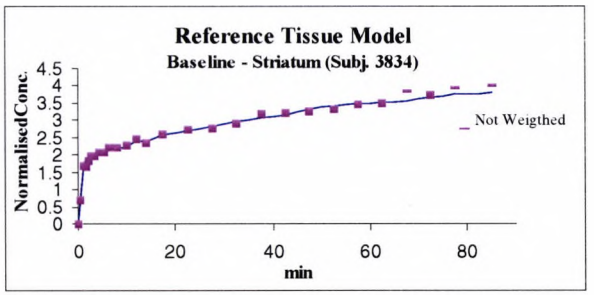
Reference Tissue Model
Baseline - Striatum (Subj. 3834)
NormalisedConc.
Not Weigthed
min

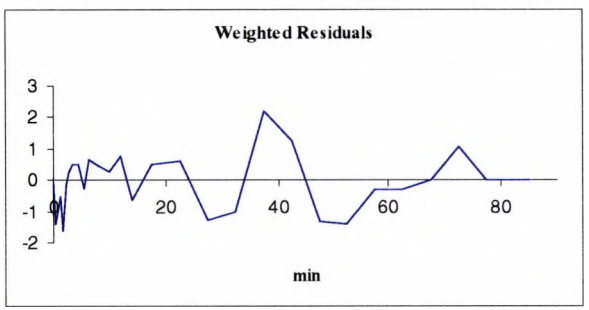
Weighted Residuals
min

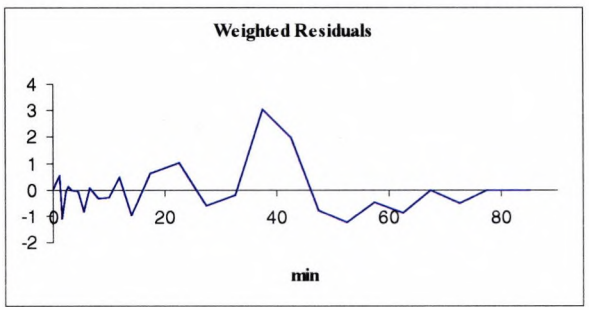
Weighted Residuals
min

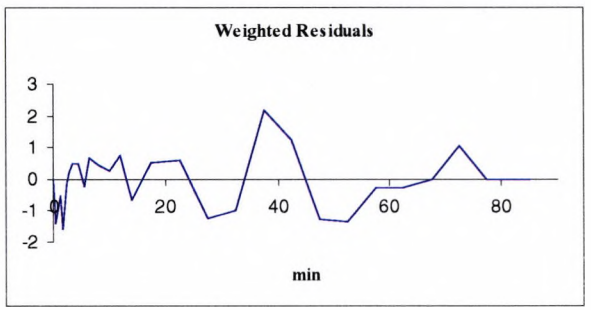
Weighted Residuals
min

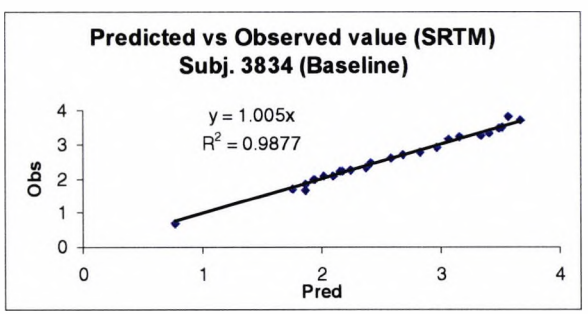
Predicted vs Observed value (SRTM)
Subj. 3834 (Baseline)
y = 1.005x
R2 = 0.9877
Obs
Pred

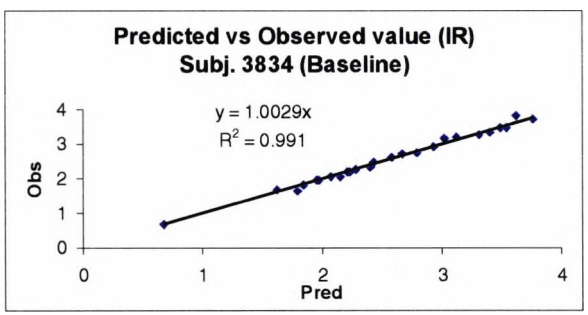
Predicted vs Observed value (IR)
Subj. 3834 (Baseline)
y = 1.0029x
R2 = 0.991
Obs
Pred

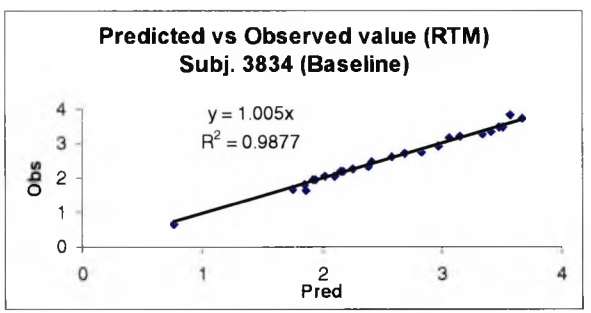
Predicted vs Observed value (RTM)
Subj. 3834 (Baseline)
y = 1.005x
R2 = 0.9877
Obs
Pred

Appendix C

In this Appendix the results of the iv human study for all the other regions of interest are presented. All the analyses were performed using the selected Simplified Reference Tissue Model.

Also the table of the HPLS analysis of metabolites is included.

TABLES

TABLE I: Estimates of the parameters and their precision (expressed in %CV) for the Simplified Reference Tissue Model. Receptor Occupancy (RO) is derived from the estimates BP. Subjects treated with 5 mg dose.

Lat.temp- Subj. 3827

	BP	CV(%)	R	CV(%)	k_2 (min^{-1})	CV(%)	RO	CV(%)
Baseline	0.611	9	0.765	3	0.035	11		
T2	0.044	31	0.855	2	0.040	24	93%	32
T4	0.008	93	0.783	2	0.045	13	99%	94
T24	0.061	22	0.815	1	0.030	15	90%	24
T28	0.038	29	0.817	1	0.031	14	94%	30
T48	0.022	61	0.789	1	0.024	13	96%	62

Lat.temp-Subj. 3825

	BP	CV(%)	R	CV(%)	k_2 (min^{-1})	CV(%)	RO	CV(%)
Baseline	1.617	13	0.927	2	0.022	10		
T2	0.119	8	0.943	1	0.036	16	95%	16
T4	0.109	12	0.909	1	0.032	18	95%	18
T24	0.106	12	0.931	2	0.039	25	95%	18
T28	0.082	11	0.906	2	0.044	18	96%	17
T48	0.118	23	0.910	1	0.020	24	95%	26

Med.temp-Subj. 3827

	BP	CV(%)	R	CV(%)	k_2 (min^{-1})	CV(%)	RO	CV(%)
Baseline	1.348	43	0.668	3	0.016	21		
T2	0.181	60	0.683	2	0.013	25	87%	73
T4	0[a]		0.653	3	0.016	10	100%	
T24	0.032	130	0.649	2	0.020	19	98%	137
T28	0.003	1060	0.627	3	0.022	18	100%	1061
T48	0.261	93	0.624	2	0.008	32	81%	102

[a] fixed to zero by the algorithm itself

Med.temp-Subj. 3825

	BP	CV(%)	R	CV(%)	k_2 (min^{-1})	CV(%)	RO	CV(%)
Baseline	0.935	14	0.811	3	0.025	13		
T2	0.139	12	0.837	2	0.032	14	94%	19
T4	0.103	21	0.822	2	0.031	19	96%	26
T24	0.215	40	0.821	2	0.018	33	91%	42
T28	0.105	16	0.811	2	0.036	17	95%	22
T48	0.215	28	0.838	1	0.016	23	91%	32

Oc.cortex-Subj.3827

	BP	CV(%)	R	CV(%)	k_2 (min^{-1})	CV(%)	RO	CV(%)
Baseline	1.315	9	1.15	2	0.04	14		
T2	0[a]		1.12	1	0.01	13	100%	
T4	0[a]		1.11	1	0.01	20	100%	
T24	0.094	8	1.12	2	0.07	148	93%	12
T28	0.058	21	1.15	2	0.04	49	96%	23
T48	0.064	58	1.08	1	0.01	320	95%	59

[a] fixed to zero by the algorithm itself

Oc.cortex-Subj.3825

	BP	CV(%)	R	CV(%)	k_2 (min^{-1})	CV(%)	RO	CV(%)
Baseline	1.990	9	1.177	2	0.033	10		
T2	0.158	4	1.384	1	0.054	13	93%	10
T4	0.125	7	1.349	1	0.059	18	95%	11
T24	0.106	10	1.225	1	0.038	30	95%	13
T28	0.043	91	1.228	1	0.019	48	98%	92
T48	0.151	16	1.418	1	0.026	24	93%	19

TABLE II: Estimates of the parameters and their precision (expressed in %CV) for the Simplified Reference Tissue Model. Receptor Occupancy (RO) is derived from the estimates BP. Subjects treated with 0.1 mg dose.

Lat.temp-Subj. 3830

	BP	CV(%)	R	CV(%)	k_2 (min^{-1})	CV(%)
Baseline	0.172	10	0.918	1	0.025	14
T2	0.471	11	0.916	1	0.019	12
T4	0.136	81	0.889	1	0.010	56
T24	2.341	31	0.823	2	0.017	14
T48	2.387	19	0.888	1	0.014	8

Lat.temp-Subj.3831

	BP	CV(%)	R	CV(%)	k_2 (min^{-1})	CV(%)
Baseline	0.251	9	0.910	1	0.022	12
T2	0.476	4	0.913	1	0.030	7
T4	0.121	24	0.918	1	0.018	25
T24	2.584	39	0.860	2	0.017[a]	16
T48	1.683	17	0.877	1	0.019	11

[a] estimated by a Bayesian approach

Med.temp-Subj.3830

	BP	CV(%)	R	CV(%)	k_2 (min^{-1})	CV(%)
Baseline	0.408	71	0.756	1	0.010[a]	37
T2	0.673	61	0.846	3	0.014	45
T4	0.130	127	0.766	2	0.011[a]	53
T24	1.368	22	0.742	3	0.022	14
T48	0.866	24	0.801	3	0.020	19

[a] estimated by a Bayesian approach

Med.temp-Subj.3831

	BP	CV(%)	R	CV(%)	k_2 (min^{-1})	CV(%)
Baseline	0.287	40	0.724	2	0.016	25
T2	1.621	30	0.784	2	0.016	16
T4	0.098	57	0.717	2	0.017	23
T24	2.837	37	0.828	2	0.015[a]	12
T48	1.452	21	0.773	2	0.019	13

[a] estimated by a Bayesian approach

Oc.cortex-Subj.3830

	BP	CV(%)	R	CV(%)	k_2 (min^{-1})	CV(%)
Baseline	0.265	6	1.177	1	0.023	23
T2	0.466	7	1.180	1	0.025[a]	18
T4	0[b]		1.239	1	0.021	9
T24	2.964	30	1.006	2	0.021	15
T48	4.644	55	1.162	1	0.015	19

[a] estimated by a Bayesian approach
[b] fixed to zero by the algorithm itself

Oc.cortex-Subj.3831

	BP	CV(%)	R	CV(%)	k_2 (min^{-1})	CV(%)
Baseline	0.280	5	1.089	1	0.031	18
T2	0.612	5	1.247	1	0.034	18
T4	0[b]		1.225	1	0.012	10
T24	4.455	20	1.067	1	0.020[a]	7
T48	4.110	34	1.223	1	0.017	14

[a] estimated by a Bayesian approach
[b] fixed to zero by the algorithm itself

TABLE III: Estimates of the parameters and their precision (expressed in %CV) for the Simplified Reference Tissue Model. Receptor Occupancy (RO) is derived from the estimates BP. Subjects treated with 0.01 and 1 mg dose

Lat.temp-Subj. 3832

	BP	CV(%)	R	CV(%)	k_2 (min^{-1})	CV(%)	RO	CV(%)
Baseline	5.146	18	0.899	1	0.022	6		
T2	4.077	19	0.866	1	0.022	7	21%	27
T4	2.648	12	0.893	1	0.022	6	49%	22
T24	3.107	28	0.870	2	0.021	12	40%	34
T28	0.092	10	0.833	1	0.035	10	98%	21
T48	0.377	8	0.876	1	0.022	9	93%	20

Lat.temp-Subj. 3834

	BP	CV(%)	R	CV(%)	k_2 (min^{-1})	CV(%)	RO	CV(%)
Baseline	2.495	12	0.796	2	0.025	6		
T2	1.887	14	0.797	1	0.021	8	24%	19
T4	1.916	15	0.803	1	0.018	8	23%	20
T24	3.162	27	0.794	2	0.019	10	-27%	30
T28	0.051	27	0.782	1	0.025	12	98%	30
T48	0.571	19	0.776	1	0.015[a]	13	77%	22

[a] estimated by a Bayesian approach

Med.temp-Subj. 3832

	BP	CV(%)	R	CV(%)	k_2 (min^{-1})	CV(%)	RO	CV(%)
Baseline	4.033	36	1.004	2	0.021	14		
T2	3.345	29	1.125	2	0.025	16	17%	46
T4	2.191	16	1.064	2	0.027	12	46%	39
T24	2.165	23	1.028	3	0.026	17	46%	42
T28	0.579	9	0.997	3	0.036	19	86%	37
T48	0.961	15	0.989	4	0.034	22	76%	39

Med.temp-Subj. 3834

	BP	CV(%)	R	CV(%)	k_2 (min^{-1})	CV(%)	RO	CV(%)
Baseline	1.802	17	0.883	3	0.028	13		
T2	1.164	16	0.794	3	0.031	13	35%	23
T4	1.218	24	0.908	3	0.026	21	32%	30
T24	1.510	24	0.868	4	0.025	19	16%	30
T28	0.417	17	0.905	3	0.029	27	77%	24
T48	0.654	18	0.821	4	0.028	21	64%	25

Oc.cortex-Subj. 3832

	BP	CV(%)	R	CV(%)	k_2 (min^{-1})	CV(%)	RO	CV(%)
Baseline	6.072	24	1.078	2	0.028	8		
T2	12.506	35	1.184	1	0.024	6	-106%	42
T4	7.199	21	1.176	1	0.023[a]	6	-19%	32
T24	3.315	17	1.123	2	0.031	11	45%	29
T28	0.084	10	1.132	1	0.030[a]	27	99%	26
T48	0.535	8	1.081	1	0.022[a]	13	91%	25

[a] estimated by a Bayesian approach

Oc.cortex- Subj. 3834

	BP	CV(%)	R	CV(%)	k_2 (min^{-1})	CV(%)	RO	CV(%)
Baseline	4.653	14	1.137	1	0.030	7		
T2	3.804	15	1.156	1	0.026	8	18%	21
T4	3.997	22	1.145	1	0.019	9	14%	26
T24	3.964	21	1.147	2	0.028	10	15%	25
T28	0.134	5	1.164	1	0.028[a]	19	97%	15
T48	0.761	16	1.074	2	0.018[a]	19	84%	21

[a] estimated by a Bayesian approach

TABLE IV: Metabolites analysis

HPLC analysis of GLD in plasma

Experiment	Subj.	7	15	60	90
Baseline (T=0)	3825	57-75	51	18-34	x
	3827	o	x	x	o
Co-injection (T=2)	3825	74	95	62x	x
	3827	o	51	x	o
Pre-treatment (T=4)	3825	70	o	61	x
	3827	o	51	x	o
Pre-treatment (T=24)	3825	72	76	x	x
	3827	x	x	x	o
Pre-treatment (T=28)	3825	x	71	50-80	x
	3827	o	75	x	o
Pre-treatment (T=48)	3825	95	113	x	x
	3727	o	112	x	x

x represents instances where the data was not interpretable
o data non available

Appendix D

Subject 4235

Reversible model – Striatum

	R	CV(%)	k_2 (min^{-1})	CV(%)	BP	CV(%)	RO
Baseline	1.101	3	0.036	9	7.352	27	
T4	1.056	2	0.019	21	1.317	23	82%
Pre-dose day 7	1.025	2	0.035	8	3.008	11	59%
T4 day 7	1.020	1	0.015	21	1.955	36	73%

Reversible model – Lat. Temp.

	R	CV(%)	k_2 (min^{-1})	CV(%)	BP	CV(%)	RO
Baseline	0.933	1	0.024	7	3.578	17	
T4	0.854	2	0.040	13	0.195	8	95%
Pre-dose day 7	0.928	1	0.018	13	1.511	20	58%
T4 day 7	0.909	1	0.018	16	0.484	16	86%

Reversible model – Med. Temp.

	R	CV(%)	k_2 (min^{-1})	CV(%)	BP	CV(%)	RO
Baseline	0.789	3	0.023	14	3.214	33	
T4	0.838	3	0.032	24	0.296	17	91%
Pre-dose day 7	0.871	2	0.025	14	0.922	14	71%
T4 day 7	0.859	2	0.021	18	0.447	17	86%

Reversible model – Oc. Cortex..

	R	CV(%)	k_2 (min^{-1})	CV(%)	BP	CV(%)	RO
Baseline	1.166	2	0.029	13	5.316	31	
T4	1.134	2	0.032	65	0.269	13	95%
Pre-dose day 7	1.178	2	0.024	18	2.403	23	55%
T4 day 7	1.099	2	0.024	17	0.329	8	94%

[a] estimated by a Bayesian approach (0.028±0.004)

Subject 4236

Reversible model – Striatum

	R	CV(%)	k_2 (min^{-1})	CV(%)	BP	CV(%)	RO
Baseline	1.005	4	0.044	11	2.734	13	
T4	0.985	1	0.011	30	1.209	44	56%
Pre-dose day 7	0.980	2	0.023	14	2.134	21	22%
T4 day 7	0.951	1	0.013[a]	21	1.240	31	54%

[a] estimated by a Bayesian approach (0.028+0.01)

Reversible model – Lat. Temp.

	R	CV(%)	k_2 (min^{-1})	CV(%)	BP	CV(%)	RO
Baseline	0.855	3	0.028	14	1.609	20	
T4	0.897	1	0.017	27	0.235	26	85%
Pre-dose day 7	0.910	1	0.011	22	1.189	35	26%
T4 day 7	0.888	1	0.023	21	0.191	18	88%

Reversible model – Med. Temp.

	R	CV(%)	k_2 (min^{-1})	CV(%)	BP	CV(%)	RO
Baseline	0.956	3	0.034	13	1.207	12	
T4	0.981	3	0.037	17	0.652	9	46%
Pre-dose day 7	1.059	2	0.025	14	1.111	12	8%
T4 day 7	0.993	2	0.047	7	0.672	3	44%

Reversible model – Oc. Cortex.

	R	CV(%)	k_2 (min^{-1})	CV(%)	BP	CV(%)	RO
Baseline	1.154	2	0.036	9	2.699	11	
T4	1.213	1	0.030[a]	35	0.211	4	92%
Pre-dose day 7	1.146	1	0.017[a]	26	0.970	24	64%
T4 day 7	1.183	1	0.020[a]	50	0.272	11	90%

[a] estimated by a Bayesian approach (0.03±0.01)

Subject 4237

Reversible model – Striatum

	R	CV(%)	k_2 (min^{-1})	CV(%)	BP	CV(%)	RO
Baseline	0.998	2	0.028	6	6.586	23	
T4	0.972	2	0.014	48	0.447	44	93%
Pre-dose day 7	0.907	2	0.018	15	1.655	24	75%
T4 day 7	0.964	2	0.018	19	0.401	15	94%

Reversible model – Lat. Temp.

	R	CV(%)	k_2 (min^{-1})	CV(%)	BP	CV(%)	RO
Baseline	0.848	1	0.020	12	3.097	34	
T4	0.856	1	0.033	19	0.022	47	99%
Pre-dose day 7	0.871	1	0.013	21	0.423	26	86%
T4 day 7	0.883	1	0.021	24	0.086	28	97%

Reversible model – Med. Temp.

	R	CV(%)	k_2 (min^{-1})	CV(%)	BP	CV(%)	RO
Baseline	0.856	2	0.018	14	2.529	32	
T4	0.848	1	0.026	11	0.392	9	85%
Pre-dose day 7	0.840	3	0.032	16	0.502	13	80%
T4 day 7	0.862	2	0.021	31	0.377	33	85%

Reversible model – Oc. Cortex.

	R	CV(%)	k_2 (min^{-1})	CV(%)	BP	CV(%)	RO
Baseline	1.135	2	0.022	18	7.362	80	
T4	1.056	1	0.049	72	0.012	58	100%
Pre-dose day 7	0.769	34	0.011[a]	34	1.061	1	90%
T4 day 7	1.097	1	0.030[a]	35	0.073	12	99%

[a] estimated by a Bayesian approach (0.025±0.01)

Subject 4238

Reversible model – Striatum

	R	CV(%)	k_2 (min^{-1})	CV(%)	BP	CV(%)	RO
Baseline	1.066	2	0.038	6	4.182	10	
T4	0.983	3	0.018	62	0.312	43	93%
Pre-dose day 7	0.996	1	0.020	8	3.343	17	20%
T4 day 7	0.990	1	0.015[a]	21	0.796	22	81%

[a] estimated by a Bayesian approach (0.025±0.01)

Reversible model – Lat. Temp.

	R	CV(%)	k_2 (min^{-1})	CV(%)	BP	CV(%)	RO
Baseline	0.823	1	0.022	6	2.382	11	
T4	0.773	1	0.030	9	0.000[a]	****	100%
Pre-dose day 7	0.793	1	0.015	13	0.495	17	79%
T4 day 7	0.810	2	0.029	18	0.082	23	97%

[a] fixed to zero by the algorithm

Reversible model – Med. Temp.

	R	CV(%)	k_2 (min^{-1})	CV(%)	BP	CV(%)	RO
Baseline	0.840	3	0.019	16	2.100	30	
T4	0.849	2	0.044	17	0.137	11	93%
Pre-dose day 7	0.876	2	0.015	22	0.890	30	58%
T4 day 7	0.924	2	0.018	29	0.415	26	80%

Reversible model – Oc. Cortex.

	R	CV(%)	k_2 (min^{-1})	CV(%)	BP	CV(%)	RO
Baseline	1.124	1	0.032	8	3.021	14	
T4	1.135	1	0.011	26	0.000	****	100%
Pre-dose day 7	1.068	1	0.013	30	0.821	29	73%
T4 day 7	1.132	1	0.020[a]	27	0.144	7	95%

[a] estimated by a Bayesian approach (0.02±0.005)

Subject 4239

Reversible model – Striatum

	R	CV(%)	k_2 (min^{-1})	CV(%)	BP	CV(%)	RO
Baseline	0.876	2	0.027	8	6.884	35	
T4	1.125	1	0.040	46	0.223	7	97%
Pre-dose day 7	0.896	2	0.017	41	0.148	42	98%
T4 day 7	1.064	1	0.027	84	0.140	19	98%

Reversible model – Lat. Temp.

	R	CV(%)	k_2 (min^{-1})	CV(%)	BP	CV(%)	RO
Baseline	0.702	2	0.015	13	7.275	87	
T4	0.887	1	0.034	16	0.068	15	99%
Pre-dose day 7	0.858	1	0.020	21	0.087	29	99%
T4 day 7	0.881	2	0.052	18	0.050	14	99%

Reversible model – Med. Temp..

	R	CV(%)	k_2 (min^{-1})	CV(%)	BP	CV(%)	RO
Baseline	0.573	2	0.016	14	1.939	42	
T4	0.753	1	0.013	32	0.071	107	96%
Pre-dose day 7	0.803	2	0.029	17	0.204	15	89%
T4 day 7	0.811	2	0.023	22	0.201	24	90%

Reversible model – Oc. Cortex..

	R	CV(%)	k_2 (min^{-1})	CV(%)	BP	CV(%)	RO
Baseline	0.971	1	0.022	8	7.628	40	
T4	1.239	1	0.016	8	0.000[a]	****	100%
Pre-dose day 7	1.193	2	0.050	36	0.070	14	99%
T4 day 7	1.337	2	0.032	33	0.087	29	99%

[a] Fixed to zero by the algorithm

Subject 4240

Reversible model – Striatum

	R	CV(%)	k_2 (min^{-1})	CV(%)	BP	CV(%)	RO
Baseline	0.979	2	0.028	10	4.951	27	
T4	1.002	1	0.014[a]	28	0.373	22	92%
Pre-dose day 7	0.918	2	0.018	12	2.252	23	55%
T4 day 7	0.920	1	0.018	9	2.081	17	58%

[a] estimated by a Bayesian approach (0.019+0.006)

Reversible model – Lat. Temp.

	R	CV(%)	k_2 (min^{-1})	CV(%)	BP	CV(%)	RO
Baseline	0.807	2	0.018	12	4.265	40	
T4	0.859	1	0.018	30	0.119	39	97%
Pre-dose day 7	0.800	1	0.014	28	0.432	42	90%
T4 day 7	0.829	2	0.015	38	0.173	54	96%

Reversible model – Med. Temp..

	R	CV(%)	k_2 (min^{-1})	CV(%)	BP	CV(%)	RO
Baseline	0.710	5	0.024	23	1.026	31	
T4	0.669	3	0.009	57	0.253	146	75%
Pre-dose day 7	0.665	4	0.019	26	0.452	39	56%
T4 day 7	0.649	3	0.010	41	0.469	92	54%

Reversible model – Oc. Cortex..

	R	CV(%)	k_2 (min^{-1})	CV(%)	BP	CV(%)	RO
Baseline	1.233	1	0.022	11	11.566	62	
T4	1.357	2	0.063	26	0.177	5	86%
Pre-dose day 7	NO FITTING						
T4 day 7	1.229	3	0.167	69	0.160	3	87%

Subject 4241

Reversible model – Striatum

	R	CV(%)	k_2 (min^{-1})	CV(%)	BP	CV(%)	RO
Baseline	1.016	1	0.032	3	5.047	8	
T4	0.912	1	0.014	17	1.338	26	73%
Pre-dose day 7	0.907	2	0.015	15	3.732	47	26%
T4 day 7	0.919	1	0.013	19	1.509	32	70%

Reversible model – Lat. Temp.

	R	CV(%)	k_2 (min^{-1})	CV(%)	BP	CV(%)	RO
Baseline	0.835	2	0.028	7	2.341	11	
T4	0.856	1	0.020	14	0.206	15	91%
Pre-dose day 7	0.864	1	0.014	12	0.634	15	73%
T4 day 7	0.864	1	0.025	15	0.221	12	91%

Reversible model – Med. Temp..

	R	CV(%)	k_2 (min^{-1})	CV(%)	BP	CV(%)	RO
Baseline	0.901	2	0.030	8	1.396	8	
T4	0.966	2	0.028	22	0.518	14	63%
Pre-dose day 7	0.909	2	0.030	11	0.589	8	58%
T4 day 7	0.887	3	0.033	18	0.404	11	71%

Reversible model – Oc. Cortex..

	R	CV(%)	k_2 (min^{-1})	CV(%)	BP	CV(%)	RO
Baseline	1.049	1	0.035	5	3.324	7	
T4	1.151	1	0.020[a]	48	0.287	15	91%
Pre-dose day 7	NO FITTING						
T4 day 7	1.182	1	0.018	53	0.361	17	89%

[a] estimated by a Bayesian approach (0.027+0.008)

Subject 4242

Reversible model – Striatum

	R	CV(%)	k_2 (min^{-1})	CV(%)	BP	CV(%)	RO
Baseline	0.979	1	0.030	5	5.556	14	
T4	0.898	1	0.019[a]	5	1.521	8	73%
Pre-dose day 7	0.870	1	0.018	8	2.011	15	64%
T4 day 7	0.865	2	0.019	14	1.044	18	81%
[a] estimated by a Bayesian approach (0.021+0.009)							

Reversible model – Lat. Temp.

	R	CV(%)	k_2 (min^{-1})	CV(%)	BP	CV(%)	RO
Baseline	0.820	1	0.018	5	5.411	21	
T4	0.834	1	0.019	12	0.334	12	94%
Pre-dose day 7	0.810	1	0.017	9	0.375	10	93%
T4 day 7	0.773	2	0.036	11	0.130	11	98%

Reversible model – Med. Temp..

	R	CV(%)	k_2 (min^{-1})	CV(%)	BP	CV(%)	RO
Baseline	0.735	2	0.014	16	4.027	63	
T4	0.660	2	0.026	10	0.232	14	94%
Pre-dose day 7	0.695	2	0.023	10	0.331	13	92%
T4 day 7	0.658	3	0.025	15	0.219	22	95%

Reversible model – Oc. Cortex..

	R	CV(%)	k_2 (min^{-1})	CV(%)	BP	CV(%)	RO
Baseline	0.998	2	0.030	6	3.669	12	
T4	1.037	2	0.008	124	0.468	114	87%
Pre-dose day 7	1.087	2	0.014	45	0.648	35	82%
T4 day 7	NO FITTING						

Personal Bibliography

Zamuner S, Gomeni R, Bye A. Estimate the time varying brain receptor occupancy in PET imaging experiments using non-linear fixed and mixed effect modeling approach. Nuclear Medicine and Biology Journal, 29 (2002) 115-123.

Scientific communications presented at international meetings

Bertoldo A, Zamuner S, Gomeni R, Bye A, Cobelli C. NK1 receptor occupancy in the brain studied by [^{11}C]GR205171. Brain PET'01.

Zamuner S, Bertoldo A, Bergstrom M, Iavarone L, Fasth KJ, Langstrom B, Bani M, Bye A, Cobelli C. Modeling of drug-receptor interaction in the monkey brain: a PET pharmacokinetic study. Proc. 22nd IEEE-EMBS Conf., Chicago, IL, July 23-28, 2000.

A. Bertoldo, S. Zamuner, R. Gomeni, A. Bye, C. Cobelli, Binding characteristics of NK1 receptors in the brains studied by [11C]GR205171 and PET. BrainPET'01 Vth International Conference on Quantification of Brain Function with PET. Taipei, TAIWAN, June 9-13, 2001.

Zamuner S, Gomeni R, Bye A. Estimate the time varying brain receptor occupancy in PET imaging. PAGE Eleventh Meeting. Paris, France, 6 - 7 June, 2002.

Zamuner S, Gomeni R. Impact of slow receptor binding kinetics and change in Cerebral Blood Flow in receptor occupancy estimation with PET experiments. A simulation study. PAGE Twelfth Meeting. Verona, Italy, 12 - 13 June, 2003.

Reprints

Zamuner S, Gomeni R, Bye A. Estimate the time varying brain receptor occupancy in PET imaging experiments using non-linear fixed and mixed effect modeling approach. Nuclear Medicine and Biology Journal, 29 (2002) 115-123.

ELSEVIER

Nuclear Medicine and Biology 29 (2002) 115–123

NUCLEAR MEDICINE — AND — BIOLOGY

Estimate the time varying brain receptor occupancy in PET imaging experiments using non-linear fixed and mixed effect modeling approach

Stefano Zamuner, Roberto Gomeni*, Alan Bye

GlaxoSmthKline, Via A. Fleming 4, 37135 Verona, Italy

Received 4 June 2001; received in revised form 21 August 2001; accepted 21 August 2001

Abstract

Positron-Emission Tomography (PET) is an imaging technology currently used in drug development as a non-invasive measure of drug distribution and interaction with biochemical target system. The level of receptor occupancy achieved by a compound can be estimated by comparing time-activity measurements in an experiment done using tracer alone with the activity measured when the tracer is given following administration of unlabelled compound. The effective use of this surrogate marker as an enabling tool for drug development requires the definition of a model linking the brain receptor occupancy with the fluctuation of plasma concentrations. However, the predictive performance of such a model is strongly related to the precision on the estimate of receptor occupancy evaluated in PET scans collected at different times following drug treatment. Several methods have been proposed for the analysis and the quantification of the ligand-receptor interactions investigated from PET data. The aim of the present study is to evaluate alternative parameter estimation strategies based on the use of non-linear mixed effect models allowing to account for intra and inter-subject variability on the time-activity and for covariates potentially explaining this variability. A comparison of the different modeling approaches is presented using real data. The results of this comparison indicates that the mixed effect approach with a primary model partitioning the variance in term of Inter-Individual Variability (IIV) and Inter-Occasion Variability (IOV) and a second stage model relating the changes on binding potential to the dose of unlabelled drug is definitely the preferred approach.

Keywords: PET imaging; Non linear model; Fixed effect; Mixed effect

1. Introduction

Positron-Emission Tomography (PET) is an imaging technology currently used in drug development as a non-invasive measure of drug distribution and interaction with biochemical target system [10,11,26]. This method is more and more frequently applied to define neurochemical correlates of illness and to explore the interaction properties of a drug with cerebral receptor and enzyme systems [2,13]. Furthermore, PET studies can supply accurate information for a rational definition of a dosage regimen suitable to achieve expected therapeutic outcomes, assuming that the brain receptor occupancy is a surrogate marker of a pharmacological drug activity [12,21,24]. Several methods have been proposed for the analysis and the quantification of the ligand-receptor interactions investigated *in vivo* from PET data [7,8,16,17,20,23,27,28]. All the *in vivo* approaches are based on mathematical models, which describe the transport of the ligand from the blood to a free ligand brain compartment and the interaction with the ligand-receptor sub-system. One of the major issues remaining unsolved is the estimate of the value and the precision of receptor time-varying occupancy accounting for the variability induced by the complex manipulations necessary to generate the time-activity data and by the intra- (or inter occasion) and inter-subject variability in individual response. Examples of abnormal (negative) fractional receptor occupancy values based on the independent modeling of time-activity data for each subject and for each PET scan time, have been reported [1]. In addition, in a recent paper has been showed that a correct inference about subject responses to activation tasks in a fMRI study can be derived through the use of a statistical model which accounts for both within- and between-subject variance applying random-effect modeling approach in the data interpretation [19].

The aim of the present study is to evaluate alternative parameter estimation strategies based on the use of non-linear mixed effect models accounting for intra and inter-

* Corresponding author. Tel.: +39.045.921.9618; fax: +39.045.921.8192.
E-mail address: rog31390@gsk.com (R. Gomeni).

0969-8051/02/$ – see front matter
PII: S0969-8051(01)00275-X

subject variability on the time-activity and for the identification of possible source of this variability using individual covariate measurements. The effective use of PET measurement as an enabling tool for drug development requires the definition of a model linking the brain receptor occupancy with the fluctuation of plasma concentrations. However, the predictive performance of such a model is strongly related to the precision on the estimate of the time varying receptor occupancy values.

2. Materials and methods

2.1. PET study

The aim of this study was the *in vivo* evaluation of the binding kinetics of a high affinity NK_1 receptor antagonist, [11C]GR205171, in the monkey brain. The experiments were initially conducted in 5 anesthetized rhesus monkeys. Furthermore, two additional monkeys were included in the same study on a separate occasion. Following a baseline experiment, each monkey received one or two unlabelled ligand followed by a tracer injection. The unlabelled drug was injected at the doses of: 0.05 mg/kg and 0.5 mg/kg in the monkey 1, 2, and 3, 0.1 mg/kg in the monkey 4, 1 mg/kg in the monkey 5, 0.001 mg/kg in the monkey 6 and 0.01 mg/kg in the monkey 7. Cerebellum was considered the reference region (RR) without specific receptors and Striatum the region of interest (ROI) according to the information collected on previous autoradiography studies. Each scan lasted approximately 55 minutes for monkey 1, 2, 3, 4, 5 and approximately 90 minutes for monkey 6 and 7. The time activity curves were expressed in SUV (Standardized Uptake Value), which equals the radioactivity concentration divided by dose of injected radioactivity normalized to body weight (normalized dose radioactivity). The PET studies were performed in the Uppsala University PET Center and the details on equipment, experimental conditions together with preliminary results have been reported in a recent publication [5].

2.2. Time-activity model selection

The PET modeling was organized into two consecutive steps. The first one concerned the choice of the most appropriate structural model while the second one consisted on the evaluation of the most appropriate parameters estimation procedure.

The data here presented were previously analyzed using an irreversible graphical methods (Patlak) [5]. However, we decided to re-analyze the date and to compare alternative modeling options using a kinetic approach because it was shown that the simplifying assumptions underling the graphical method can lead to substantial bias [23]. Since the arterial input function was not available three models based on the reference region were used to account for a reversible and irreversible binding hypotheses. This approach estimates receptor-bound activity by subtracting the concentration of activity in a reference region, known to be devoid of the receptors of interest (non-specific binding + free tracer), from the concentration of total uptake in the region of interest (specific + non-specific binding + free activity). The level of receptor occupancy achieved by a compound can be estimated by comparing time-activity measurements from a pre-dose PET scan using the tracer alone, with the activity measured when the tracer is given following administration of the cold (unlabelled) compound. The pre-dose scan gives an estimate of the total number of receptors available to be occupied: the binding potential (BP). In subsequent scans, the PET tracer has less specific binding because the compound is occupying a defined proportion of the specific receptors. The two-tissue compartment reference tissue model (RTM) [16] and the simplified reference tissue model (SRTM) [17] were initially used. In the last approach, a modified version of the RTM, MRTM, based on irreversible binding assumption was applied. The models were compared on the basis of weighted residuals, parameter precision, Akaike criteria using a weighted non-linear least squares procedure as implemented in the SAMII software package [4]. The minimization algorithm reached a successful convergence in 100% of data sets using SRTM, 46% using MRTM and 77% using RTM. According the Akaike criteria SRTM was the preferred model in 66% of data sets, the RTM in 15% and MRTM in 19%. The results have been presented in [6] and show that the SRTM is the most appropriate model among those evaluated to describe the [11C]GR205171 binding kinetic in monkey. This one tissue-compartment and three-parameter model assumes that only the parent tracer, crossing the blood-brain barrier, diffuses from the plasma compartment to the a region devoid of specific binding sites (C_r), and to the specific compartments associated to a region of interest (C_t). Furthermore, the level of non-specific binding is assumed identical in both tissues. Moreover, the SRTM model provided well identified estimate of the model parameters with increased convergence rate in combination with increased stability when compared with alternative models. Time-activity data were analyzed using the Simplified Reference Tissue Model, considering the Cerebellum as the reference region and the Striatum as region of interest. Three alternative data analysis approaches were investigated based on the use of non-linear fixed and random-effect models.

2.3. Model A

A non-linear fixed-effects model (Equation 1) was used to independently analyze the time-activity data collected at each PET scan time as if they come from separate animals.

$$\frac{dy}{dt} = \left(k_2 - \frac{R_1 \cdot k_2}{(1 + BP)}\right) C_r(t) - \frac{k_2}{(1 + BP)} y$$
$$C_t(t) = y + R_1 \cdot C_r(t) \quad (1)$$

Were C_t and C_r are the tracer concentration in the ROI and in the RR respectively, BP is the binding potential, R_1 is the ratio of the delivery in the ROI compared to that in the RR (ratio of influx), and k_2 is the efflux rate constant from the ROI. The fractional receptor occupancy value at scan time i ($RO\%_i$) was further derived from the primary model parameters using the binding potential value estimated at the baseline (BP_0) and the one estimated at the i^{th} PET scan time (BP_i) as:

$$RO\%_i = 100\,\frac{BP_0 - BP_i}{BP_0} \tag{2}$$

2.4. Model B

All the time-activity data collected in a monkey was simultaneously analyzed using a non-linear fixed-effects approach and the Model B (Equation 3). All parameters were considered as fixed-effect parameters. R_1 and k_2 were assumed to have a typical value for each monkey constant across PET scan times. R_1 and k_2 were estimated using all the measurements at the different times, BP_0 was estimated using only baseline data while $RO\%_i$ was estimated using the measurements at time i. The model was constrained to estimate positive $RO\%_i$ values using a model re-parameterisation: the receptor occupancy (RO%) was constrained to be equal to 0 at baseline and to assume values ranging between 0 and 100% at the different PET scan times.

$$\begin{aligned}
&\frac{dy}{dt} = \left(k_2 - \frac{R_1 \cdot k_2}{(1 + BP)}\right) C_r(t) - \frac{k_2}{(1 + BP)}\, y \\
&BP = BP_0 - \frac{RO\%_i \cdot BP_0}{100} \\
&C_t(t) = y + R_1 \cdot C_r(t)
\end{aligned} \tag{3}$$

The parameters estimated in the Model B are: BP_0, R_1, k_2 + $RO\%_i$ [i = 1, number of PET scans (including baseline) –1]

2.5. Model C

The non-linear mixed-effects approach was applied using the structural model defined by equation 4. All data for each monkey and each scan time were jointly analyzed accounting for intra (or inter occasion)-and inter- monkey variability. The modeling approach (Model C-a) was based on the assumptions that: (a) typical tracer kinetic and binding parameters exist for each monkey (fixed-effect) and (b) these parameters may vary across monkey and experimental conditions within the same monkey according to two variability sources: an Inter-Occasion Variability (IOV) and Inter-Individual Variability (IIV). IIV was estimated as a first level random-effect parameter while occasion-specific departure of the parameter from the individual typical values (IOV) was accounted by a second level random-effect model component.

Table 1
Parameter values estimated using the Model A

Monkey		R_1	k_2	BP	RO%
1	Baseline	0.840	0.0349	2.620	0
	Scan 1	1.360	0.3270	0.209	92.0
	Scan 2	1.050	0.0354	0.300	88.5
2	Baseline	0.778	0.0290	4.550	0
	Scan 1	0.778	0.0405	0.418	90.8
	Scan 2	0.848	0.1100	0.109	97.6
3	Baseline	0.863	0.0245	3.340	0
	Scan 1	0.905	0.0418	0.234	93.0
	Scan 2	1.000	0.0651	0.221	93.4
4	Baseline	*	*	*	—
	Scan 1	*	*	*	—
5	Baseline	1.070	0.0341	3.860	0
	Scan 1	*	*	*	—
6	Baseline	1.040	0.0433	0.848	0
	Scan 1	0.938	0.0151	1.020	−20.3
7	Baseline	1.090	0.0323	1.710	0
	Scan 1	1.010	0.0076	0.932	45.5

* Non-linear regression procedure failed to reach convergence.
– Parameter not estimated.

$$\begin{aligned}
&\frac{dy}{dt} = \left(k_2 - \frac{R_1 \cdot k_2}{(1 + BP)}\right) C_r(t) - \frac{k_2}{(1 + BP)}\, y \\
&C_t(t) = y + R_1 \cdot C_r(t)
\end{aligned} \tag{4}$$

2.6. Model for IIV and IOV

Denoting the ith subject's average parameter value P_i, and its value at the jth occasion P_{ij}, a general model for IOV was:

$$\begin{aligned}
&P_i = f(P^*,\ \eta_i) \\
&Pij = g(Pi,\ kij)
\end{aligned} \tag{5}$$

where P^* is a typical value of P in the population and η_i and k_{ij} are assumed to be independently, normally distributed parameters both with zero mean and variance ω^2 and π^2, respectively. The η represents the between individual difference (IIV) and the k the between occasion difference within an individual (IOV). The following exponential models were evaluated to describe IIV and IOV variability:

Table 2
Parameter values estimated using the Model B

Monkey	R_1	k_2	BP_0	$RO\%_1$	$RO\%_2$
1	1.1	0.0142	119	99.6	99.7
2	0.83	0.0302	2.97	82.6	87.9
3	0.946	0.0217	2.95	86.9	79.6
4	0.613	0.0211	282	100	
5	1.09	0.0246	16.8	98	
6	0.968	0.0429	0.932	63.2	
7	1.03	0.0392	1.59	83.6	

$RO\%_1$, $RO\%_2$: receptor occupancy estimated at the first and second scans time.

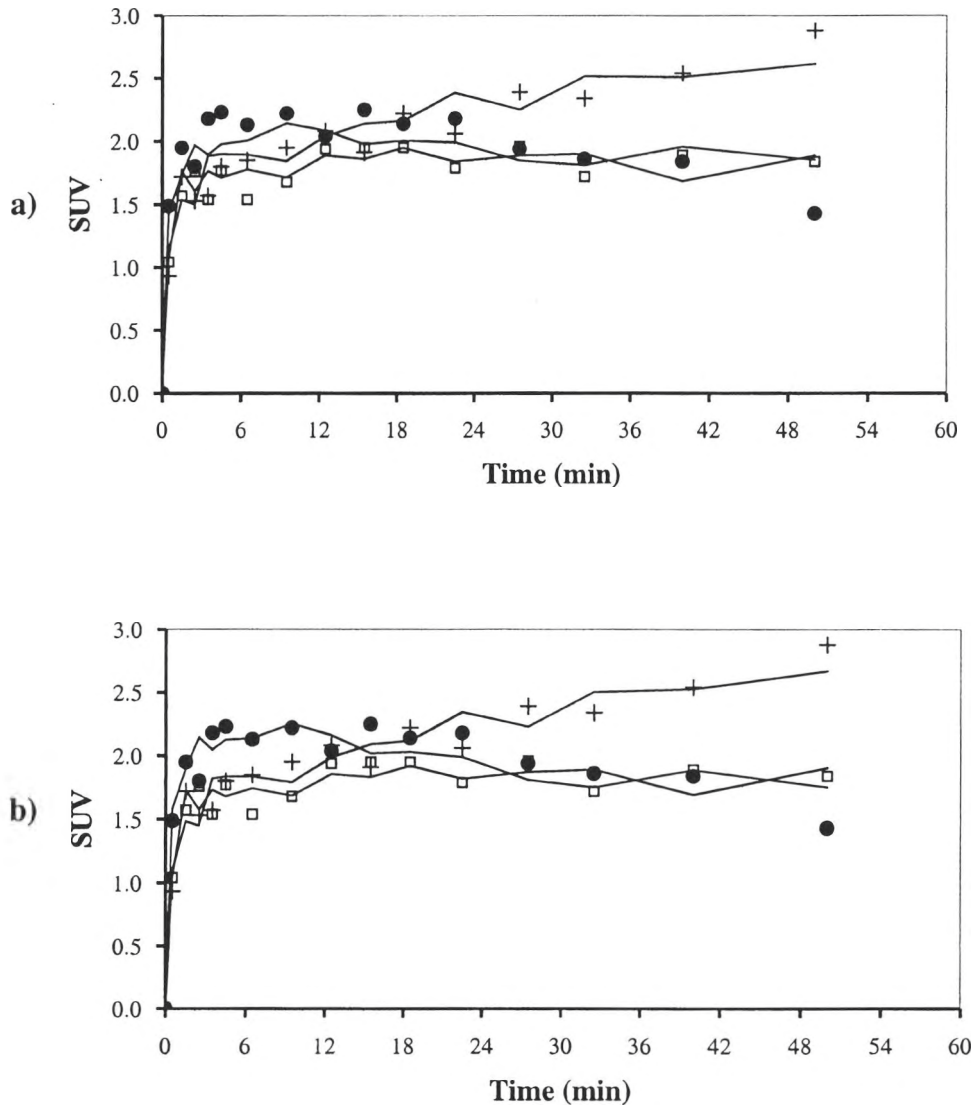

Fig. 1. Monkey 2: Individual observed time-activity (SUV) data with model predicted values (continuos line) using fixed effect model B (panel a) and random effect model C-c (panel b) at (+) baseline, ( ) scan 2, (●) scan 3.

$$P_{ij} = P^* \cdot e^{(\eta_i + k_{ij})}$$
$$\eta_i \approx N(0, \omega^2) \quad (6)$$
$$k_{ij} \approx N(0, \pi^2)$$

Using this approach, the model parameters were partitioned in fixed-effect (R_I, k_2, BP), random-effect (ωR_I, ωk_2 and ωBP), and residual error (σ) parameters. All the parameters (fixed and random) were estimated using all the collected measurements. R_I, k_2 and BP were assumed to vary across PET scan times taking values from two distributions having typical values equal to R_I^*, k_2^* and BP* and a dispersion proportional to ωR_I, ωk_2 and ωBP to account for IIV and to πR_I, πk_2 and πBP to account for IOV variance component.

Table 3
Non-linear mixed effect modelling: comparison of the objective function values estimated using an additive and a proportional error model assumption

	Model C-a	Model C-b	Model C-c
Proportional error model	−643.112	−647.658	−687.345
Additive error model	−622.654	−630.683	−663.933

2.7. Model for residual error

The residual error on the time-activity measurements was modeled using either additive or proportional model. This error term component represents the residual departure of the model from the observations and contain contribu-

tions from unexplained variability, measurement error and model misspecification for the dependent variable.

2.8. Covariate effects

The dose of unlabelled ligand was expected to affect the BP values estimated in different occasions. Therefore, the dose of unlabelled ligand was considered as a covariate potentially explaining the variability observed on the BP fixed-effect parameter value. The procedure used to investigate the influence of the covariate was based on the analysis of the individual Bayesian parameter estimates plot vs. the covariate values [18] and on the log-likelihood ratio test. The exponential (Model C-b, Equation 7) and the sigmoid (Model C-c, Equation 8) models were investigated as potentially explanatory models.

$$BP_{ij} = BP_0 \cdot e^{-Dose_{ij}\beta} \quad (7)$$

$$BP_{ij} = BP_{\cdot} - \frac{Emax \cdot Dose_{ij}}{ED_{50} + Dose_{ij}} \quad (8)$$

where BP_0 is the binding potential at baseline, BP_{ij} is the binding potential at i^{th} scan for j^{th} subject, β is a slope factor, Emax represents the maximum BP reduction and ED_{50} the dose giving 50% of the maximum BP reduction.

The model retained was included as a second stage model in the equation 4. The predictive accuracy of the individual Bayesian estimates of the time activity data was evaluated by comparing the scatter plot of the individual predictions vs. the observed data with the unitary slope reference line.

2.9. Data analysis

All analyses were performed using the first-order estimate method as implemented in NONMEM Version 5.1 [3]. Furthermore, using the population parameter the bayesian individual estimates of kinetic parameters were then estimated. Minimizing the objective function provided by NONMEM is equivalent to maximize the likelihood of data. Hypothesis testing was performed by comparing the changes in the objective function (OF) when the value of one or more parameters have been fixed in the regression model. The difference in OF values is asymptotically distributed as χ^2 with a degree of freedom equal to the difference in the number of parameters between the two regression models. Any reduction in OF greater than 3.84 and 5.99 (χ^2, $p < 0.05$ with 1 and 2 *df*) was considered to be significant and the parameter(s) concerned retained in the model according to the log-likelihood ratio test [9].

3. Results

The parameters estimated using the fixed-effect modeling approach (Model A) are shown in Table 1. The computational algorithm failed to reach convergence for monkey 4 at baseline and at scan 1 and for monkey 5 at scan 1 probably due to the variability on time-activity data. Furthermore, inconsistent negative value for receptor occupancy was estimated for monkey 6. In the Model B, all the time-activity observations collected in the same monkey at different scan times were simultaneously analyzed using a re-parameterised model where the RO% value was fixed to 0 at baseline and to a value ranging between 0 and 100% at the different scan times. The parameters estimated using this modeling approach are shown in Table 2. The scatter plot of the observed and model predicted time activity data of a typical individual (monkey 2) vs. time is displayed in Figure 1a. Two sets of analyses were conducted using the non-linear mixed effect to evaluate the influence of additive and proportional error model. The analysis database included 7 monkey with 17 time-activity curves and a total of 267 measurements. The results, shown in Table 3, indicate that the proportional error model significantly improved the OF values for all the modeling approaches used. The fixed and random parameter values estimated with the Model C-a, C-b, and C-c using the proportional error model are shown in Table 4. The results of this analysis indicate that the fixed influx/efflux parameter R_I and k_2 estimated from the 4 models have similar values at the exception of k_2 in the model C-c which shows an higher value. The comparison of random effects estimates indicates that IOV variability seems to represent the most important component of the total variability and that the inclusion of the Emax model, as a second stage regression model, significantly ($P < 0.01$) explains the observed variability on BP as a function of the unlabelled drug dose administered at the different scan times. The time activity plot of the observed and mixed effect model predicted values of a typical individual (monkey 2) is displayed in Figure 1b while the individual ob-

Table 4
Non-linear mixed effect modelling fixed and random effect parameter values.

Parameters	Model C-a	Model C-b	Model C-c
R_1	0.982	0.981	1.0
k_2	0.0171	0.0196	0.0268
BP	1.19	β = 2.19	BPo = 3.31
		BPo = 1.23	Emax = 3.05
			ED50 = 0.0000323
ωR	15	15	16
$\omega k2$	<1	<1	<1
ωBP	<1	<1	<1
πR_1	11	12	11
πk_2	35	33	<1
πBP	182	145	56
σ	8	8	7
OF	−643.112	−647.658	−687.345
ΔOF	0	4.56	44.233
Probability		df = 1	df = 2
		$P < 0.05$	$P < 0.01$

The ICV, IIV, IOV and residual error variability are expressedas CV%.

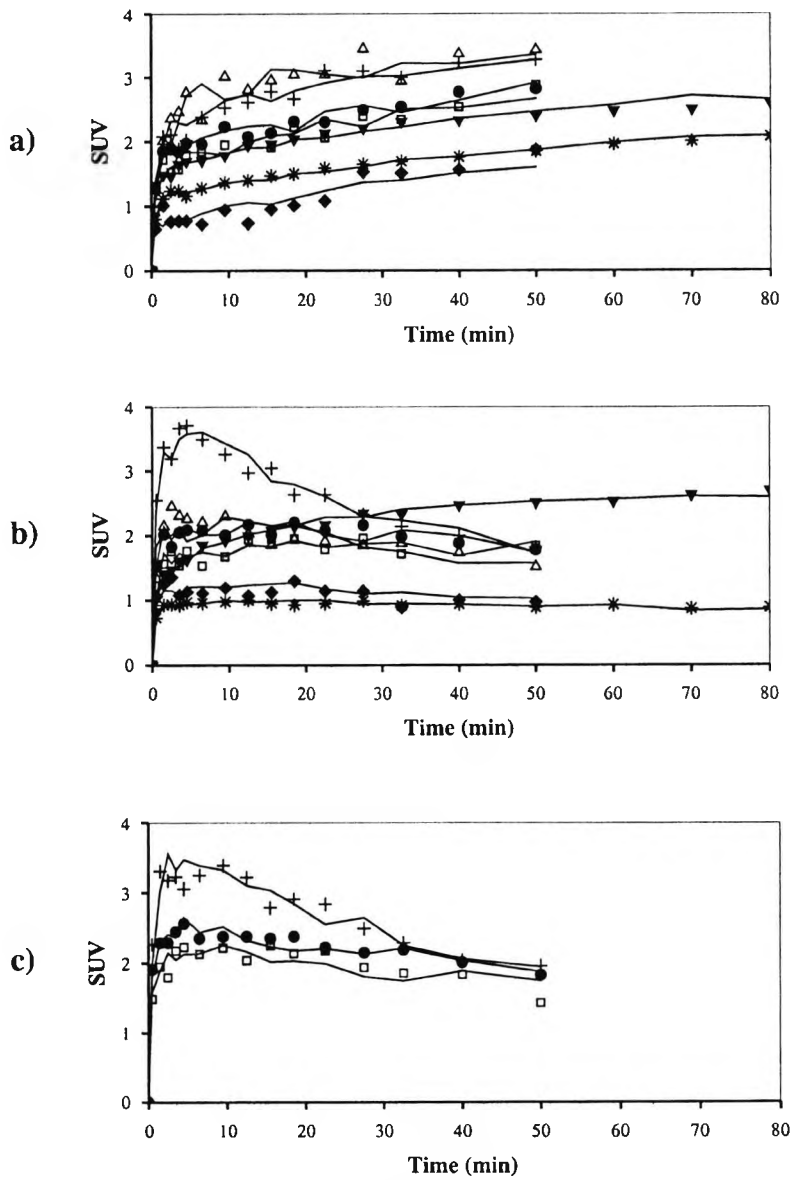

Fig. 2. Individual observed time-activity (SUV) data with the posterior individual predicted values (continuos line) at baseline (panel a), at the second scan time (panel b) and at the third scan time (panel c) for each monkey enrolled in the study: (+) monkey 1, ( ) monkey 2, (●) monkey 3, (◆) monkey 4, (▵) monkey 5, (▼) monkey 6, (*) monkey 7.

served time activity data with the posterior model predicted values for the 7 monkeys at baseline and at the first and second scan time are display in Figure 2. The overall evaluation of the fitting obtained with the C-c model is illustrated by the excellent agreement between individual prediction vs. observed RO% values with the unitary slope reference line (Figure 3).

4. Discussion

PET offers unique possibilities to investigate physiology, metabolism, pharmacokinetic, pharmacodynamic, and modes of action of drugs from animal and human studies. Several methods have been proposed for the analysis and the quantification of *in vivo* ligand-receptor interactions from PET data even if no universally "best" method has been recognized [25]. In any case, the modeling approach based on the arterial plasma input function appears as the method of choice [26]. However, in absence of arterial input function, mainly dues to the impossibility of properly identify and measure metabolite concentrations, the reference tissue methods remain, at the moment, a preferred modeling strategy despite the limitation and the known problems associated to this approach. In the present paper, STRM has

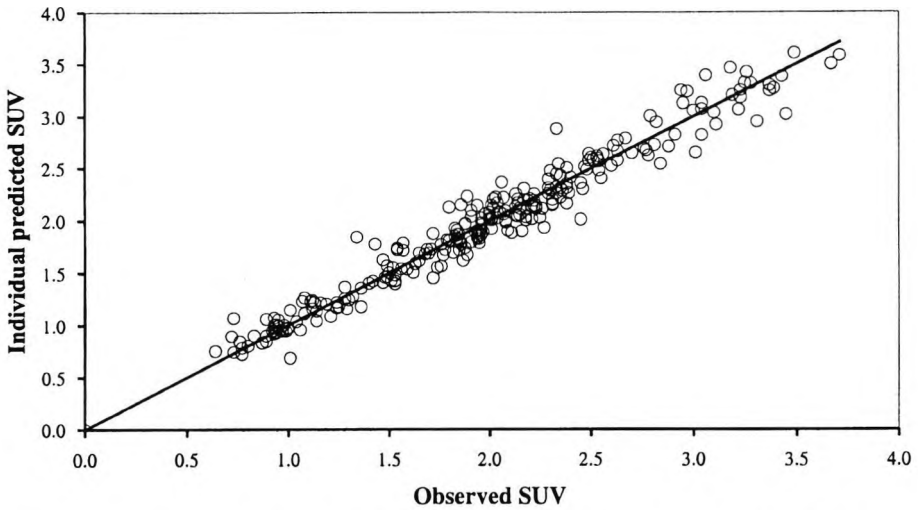

Fig. 3. Individual predicted versus observed time-activity data (SUV) with the reference unitary slope line (continuos line).

been selected according to statistical and goodness of fit criteria. At variance from the graphical method, which provides biased parameter estimates, the SRTM usually supplies well identified but, some time, underestimated parameter values.

A reliable estimate of the time-varying fraction of receptor occupancy integrated with the drug pharmacokinetic properties will enable researcher to build predictive models necessary to optimize the drug development process. Monte Carlo simulations have demonstrated that ignoring the presence of the inter-occasion variability may lead to biased and more variable parameter estimates [14,15] in pharmacokinetic/pharmacodynamic studies. For this reason, similar problems are expected in the analysis of PET experiments due to the repeated measure structure of the time-activity data and the complex mathematical models used to describe the response. The presence of intra-and inter-subject variability can be detected by inspecting the changes over time of the time-activity data measured in a RR following the same tracer injection. By definition, the RR is expected to be drug receptor free, therefore the variability observed on the time-activity kinetics in this region is assumed to reflect only inter- and intra-subject variability. This can be quantified by using the distribution property of the area under the time-activity curve estimated using the linear trapezoidal rule from 0 to 50 minutes (Mean = 82.7, Min = 42.1, Max = 110.4, S.D. = 19.2, CV% = 23.4). Some of this variation can be linked to experimental conditions associated to the PET technology (such as equipment calibration and tuning, procedures to collect and process data, sensitivity and detection limits, etc.) or to physiological processes associated to individual behavior. On these conditions, the use of non-linear mixed effect modeling approaches seems appropriate to better estimate the receptor occupancy parameter accounting for the different sources of variability. The evaluation of the different modeling approaches revealed that one of the major limitations of Model A is related to the underlying assumption considering each time-activity curve as a measurement coming from a separate individual. This assumption aggregates the within subject and the measurement error variability into an overall measurement noise, which therefore results artificially inflated. The final consequence of this assumption was the estimate of misleading parameters such as a negative receptor occupancy value and, in some cases, the impossibility to reach convergence in the minimization algorithm. This finding is in agreement with previously reported observations [1,22]. To overcome these limitations the Model B approach was proposed. In this approach the whole set of observations collected at different scan times on each monkey were simultaneously fitted together and the model was constrained to estimate positive RO% values. Furthermore, R_1 and k_2 were estimated on all the individual data, assuming that these values remain constant on the same monkey, while the observations at baseline and at the different scan times were used to estimate BP_0 and the RO% at the different scan times. Using this approach we did not observe any computational problem and any inconsistency on the estimated parameter values. However, two major limitations persist: (a) the R_1 and k_2 values are not constant over time for an individual but they may change on time, (b) this approach does not account for intra-individual variability which was, again, lumped into the measurement noise. Finally, three mixed effect models were investigated: the first one (Model C-a) only accounted for IIV and IOV while the Model C-b and C-c included two alternative second stage models to explain variability on BP as a function of the dose of unlabelled drug administered. The comparison of the different models indicates that the mixed effect approach with a primary model partitioning the variance in term of IIV and IOV and a second stage model relating the changes of binding potential to the dose of unlabelled drug

Table 5
Brain receptor occupancy (%) estimated using fixed and mixed effect modelling approach

Monkey	Scan	Model A	Model B	Model C
1	1	92.0	99.6	92.5
	2	88.5	99.7	91.3
2	1	90.8	82.6	86.4
	2	97.6	87.9	93.3
3	1	93.0	86.9	85.6
	2	93.4	79.6	84.8
4	1	*	100	97.
5	1	*	98	95.1
6	1	−20.3	63.2	50.1
7	1	45.5	83.6	85

* The non-linear regression procedure failed to reach convergence.

with an Emax model is definitely the preferred approach. However, the limited number of subjects (7 monkeys) and the limited number of occasions for subject (3 occasions in 3 monkeys and 2 occasions in 4 monkeys) suggests that the estimate of each variance term component must be cautiously interpreted even if the overall database used in the analysis (267 observations) was sufficiently large to allow a proper parameter estimation. In any case, the contribution of the IOV to the overall variance remains larger than the one of the IIV indicating the presence of an important intra-subject variability in the time-activity data collected during a PET experiment in the same subject. In addition, the relative error affecting the receptor occupancy seems inversely proportional to its value: the lowest is the value, the highest is the discrepancy between the RO% values estimated with the different methods as reported in Table 5. This observation indicates that the influence of the estimation procedure may become a critical factor for the appropriate evaluation of this parameter in particular at low RO% values (i.e. $< 50\%$). These findings may be of particular interest in the analysis of the experiments designed for the evaluation of receptor occupancy kinetic profile over time where several PET scans are collected in the same individual and where the extent of intra-subject variability may introduce artifact and/or bias in the evaluation of the results.

In conclusion, the non-linear mixed effect modeling seems to represent a valid alternative analysis approach mainly because it accounts for the repeated-measurement structure of the data and supply an estimate of the different variability components on the parameter values. In addition, this approach allows to integrate a second stage regression model to investigate the sources of variability in term of concomitant measurements (covariates). In our example only dose was included in this second stage model, however this approach can be easily extended to account for other factors such as demographical, pathophysiological, genetic factors which can potentially be used to investigate sources of variability in brain receptor occupancy.

References

[1] P. Abadie, P. Rioux, B. Scatton, E. Zarifian, L. Barré, A. Patat, J.C. Baron, Central benzodiazepine receptor occupancy by zolpidem in the human brain as assessed by positron emission tomography, Eur. J. Pharmacol. 295 (1996) 35–44.

[2] B. Andrée, C. Halldin, S.O. Thorberg, J. Sandell, L Farde, Use of PET and the radioligand [Carbonyl ^{11}C]WAY-100635 in psychotropic drug development, Nuclear Med. & Biol. 27 (2000) 515–521.

[3] S.L. Beal, L.B. Scheiner, NONMEM Users Guide, NONMEM Project Group, USCF, San Francisco, CA, 1992.

[4] P.H.R. Barrett, B.M. Bell, C. Cobelli, H. Golde, A. Schumitzky, P. Vicini, D.M. Foster, SAMII: simulation, analysis, and modeling software for tracer and pharmacokinetic studies. ¢rauth0¢rdate643343239 Metabolism 47 (1998) 484–492.

[5] M. Bergstrom, K.J. Fasth, G. Kilpatrick, P. Ward, K.M. Cable, M.D. Wipperman, D.R. Sutherland, B. Langstrom, Brain uptake and receptor binding of two [^{11}C]labelled selective high affinity NK1-antagonists, GR203040 and GR205171–PET studies in rhesus monkey, Neuropharmacology 39 (2000) 664–670.

[6] A. Bertoldo, S. Zamuner, R. Gomeni, A. Bye, C. Cobelli, Binding characteristics of NK1 receptors in the brains studied by [11C]GR205171 and PET. BrainPET'01 Vth International Conference on Quantification of Brain Function with PET, Taipei, TAIWAN, June 9–13 (2001).

[7] J. Delforge, A. Syrota, B.M Mazoyer, Identifiability analysis and parameter identification of an in vivo ligand-receptor model from PET data, IEEE Trans. Biomed. Eng. 37 (1990) 653–661.

[8] J. Delforge, The in vivo quantification of the receptor site concentration using ligand-receptor interaction modeling, Drug Inf. Journal 31 (1997) 1019–1027.

[9] A.J. Dobson, An introduction to statistical modelling, Chapman and Hall, New York, 1983.

[10] L. Farde, PET in neuropsychiatric drug development, in: D. Comar (Ed.), PET for drug development and evaluation, Kluwer Accademic Publisher, Dordrech, 1995, pp. 51–92.

[11] L. Farde, The advantage of using positron emission tomography in drug research, Trends Neurisci. 19 (1996) 211–214.

[12] P.B. Fitzgerald, S. Kapur, G. Remington, P. Roy, B. Zipursky, Predicting haloperidol occupancy of central dopamine D2 receptors from plasma levels, Psychopharmacology 149 (2000) 1–5.

[13] P.M. Grasby, Imaging strategies in depression, J. Psychopharmacology, 13 (1999) 346–351.

[14] M.O. Karlsson, L.B. Sheiner, The importance of modeling interoccasion variability in population pharmacokinetic analyses, J. Pharmacokin. Biopharm. 21 (1993) 735–750.

[15] R.L. Lalonde, D. Ouellet, E.K. Kimanani, D. Potvin,, L.M. Vaughan, M.R. Hill, Comparison of different methods to evaluate population dose-response and relative potency: importance of interoccasion variability, J. Pharmacokin. Biopharm. 27 (1999) 67–83.

[16] A.A. Lammertsma, C.J. Bench, S.P. Hume, S. Osman, K. Gunn, D.J. Brooks, R.S. Frackowiak, Comparison of methods for analysis of clinical [11C]raclopride studies, J. Cereb. Blood Flow Metab. 16 (1996) 42–52.

[17] A.A. Lammertsma, S.P. Humes, simplified reference tissue model for PET receptor studies, Neuroimage 4 (1996) 153–158.

[18] P.O. Maitre, M. Buhrer, D. Thomson, D.R. Stanski, A three-step approach combining Bayesian regression and NONMEM population analysis: application to Midazolam, J. Pharmacokin Biopharm. 19 (1991) 377–384.

[19] D.J. McGonigle, A.M. Howseman, B.S. Athwal, K.J. Friston, R.S.J. Frackowiak, A.P. Holmes, Variability in fMRI: an examination of intersession differences, Neuroimage 11 (2000) 708–734.

[20] M.A. Mintum, M.E. Raichle M.E., M.E. Kilbourn, G.F. Wooten, M.J. Welch, A quantitative model for the in vivo assessment of drug binding sites with PET, Ann. Neurol. 15 (1984) 217–227.

[21] A.M.J. Paans, W. Vaalburg, Positron emission tomography in drug development and drug evaluation, Current Pharm. Design 6 (2000) 1583–1591.

[22] R.V. Parsey, M. Slifstein, D.R. Hwang, A. Abi-Dargham, N. Simpson, O. Mawlawi, N.N. Guo, R. Van Heertum, J.J. Mann, M Laruelle, Validation and reproducibility of measurements of 5-HT_{1A} receptor parameters with [*carbonyl*-^{11}C]WAY-100635 in humans: comparison of arterial and reference tissue input function, J. Cereb. Blood Flow Metab. 20 (2000) 1111–1133.

[23] J.S. Perlmutter, K.B. Larson, M.E. Raichle, J. Markham, M.A. Mintun, M.R. Kilbourn, M.J.Welch, Strategies for in vivo measurement of receptor binding using positron emission tomography, J. Cereb. Blood Flow Metab. 6 (1986) 154–69.

[24] A.L. Nordstrom, L. Farde, F.A. Wiesel, K. Forslund, S. Pauli, C. Halldin, G. Uppfeldt, Central D2-dopamine receptor occupancy in relation to antipsychotic drug effect–a double blind PET study of schizophrenic patients, Biol. Psychiatry 33 (1993) 227–235.

[25] M. Slifstein, M. Laruelle, Models and methods for derivation of in vivo neuroreceptor parameters with PET and SPECT reversible radiotracers, Nucl. Med. Biol. 28 (2001) 595–608.

[26] A. Van Waarde, Measuring receptor occupancy with PET, Current Pharm. Design 6 (2000) 1593–1610.

[27] D.F. Wong, A. Gjedde, H.N. Wagner Jr, R.F. Dannals, K.H. Douglass, J.M. Links, M.J. Kuhar, Quantification of Neuroreceptors in the living human brain. II. Inhibition studies of receptor density and affinity, J. Cereb. Blood Flow Metab. 6 (1986) 147–153.

[28] D.F. Wong, A. Gjedde, H.N. Wagner Jr, Quantification of neuroreceptors in the living human brain. I. Irreversible binding of ligands, J. Cereb. Blood Flow Metab. 6 (1986) 137–146.